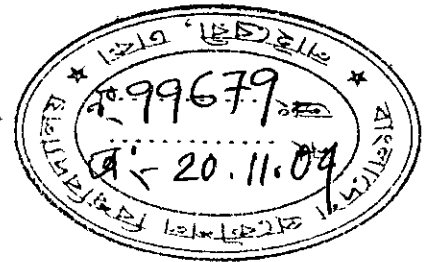


Performance of a Two-Phase Thermosyphon: Response to Evaporator Geometry and Working Fluid

by

Kamal Uddin Ahmed



A Thesis

Submitted to the Department of Mechanical Engineering, Bangladesh University of Engineering and Technology, Dhaka, in partial Fulfillment of the Requirement for the Degree of Master of Science in Mechanical Engineering.



#99679#

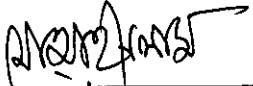
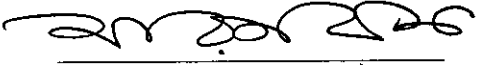

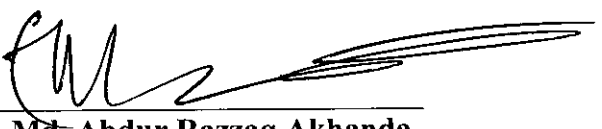
Department of Mechanical Engineering
Bangladesh University of Engineering & Technology
Dhaka-1000, Bangladesh

2004

Certificate of Thesis Approval

The thesis titled **Performance of a Two-Phase Thermosyphon: Response to Evaporator Geometry and Working Fluid** submitted by **Kamal Uddin Ahmed, Roll No. 040010043P**, Session: April 2000 has been accepted as satisfactory in partial fulfillment of the requirement for the degree of Master of Science in Mechanical Engineering on 2 October 2004.

BOARD OF EXAMINERS

1. 
Dr. Md. Ashraful Islam
Associate Professor
Department of Mechanical Engineering
BUET, Dhaka
Chairman
2. 
Dr. M. A. Rashid Sarkar
Professor
Department of Mechanical Engineering
BUET, Dhaka
Member
3. 
Dr. Md. Quamrul Islam
Professor and Head
Department of Mechanical Engineering
BUET, Dhaka
Member
(Ex-officio)
4. 
Dr. Md. Abdur Razzaq Akhanda
Professor (On leave)
Department of Mechanical Engineering
BUET, Dhaka
Member
(External)

DECLARATION

It is hereby declared that this thesis or any part of it has not been submitted elsewhere for the award of any degree or diploma.

Kamal Uddin Ahmed

Kamal Uddin Ahmed
Roll No. 040010043P

Dedicated to my

Parents

CONTENTS

	<u>Page No.</u>
List of Figures	viii
List of Tables	x
Nomenclature	xii
Acknowledgement	xiii
Abstract	xiv
Chapter-1 INTRODUCTION	1-3
1.1 General	1
1.2 Motivation	1
1.3 Objectives	3
Chapter-2 LITERATURE REVIEW	4-12
2.1 Background	4
2.2 Regimes of Subject Matter	8
2.2.1 Pool Boiling	8
2.2.2 Boiling Curve	8
2.2.3 Rohsenow Correlation	10
2.2.4 Stephan and Abdelsalam Correlation	11
2.2.5 Critical Heat flux and Kutateladze Correlation	11
Chapter-3 EXPERIMENTAL SETUP AND PROCEDURE	13-23
3.1 General	13
3.2 Experimental Setup	13
3.2.1 Loop Thermosyphon	13
3.2.2 Evaporator Surface	16
3.2.3 Heat Supply System	19
3.2.4 Measurement System	19
3.2.5 Working Fluids	19
3.3 Experimental Procedure	22
3.3.1 Data Collection Procedure	22
3.3.2 Data Reduction Procedure	23
Chapter-4 RESULTS AND DISCUSSIONS	24-59
4.1 General	24
4.2 Boiling Curves (q vs. ΔT)	24
4.3 Effects of Evaporator Surface on Boiling Curves	26
4.4 Effects of Working Fluids on Boiling Curves	27
4.5 Boiling Curves (h vs. ΔT)	28
4.6 Effects of Evaporator Surface on h	28
4.7 Effects of Working Fluids on h	29

Chapter-5 CONCLUSIONS	60-61
5.1 Conclusions	60
5.2 Recommendations	61
REFERENCES	62-65
APPENDICES	66-98
APPENDIX-A Experimental Data	66
APPENDIX-B Sample Calculations	93

LIST OF FIGURES

Fig. 2.1	General Pool Boiling Curve	4
Fig. 3.1	Schematic Diagram of Two-Phase Compact Thermosyphon	14
Fig. 3.2	Evaporator Section of the Loop Thermosyphon	15
Fig. 3.3	Detail of Evaporator Assembly	17
Fig. 3.4	Evaporator Surfaces	18
Fig. 4.1	Boiling Curve for HRO-Acetone	30
Fig. 4.2	Boiling Curve for HRI-Acetone	31
Fig. 4.3	Boiling Curve for HR+-Acetone	32
Fig. 4.4	Boiling Curve for HRO-Ethanol	33
Fig. 4.5	Boiling Curve for HRI-Ethanol	34
Fig. 4.6	Boiling Curve for HR+-Ethanol	35
Fig. 4.7	Boiling Curve for HRO-Methanol	36
Fig. 4.8	Boiling Curve for HRI-Methanol	37
Fig. 4.9	Boiling Curve for HR+-Methanol	38
Fig. 4.10	Effect of Evaporator Surface on the Boiling Curve for Acetone	39
Fig. 4.11	Effect of Evaporator Surface on the Boiling Curve for Ethanol	40
Fig. 4.12	Effect of Evaporator Surface on the Boiling Curve for Methanol	41
Fig. 4.13	Effect of Working Fluids on the Boiling Curve for HRO	42
Fig. 4.14	Effect of Working Fluids on the Boiling Curve for HRI	43
Fig. 4.15	Effect of Working Fluids on the Boiling Curve for HR+	44
Fig. 4.16	Variation of Heat Transfer Coefficient, h for HRO-Acetone	45
Fig. 4.17	Variation of Heat Transfer Coefficient, h for HRI-Acetone	46
Fig. 4.18	Variation of Heat Transfer Coefficient, h for HR+-Acetone	47

Fig. 4.19	Variation of Heat Transfer Coefficient, h for HRO-Ethanol	48
Fig. 4.20	Variation of Heat Transfer Coefficient, h for HRI-Ethanol	49
Fig. 4.21	Variation of Heat Transfer Coefficient, h for HR+-Ethanol	50
Fig. 4.22	Variation of Heat Transfer Coefficient, h for HRO-Methanol	51
Fig. 4.23	Variation of Heat Transfer Coefficient, h for HRI-Methanol	52
Fig. 4.24	Variation of Heat Transfer Coefficient, h for HR+-Methanol	53
Fig. 4.25	Effects of Evaporator Surfaces on Heat Transfer Coefficient, h for Acetone	54
Fig. 4.26	Effects of Evaporator Surfaces on Heat Transfer Coefficient, h for Ethanol	55
Fig. 4.27	Effects of Evaporator Surfaces on Heat Transfer Coefficient, h for Methanol	56
Fig. 4.28	Effects of Working Fluids on Heat Transfer Coefficient, h for HRO	57
Fig. 4.29	Effects of Working Fluids on Heat Transfer Coefficient, h for HRI	58
Fig. 4.30	Effects of Working Fluids on Heat Transfer Coefficient, h for HR+	59

LIST OF TABLES

Table-3.1:	Properties of the Working Fluids at Atmospheric Pressure	21
Table-A1:	Collected data during the 1st experiment evaporator plain surface with acetone	66
Table-A2:	Collected data during the 2nd experiment evaporator plain surface with acetone	67
Table-A3:	Collected data during the 3rd experiment evaporator plain surface with acetone	68
Table-A4:	Collected data during the 1st experiment evaporator with integrated rectangular fins with acetone	69
Table-A5:	Collected data during the 2nd experiment evaporator with integrated rectangular fins with acetone	70
Table-A6:	Collected data during the 3rd experiment evaporator with integrated rectangular fins with acetone	71
Table-A7:	Collected data during the 1st experiment evaporator with integrated cross fins with acetone	72
Table-A8:	Collected data during the 2nd experiment evaporator with integrated cross fins with acetone	73
Table-A9:	Collected data during the 3rd experiment evaporator with integrated cross fins with acetone	74
Table-A10:	Collected data during the 1st experiment evaporator plain surface with ethanol	75
Table-A11:	Collected data during the 2nd experiment evaporator plain surface with ethanol	76
Table-A12:	Collected data during the 3rd experiment evaporator plain surface with ethanol	77
Table-A13:	Collected data during the 1st experiment evaporator with integrated rectangular fins with ethanol	78
Table-A14:	Collected data during the 2nd experiment evaporator with integrated rectangular fins with ethanol	79

Table-A15:	Collected data during the 3rd experiment evaporator with integrated rectangular fins with ethanol	80
Table-A16:	Collected data during the 1st experiment evaporator with integrated cross fins with ethanol	81
Table-A17:	Collected data during the 2nd experiment evaporator with integrated cross fins with ethanol	82
Table-A18:	Collected data during the 3rd experiment evaporator with integrated cross fins with ethanol	83
Table-A19:	Collected data during the 1st experiment evaporator plain surface with methanol	84
Table-A20:	Collected data during the 2nd experiment evaporator plain surface with methanol	85
Table-A21:	Collected data during the 3rd experiment evaporator plain surface with methanol	86
Table-A22:	Collected data during the 1st experiment evaporator with integrated rectangular fins with methanol	87
Table-A23:	Collected data during the 2nd experiment evaporator with integrated rectangular fins with methanol	88
Table-A24:	Collected data during the 3rd experiment evaporator with integrated rectangular fins with methanol	89
Table-A25:	Collected data during the 1st experiment evaporator with integrated cross fins with methanol	90
Table-A26:	Collected data during the 2nd experiment evaporator with integrated cross fins with methanol	91
Table-A27:	Collected data during the 3rd experiment evaporator with integrated cross fins with methanol	92

NOMENCLATURE

A	Area, m ²
C _l	Specific heat of saturated liquid, J/kg, °C
C _{sf}	Coefficient for various liquid surface combinations
g	Gravitational acceleration, m/s ²
g _c	Conversion factor
h	Boiling heat-transfer coefficient, W/m ² .°C
h _{fg}	Enthalpy of vaporization, J/kg
HRI	Evaporator with integrated rectangular fins
HR+	Evaporator with integrated cross fins
HRO	Evaporator with plain surface
k	Thermal conductivity of material, W/m.°C
P _{rl}	Prandtl number of saturated liquid
Q	Heat Input, W
q	Heat Flux, MW/m ²
q _L	Heat loss, MW/m ²
q _R	Heat Flux from Rohsenow correlation, MW/m ²
q _S	Heat Flux from Stephan & Abdelsalam correlation, MW/m ²
q _{crit}	Critical Heat Flux by Kuateledze correlation
r	Radius of heater assembly, cm
T _{sat}	Saturation temperature of working fluids, °C
T _{X1}	Temperature at the point 1 of evaporator assembly, °C
T _{X2}	Temperature at the point 2 of evaporator assembly, °C
T _{X3}	Temperature at the point 3 of evaporator assembly, °C
T _{X4}	Temperature at the point 4 of evaporator assembly, °C
T _w	Wall temperature, °C
T _∞	Ambient temperature, °C
ΔT	Temperature excess or wall superheat, °C
μ _l	Liquid viscosity, kg/m.s
ρ _l	Density of saturated liquid, kg/m ³
ρ _v	Density of saturated vapor, kg/m ³
σ	Surface tension of liquid-vapor interface, N/m

ACKNOWLEDGEMENT

The author wishes to express his heartiest and sincerest gratitude to Dr. Md. Ashraful Islam, Associate Professor of Mechanical Engineering Department, Bangladesh University of Engineering and Technology, Dhaka for his guidance, inspiration, constructive suggestions and close supervision throughout the entire period of the experiment investigation.

The author also expresses thankful gratitude to Prof. Md. Abdur Razzaq Akhanda, Prof. Md. Quamrul Islam and Prof. M. A. Rashid Sarkar for kindly examining the manuscript and offering valuable comments.

The author acknowledges his gratefulness to the Mechanical Engineering Department for providing required facilities. The author is thankful to Instructors, Operators and Technicians of Machine Shop and Welding shop.

The author gratefully acknowledges the contribution of Mr. Hasan Md. Mostofa Afroz for organizing thesis and analyzing data and of Mr. A.Z.M Ariful Islam and Mr. Al Amin in building experiential setup.

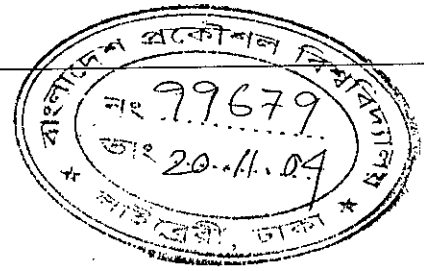
A lot of thanks are due to Mr. Dewan Md. Amir Hossain, Senior Lab. Instructor Cum-Store-Keeper of Heat Transfer Laboratories, Mr. Md. Abdul Awal, Senior Lab. Attendent of Fuel Testing Laboratory and Mr. Md. Masudur Rahman, Assistant Instrument Engineer, Measurement and Control Laboratories, Mr. Md. Fakhru Islam Hazra, Assistant Accountant of Mechanical Engineering Department for their cooperation all through the research work.

Author

ABSTRACT

A two-phase loop thermosyphon had been designed, fabricated and experimented with a view to cooling high heat flux electronic components. The thermosyphon has four components in a loop: an evaporator with boiling enhancement structure, vapor rising tube, condenser and condensate return tube. Experiments were conducted to assess the effects of working fluids and evaporator geometry. Three different working fluids were used in this study, namely Acetone, Ethanol and Methanol. Boiling heat transfer was studied for three different evaporator surfaces: plain surface (HRO), integrated rectangular finned surface (HRI) and integrated cross finned surface (HR+). The supplied electrical energy and temperatures at different locations of evaporator surfaces were measured in this study for different working fluids. From the measured parameters, boiling curves were plotted in nucleate boiling regime and were analyzed for different geometry and working fluids.

The temperature very close to evaporator surface was as high as 99°C to transfer heat flux of 28 W/cm². These temperatures were 88, 99 and 85°C for Methanol, Ethanol, and Acetone respectively. The respective heat fluxes were 27.5, 28.0, 27.5 W/cm². Enhanced surfaces can transfer more heat compared to the surface without it. The enhanced surfaces HR+ can transfer a heat flux of 27.5 W/cm² boiling Methanol and keeping evaporator surface temperature very close to 85°C. The heat transfer coefficient in this study was as high as $9 \times 10^4 \text{ W/m}^2 \text{ } ^\circ\text{C}$.



1.1 General

The feature size in microprocessors has been reducing with the development of electronics field. Consequently, the number of active semi-conductor devices per unit chip area has been increasing. In the last decade, the number of active semi-conductor devices per unit chip area has almost quadrupled (Semi-conductor Industries Association Roadmap, 1994, Ramaswamy et al. 1998). As an example, the minimum feature size in microprocessors has reduced from 0.35 μm in 1990 to 0.25 μm in 1997 and is slated go down further to 0.05 μm by the year 2012 (Semi-conductor Industries Association Roadmap, 1997, Ramaswamy et al 1999). This has increased the heat dissipation density for desktop microprocessors. As an example the heat flux has increased from $\sim 2\text{W}/\text{cm}^2$ for an Intel 486 microprocessor to almost $21\text{ W}/\text{cm}^2$ for the Intel P II 300-400 MHz microprocessors. (Intel Web page, 1998, Ramaswamy et al 1999). The current heat dissipation rates for some desktop computer is approximately $25\text{ W}/\text{cm}^2$. As per Bergles et al. (1990), it is expected that the microprocessor chips for some of the next generation work stations would dissipate 50-100 W/cm^2 . Development of efficient thermal management scheme is essential to dissipate these high heat fluxes and maintain the chip junction temperature below 85°C . Liquid cooling, with phase change, is a very efficient heat transfer process and is good alternative to existing air-cooled designs.

1.2 Motivation

A thermosyphon is a kind of device that transfers heat, momentum, and mass with the assistance of buoyancy force on a fluid contained in a system. It is such a device, which successfully implements two phase liquid cooling by indirect contact with

electronics. A two phase thermosyphon basically consists of an evaporator and a condenser, which are connected through a passage or a loop. Heat is transferred from the source through an interface to the evaporator where the liquid vaporizes by taking the latent heat. The vapor then moves to the condenser, where it is condensed. The released heat is dissipated to the ambient from the condenser and the condensed liquid is returned to the evaporator, thus completing a closed loop. The density difference between the liquid and vapor creates a pressure head, which drives the flow through the loop, and as such no driving force is needed. Thermal resistance at the interface between the heat sources and the evaporator is a key design parameter. This must be minimized in order to get the benefit of low thermal resistance of the evaporator.

To design effective devices for heat transfer augmentation and temperature control, scientists all over the world have been paying their attention for many years on different types of geometric arrangements. Among those devices, thermosyphon is the one, which has been being studied since the middle of last century due to its high effective heat transfer co-efficient. Some highlighted studies are being described here and remaining works about thermosyphon will be described more elaborately in the Chapter-2. Mudawar and Anderson (1993) performed pool boiling studies using structures with multiple levels of enhancement and dielectric fluorinerts as the working fluid (FC-72 and FC-87). The maximum heat flux attained with the same structure, with a surface temperature below 85°C was $\sim 105 \text{ W/cm}^2$. Nakayama et al.(1984) employed a 3-D porous structure and attained a heat dissipation of 100 W/cm^2 at a wall superheat of 27.8°C with FC-72. The wall superheats are based on thermodynamically saturated fluid for the above mentioned studies. Ramaswamy et al. (1998) performed a study of a compact two-phase thermosyphon in the effect of variation of liquid fill volume. The fill ratio tested were 100%, 50%, 15% and 11%. The 11% fill level was chosen to simulate a case, where the enhanced surface was just about immersed in the liquid. Their results showed that the liquid fill volume has negligible effect on the boiling performance of a enhanced structure as long as it immersed in the liquid at all times. This could be a limiting factor in the design of very compact evaporators.

1.3 Objectives

The specific objectives of this study are to

1. Design and fabricate an experimental facility for studying thermal performance of a two-phase loop thermosyphon.
2. Measure temperature at different location of the system.
3. Study the effects of the working fluids, shape of the evaporator and surface.
4. Analyze the heat transfer performance.
5. Compare the results of this experiment with those of similar previous works.

LITERATURE REVIEW

2.1 Background

Development of the world depends on the development of various fields e.g. environment, education, houses, transport, tools and equipments, corresponding media and electronics media etc. Among those, electronics plays a vital part. With the development of electronics, the feature size in microprocessor has been reducing day by day and with the reducing of feature size increasing the number of active semiconductor devices per unit chip area as well as increasing the heat dissipation density. For efficient thermal management, it is essential to dissipate these high heat fluxes and maintain the chip junction temperature below 85°C (a maximum limit for most commercial electronics). Thus it will be a great problem for some next generation workstation, although scientists all over the world have been working to overcome the problem from middle of last century. Personal computers are currently air cooled by either free or forced convection. Fans attached to the central processing unit (CPU) are the most popular cooling devices for low power dissipation systems. They are popular because of reliability, cost, efficiency and ease of implementation. However, for higher frequency chips (above 1000 MHz), the air-cooled heat sinks have some limitations in the form of bulky size, noise and insufficient cooling performance. As a result, current practice of dense packaging of electronics in compact spaces demands novel ways of heat dissipation, which will be able to dissipate as much as 100 W/cm² at chip levels while maintaining the device at acceptable temperature. As the size of heat sinks becomes too large and unwieldy for compact systems, indirect liquid cooling is a potential candidate for more efficient thermal management.

Liquid cooling techniques may be classified as direct and indirect. Direct liquid cooling involves immersing the electronics directly in a pool of inert liquid. [Incropera (1990), Nakayama and Bergles (1990) and Cohen (1993)]. Two issues that have been addressed in most studies are the reduction of incipience excursion results

in a sudden drop in the surface temperature to transition from natural convection to nucleate boiling and act as a thermal shock for the electronic component. Critical heat flux (CHF) is the point where a vapor film forms around the boiling surface and deteriorates the heat transfer significantly. Indirect liquid cooling is usually implemented using thermosyphons and heat pipes. The early studies on thermosyphons were on single-phase heat transfer and fluid flow processes. But the latest researches are on two-phase thermosyphon. Many great studies of thermosyphon show the existence of several operating limits that depend on the heat addition, geometry, liquid filling ratio and fluid characteristics.

As the size of the evaporator is reduced, the liquid/vapor space around the enhanced structure reduces. This could affect the heat transfer performance of the system. Katto et al. (1977) examined the effect of placing a plate parallel to the boiling surface at very close distance (0.2 - 10 mm) with saturated distilled water as the working fluid. The boiling surface was a 11 mm diameter horizontally oriented copper plate. They found degradation in the heat transfer performance with reduction of vapor space. Tubes with enhanced surfaces have been used in the refrigeration and chemical industries extensively to reduce the incipience super heat and increase the critical heat flux. An analysis of the variation in super heat with sub-cooling was carried out by Judd et al. (1991). They found an increase in the wall super heat with increase in sub-cooling initially, followed by a reduction. They attributed the initial increase to changes in boiling parameters-nucleation site density micro-layer evaporation and enthalpy transport. As the sub-cooling was further increased, natural convection played a dominant role and the wall super heat was lower. Miller (1991) developed re-entrant cavities on a silicon substrate and conducted pool boiling studies. With FC-72 as the working fluid, the heat flux obtained was about 10 W/cm^2 at a super heat of 10°C . Bhavnani et al. (1993) developed similar structures and reported maximum heat dissipation rates of 55 W/cm^2 with a super heat of 42°C using FC-72 as the working fluid. The efficient performance of enhanced structures in pool boiling makes them good candidates for incorporating into the evaporator section of thermosyphons to accommodate higher heat fluxes.

Nowell et al. (1994) conducted a similar study with a micro configured heat sink which was etched in silicon and oriented vertically. The parallel plate was also

made of silicon and the distance was varied from 1-6 mm. Results showed an improvement in heat transfer performance with a reduction in the gap. For the 1 mm gap, the performance was very similar to pool boiling. They attributed this improvement to a local thermosyphon effect, where some of the vapor generated was condensed at the parallel plate.

Palm and Tengblad (1996) have reviewed some of the current research on thermosyphons. To accommodate the higher heat fluxes, enhancement schemes have been used in the evaporator section. There is an extensive database of pool boiling studies on enhanced surfaces and, considering their efficient performance in immersion cooling, they seem to be good candidates for the evaporator section of thermosyphons. Since most of the enhanced surfaces have small feature sizes ($\sim 200 \mu\text{m}$), a very compact evaporator section can be designed with these structures. Thermosyphons using these compact evaporators are an attractive cooling technique for point applications (e.g. single chip microprocessors). Webb et al. (1996) have used enhanced surfaces in the evaporator and condenser sections of a thermosyphon for cooling the hot side of thermoelectric coolers. Using a "bent-fin" structure, they have achieved a heat flux of about 18 W/cm^2 in refrigerant R-134a. Performance evaluation was carried out over a range of velocities for the forced convection cooled condenser. Ramaswamy et al. (1997) investigated the effect of confinement of the evaporator section. Plexiglass blocks were inserted in to the enclosure to reduce the liquid space around the enhanced structure. Results showed that the effect of confining the space in the evaporator (simulating a compact evaporator) on boiling heat transfer was negligible. In another study by Ramaswamy et al. (1998) liquid/vapor space confinement in the evaporator section was studied, and the results showed a negligible effect on the performance of the system. The incipience excursion in the partial vacuum case was 6.3°C at a heat flux of 3 W/cm^2 . There was some hysteresis observed in the high-pressure case where the decreasing heat flux showed higher wall super heat values compared to the increasing heat flux. Also the pressure build up in the case was only 320 kPa at 18 W/cm^2 . The Plexiglass blocks placed in the evaporator could have spread the heat more effectively to the cover, thereby improvement the heat transfer and reducing the liquid temperature and pressure in the system.

Another study by Ramaswamy et al. (1999) based on the use of boiling enhancement structures in the evaporator section; a three-dimensional stacked micro-channel structure with interconnected pores was used to dissipate heat fluxes of about 70 W/cm^2 in dielectric liquid FC-72 with the maximum heat source temperature below 100°C . Sunil et al. (2000) studied single chamber compact thermosyphons with micro-fabricated components. Incorporation of the enhancement structure resulted in an improvement in the thermosyphon performance by decreasing the wall temperature at the evaporator by 8°C , for a power dissipation of 36 W/cm^2 at an air speed of 1 m/sec . The maximum heat flux obtained based on a maximum evaporator temperature of 75°C for an air speed of 1 m/s was 42.5 W/cm^2 . Long et al. (2001) studied the effects of imposed circulation and location of condenser on the performance of a two-phase thermosyphon in a confined space. They reported imposed circulation using a pump could make the thermosyphon successfully operate even when the condenser is placed below the evaporator. The effect of the relative placement of condenser and evaporator is marginal in the imposed circulation thermosyphon. Increasing the pumping flow rate decreases the total thermal resistance of the thermosyphon for each heat input. Aniruddha et al. (2002) studied the performance evaluation of a compact thermosyphon. They tested the thermosyphon with two fluids- deionized ultra filtered (DIUF) water and PF 5060, a dielectric liquid. The loop thermosyphon (LTS) is mounted on a test stand and $0.0075 \text{ m}^3/\text{s}$ of cooling air is passed over the condenser fin stack. The parameters measured at various power inputs for two different working fluids. They reported that water is a better working fluid, as the thermal properties of water are better than that of PF 5060. The high thermal resistance in PF 5060 may be attributed to the high amount of dissolved gases in it. It has been shown that the dissolved gases enhance heat transfer coefficient; however, they lead to a decrease in critical heat flux, thus increasing thermal resistance. The pressure of the dissolved gases may also have an adverse effect on the condenser and lead to overall performance degradation. However, with proper degassing procedure before charging the system, it may be possible to improve the performance of the PF 5060 charged system.

Present study will estimate the maximum amount heat that can be transferred using newly designed evaporator having enhanced structures. It will also evaluate the

effects of size and shape of the evaporator. The response of different working fluids will also be evaluated in this study.

2.2 Regimes of Subject Matter

2.2.1 Pool Boiling

Boiling at the surface of a body immersed in an extensive pool of motionless liquid is generally referred to as pool boiling. This type of boiling process is encountered in a number of applications, including metallurgical quenching processes, flooded tube and shell evaporators, immersion cooling of electronic components and boiling of water in a pot on the burner of a stove. The nature of pool boiling process varies considerably depending on the conditions at which boiling occurs. The level of heat flux, the thermophysical properties of the liquid and vapor, the surface material and finish and the physical size of the heated surface all may have an effect on the boiling process.

2.2.2 Boiling Curve

The regimes of pool boiling are most easily understood in terms of the boiling curve; a plot of heat flux q versus wall superheat $T_w - T_{sat}$ for the circumstances of interest. The different regions of boiling are indicated in Fig. 2.1 where heat-flux data from an electrically heated platinum wire submerged in water are plotted against wall superheat. In region I free convection currents are responsible for motion of the fluid near the surface. In this region the liquid near the heated surface is superheated slightly and it subsequently evaporates when it rises to the surface. In region II bubbles begin to form on the surface of the wire and are dissipated in the liquid after breaking away from the surface. This region indicates the beginning of nucleate boiling. As the temperature excess is increased further bubbles form more rapidly and rise to the surface of the liquid where they are dissipated. This is indicated in region III. Eventually, bubbles are formed so rapidly that they blanket the heating surface and prevent the inflow of fresh liquid from taking their place. At this point the bubbles coalesce and form a vapor film, which covers the surface. The heat must be conducted through this film before it can reach the liquid and effect the boiling process. The thermal resistance of this film causes a reduction in heat flux, and this phenomenon is illustrated in region IV, the film-boiling region. This region represents

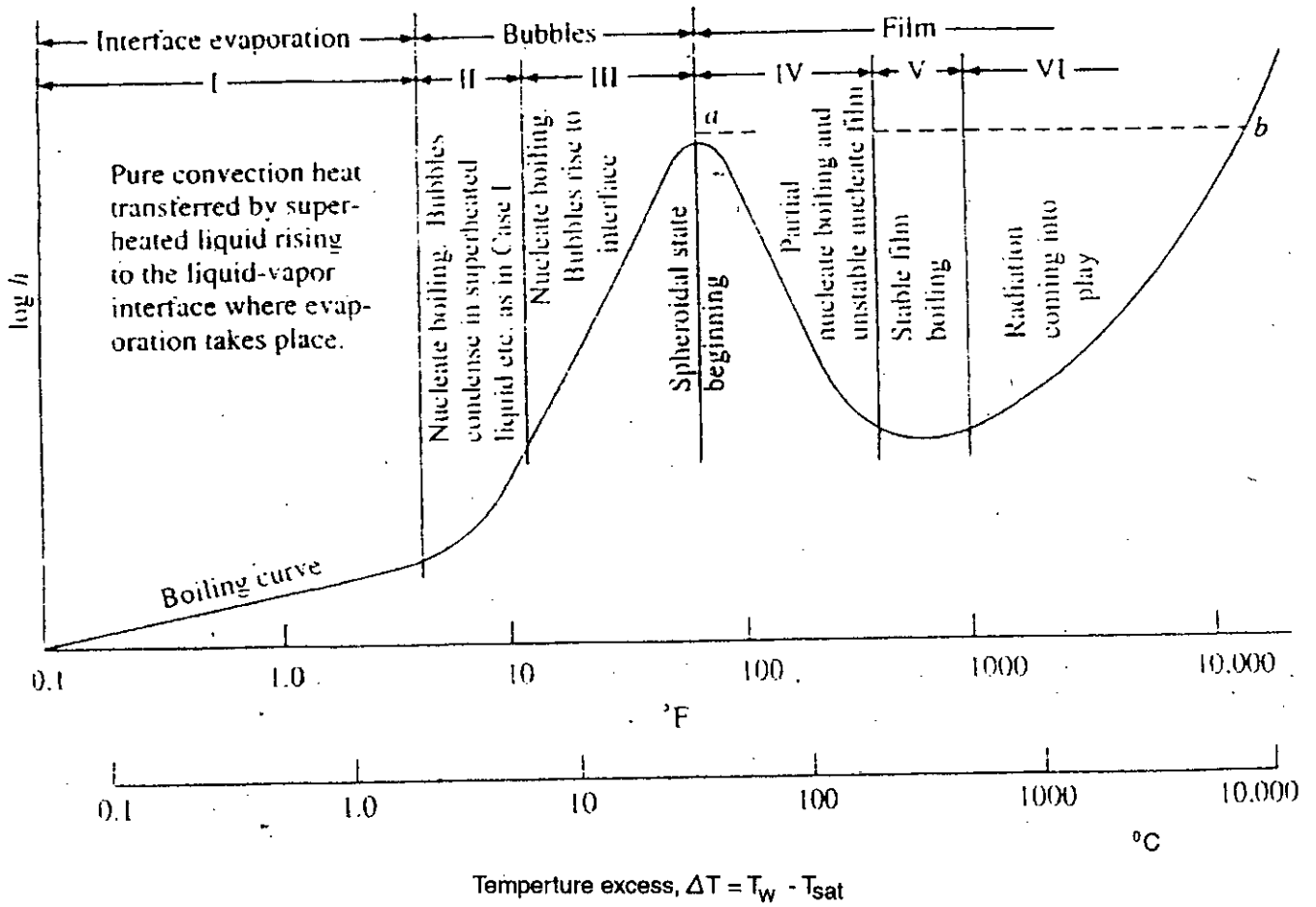


Figure : 2.1 Boiling Curve

Ref. Farber and Scoriah (1948)

a transition from nucleate boiling to film boiling and is unstable. Stable film boiling is eventually encountered in region V. The surface temperatures required to maintain stable film boiling are high and once this condition is attained, a significant portion of the heat loss by the surface may be the result of thermal radiation, as indicated in region VI. In the present study, experiments are conducted in regions II-III.

2.2.3 Rohsenow Correlation

Many of the very early models of the nucleate boiling process were based on the assumption that the process of bubble growth and release induced motion of the surrounding liquid facilitated convective transport of heat from the adjacent surface. Perhaps the most successful application of this approach was made by Rohsenow, who postulated that heat flows from the surface first to the adjacent liquid, as in any single phase convection process and that the high heat transfer coefficient associated with nucleate boiling is a result of local agitation due to liquid flowing behind the wake of dependent bubbles. Rohsenow (1955) correlated experimental data for nucleate pool boiling as follows.

$$\frac{C_l \Delta T}{h_{fg} Pr_l^s} = C_{sf} \left[\frac{q_R}{\mu_l h_{fg}} \sqrt{\frac{g_c \sigma}{g(\rho_l - \rho_v)}} \right]^{0.33} \quad (2.1)$$

- where C_l = specific heat of saturated liquid, J/kg.°C
 ΔT = temperature excess = $T_w - T_{sat}$, °C
 h_{fg} = enthalpy of vaporization, J/kg
 Pr_l = Prandtl number of saturated liquid
 q_R = heat flux from Rohsenow correlation, W/m².
 μ_l = liquid viscosity, kg/m.s
 σ = surface tension of liquid-vapor interface, N/m
 g = gravitational acceleration, m/s²
 ρ_l = density of saturated liquid, kg/m³
 ρ_v = density of saturated vapor, kg/m³
 C_{sf} = coefficient for various liquid surface combinations
 s = 1.0 for water and 1.7 for other liquids

2.2.4 Stephan and Abdelsalam Correlations

In a more recent study, Stephan and Abdelsalam (1980) proposed the following correlation based on dimensional analysis and optimal fits to experimental data:

For hydrocarbons

$$q_s = \{C_2(T_w - T_{sat})\}^{1/0.33} \tag{2.2}$$

Values of the constants C_2 for materials of the indicated types are found from Fig. 7.10 through 7.13 in the Book by Carey (1994).

2.2.5 Critical Heat Flux (CHF) and Kutateladze Correlation

If the surface temperature is held constant and uniform, dry portions of the surface covered with a vapor film will locally transfer a much lower heat flux than wetted portions of the surface where nucleate boiling is occurring. Because of the reduction of heat flux from intermittently dry portions of the surface, the mean overall heat flux from the surface is reduced. Thus increasing the wall temperature within the slugs and columns region ultimately results in a peaking and rollover of the heat flux. The peak value of heat flux is called the critical heat flux (CHF), designated as point *a* in the boiling curve (Fig. 2.1).

Kutateladze (1948) apparently was among the first investigators to note the similarity between flooding phenomena in distillation columns and the CHF condition in pool boiling. He used dimensional analysis arguments to derive the following relation for the maximum heat flux.

$$q_{crit} = C_k \rho_v^{1/2} h_{fg} [g(\rho_l - \rho_v)\sigma]^{1/4} \tag{2.3}$$

- where q_{crit} = critical heat flux for W/m^2
- ρ_v = density of saturated vapor, kg/m^3
- h_{fg} = enthalpy of vaporization, J/kg
- σ = Surface tension of liquid-vapor interface, N/m
- g = gravitational acceleration, m/s^2
- ρ_l = density of saturated liquid, kg/m^3

$$C_k = 0.16, \text{ constant for pool boiling}$$

Strictly speaking, the flooding analogy used to obtain this relation is applicable only to one-dimensional flow associated with boiling from a flat heated surface of infinite extent.

3.1 General

In order to study the performance of a compact two-phase loop thermosyphon, an experimental facility has been designed, fabricated and installed in the Heat Transfer Laboratory of BUET. A detailed description of the thermosyphon, heating systems, measurement system is presented in the subsequent sections of this chapter.

3.2 Experimental Setup

A schematic diagram of the experimental setup is shown in Fig. 3.1, which consists mainly of loop thermosyphon (evaporator, condenser and copper tubing), heat supply system, and measurement systems. Three different evaporator surfaces having enhanced structure are considered in this study. Three different working fluids are also used to transport heat from evaporator to condenser. These are described briefly in the following sections.

3.2.1 Loop Thermosyphon

A thermosyphon is a device consisting of evaporator, condenser and adiabatic sections. In this loop type one we experimented with the condenser is placed at a higher elevation with respect to the evaporator for liquid return by gravity (as shown in Fig. 3.1) through copper tubing.

Evaporator Section: A schematic diagram of the evaporator section is shown in Fig. 3.2. It is a mild steel enclosure made from a circular cross-sectional hollow cylinder with top and bottom flanges welded there. Proper fittings and provisions are

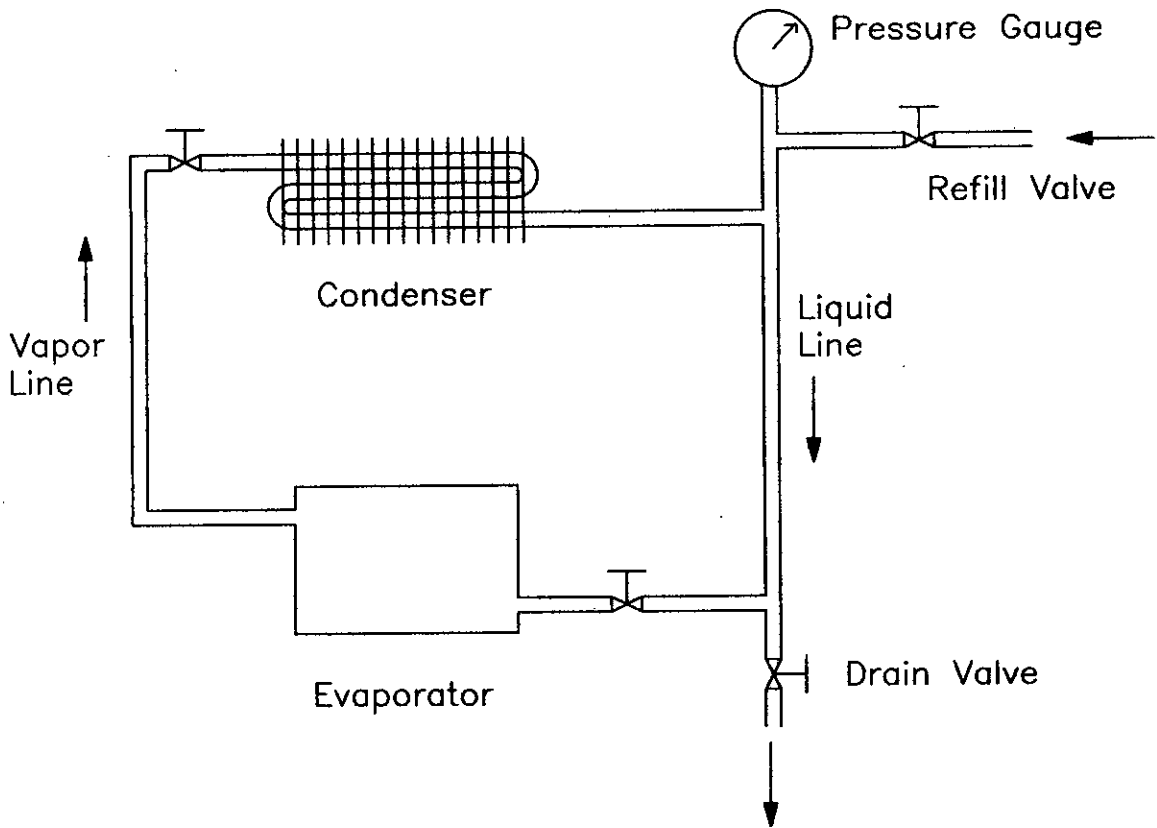


Fig. 3.1 Schematic diagram of two-phase thermosyphon

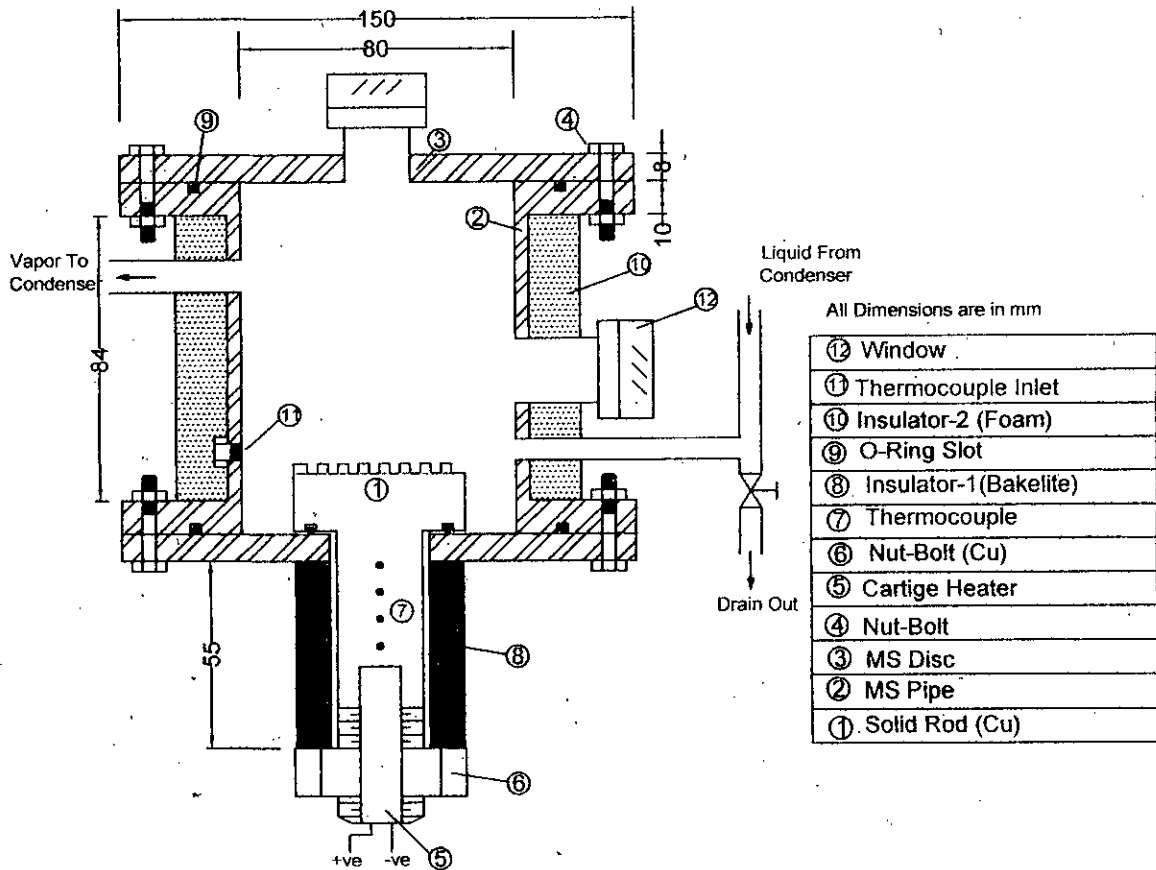


Fig. 3.2 Evaporator section

there so that liquid cannot leak out of it and boiling can be observed clearly. It has one vapor outlet port, condensed liquid inlet port and two looking windows. All the body of the evaporator section is properly insulated with glass-wool and asbestos tape. One thermocouple is embedded inside the enclosure to measure the temperature of boiling liquid.

Condenser Section: A line diagram of condenser is shown in Fig. 3.1. It is of tube-in-fin type and is cooled by air. Aluminum fins (104 mm x 80 mm x 0.8 mm thickness) are fixed to a bent copper tube (6 mm ID and 1.0 mm thick at 8 mm spacing). The total number of fins is 24. It was not possible for us to fix the fins with copper tubes to provide a solid metallic contact.

Copper Tubing: It consists mainly of vapor line and condensate line. The former one is insulated and have larger dimension and fittings (valves etc.). Vapor line is from evaporator top port to condenser top port and liquid line is from condenser bottom port to evaporator bottom port. Four valves are fixed in the whole system. One is in between evaporator and condenser, next one is in after condenser for filling the fluid or reflux the condenser, next one is in under side of the system for drain out the fluid when need and last one is in between condenser in the liquid line. A pressure gauge (range from -30 inch. of Hg to 250 psig) is attached to the loop near the exit of the condenser to monitor the loop pressure and the pressure during the leak test of the setup (in vacuum and under pressure). A plate fin condenser is employed with the aluminum fin spacing optimized for operation in convection.

3.2.2 Evaporator Surface

Three types of evaporator surfaces are experimented in this study. Namely evaporator with plane surface (HRO), evaporator with integrated rectangular fins (HRI), evaporator with integrated cross fins (HR+). The evaporator assembly is shown in Fig. 3.3. The dimensions of the evaporator and thermocouple location are also shown in the figure. The schematic of all the surfaces of evaporator are shown in Fig. 3.4. All the surfaces are of similar dimension and of same material. The differences are in enhanced structures.

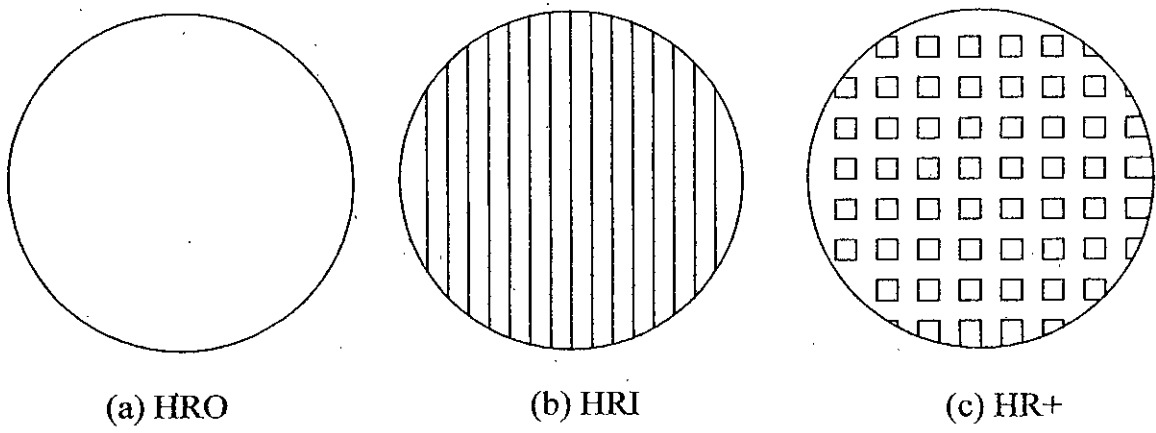


Fig.3.4 Evaporator Surface

3.2.3 Heat Supply System

The heat supplied to the evaporator through Joule heating. A cartridge heater is fitted in the evaporator as shown in Fig. 3.2 – 3.3. Regulated electrical energy is supplied to the heater during the experiment. The maximum heater capacity is 500 W.

3.2.4 Measurement System

During experiment, the power supplied to the heater was measured by measuring voltage and current by voltmeter and Clipon-meter respectively. At the same time, temperatures at the location mentioned in Fig. 3.2 are measured by thermocouples and meter assembly. all the measured values are recorded manually.

3.2.5 Working Fluids

Heat transfer fluids carry heat from cartridge heater via evaporator surface. The fluids used in this study are Methanol (CH_3OH), Ethanol ($\text{C}_2\text{H}_5\text{OH}$) and Acetone (CH_3COCH_3). Fluids heated up in the evaporator, boils and vapor pass to condenser through copper tubing. After condensing the condensed liquid return to condenser by gravity. Some important properties of these three working fluids are mentioned below.

Methanol: Methanol or Methyl alcohol is a colorless, flame-able liquid. Pure methanol melts at 175.2°K boils at 327.85°K and molecular weight is 32.00. Thermophysical properties of methanol are given in Table 3.1. The commercial use of methanol has sometimes been prohibited. Large amount of it are used in the synthesis of formaldehyde Methanol is often called wood alcohol because it was once produced chiefly as a by-product of the destructive distillation of wood. Methanol is also used as a solvent for varnishes and lacquers as antifreeze and as gasoline extender in the production of gasohol.

Ethanol: Ethanol or Ethyl alcohol can be produced by fermentation of carbohydrates, which occur naturally and abundantly in some plants like sugarcane and from starchy materials like potatoes and corn. It boils at 351.3°K. Ethanol and

Methanol both are also used as fuels in SI Engines. Important properties of ethanol are given in Table 3.1.

Acetone: Acetone is a flame-able, colorless liquid. It is the simplest of the organic chemical called ketones. It is completely soluble in water. It has a mild pleasant odor. It boils at 329°K and melts at 178°K . Enormous quantities are used as solvents for cellulose acetate in the production of rayon and as a gelatinizing for explosive. Acetone is also used as an ingredient in lacquer solvent and to dissolve gums and resins. It is used as a solvent in formulations for surface coatings and related washes and thinners. Important properties of Acetone are given in Table 3.1.

Table-3.1: Properties of the Working Fluids at Atmospheric Pressure.

Name of Working Fluid	Density of liquid at T_{sat} ρ_l (kg/m ³)	Density of vapor at T_{sat} ρ_v (kg/m ³)	Boiling Point T_{sat} °K	Specific heat of liquid at T_{sat} C_{pl} (kJ/kg.K)	Specific heat of vapor at T_{sat} C_{pv} (kJ/kg.K)	Latent heat of vaporization at T_{sat} h_{fg} (kJ/kg)	Liquid viscosity μ_l (μ Ns/m ²)	Vapor viscosity μ_v (μ Ns/m ²)	Prandtl number of liquid (Pr_l)	Surface tension of vapor liquid interface σ (mN/m)
Acetone CH ₃ COCH ₃	750.0	2.23	329.25	2.28	1.41	506.0	235.0	9.4	3.77	18.40
Ethanol CH ₃ CH ₂ OH	757.0	1.435	351.30	3.00	1.83	963.0	428.7	10.4	8.37	17.7
Methanol CH ₃ OH	751.0	1.222	337.50	2.88	1.55	1101.0	326.0	11.1	5.13	18.75

Ref. Carry (1994)

3.3 Experimental Procedure

Before starting the experiment the whole system is examined for leak proof for both vacuum and pressurized condition. When it is confirmed that the system is fully leak proof then evaporator is charged with the relevant fluid. About two-third of the volume is charged. Each experimental run is preceded by a degassing operation. The vent valve is opened and a very high heat flux ($\sim 700 \text{ kW/m}^2$) is supplied to the heater. The boiling is continued for one hour. Then the heater is switched off and the test section is allowed to cool down about two hours. During the cool down the vent valve is kept closed. By this time the system reached room temperature, pressure gauge indicates negative pressure. This procedure ensured that the dissolved gas concentration of non-condensable is uniform in all time if not zero. Now the setup is ready for experiment. The vent valve is again opened just before the experiment. For ensuring atmospheric conditions the vent valve is kept open during the experiments. The initial heat input in this experiment is 5W and increased in steps of 1W until the fluid gains boiling temperature. Subsequently, the increments are increased to about 5W. After reaching the boiling temperature, temperature of four points e.g. T_{x1} , T_{x2} , T_{x3} , T_{x4} of heater geometry; voltage reading from multi-meter, current reading from digital Clip-on meter are recorded carefully. The test is continued until the surface temperature is exceeded 85°C (a maximum limit for most commercial electronics) for each working fluid, a set of procedure is always followed. Again for each experimental run, similar arrangements are taken. For particular working fluid and condition, three sets of data are recorded for ensuring reproducibility of the data.

3.3.1 Data Collection Procedure

In every step the temperatures are monitored continuously and the heat input incremented after the system reached steady state. When temperature rise 0.1°C in a span of 10 minutes or thermometer shows lessen the temperature then reading is taken.

3.3.2 Data Reduction Procedure

As mentioned earlier, electrical power supply and temperatures are measured during each experimental run. From these data, boiling curves are drawn for different working fluids and heater surfaces.

Heat flux is calculated using the following equation:

$$q = (V I \cos\theta - q_L) / A \quad (3.1)$$

where

V = Voltmeter reading, Volt

I = Clip-on meter reading, ampere

$\cos\theta$ = power factor = 0.85

q_L = heat loss from the heater assembly \approx 2% as per heat transfer calculation
Appendix-B

A = cross sectional area of the copper rod conduction heat to the evaporator surface, m^2

Again, the wall superheat is calculated using the following relation

$$\Delta T = T_{X_4} - T_{sat} \quad (3.2)$$

where,

T_{X_4} = Temperature of the top thermocouple. As the evaporator surface temperature was not possible to measure / estimate correctly.

T_{sat} = Saturation temperature of the working fluid.

Boiling heat transfer coefficient, h was also calculated using the following relation.

$$h = \frac{q}{\Delta T} \quad (3.3)$$

In the next chapter, these are well explained analyzed and compared with existing results.

RESULTS AND DISCUSSIONS

4.1 General

During experiment temperatures of four points (T_{x1} , T_{x2} , T_{x3} , T_{x4}) on the different evaporator surfaces are measured for the three different working fluids (Acetone, Ethanol and Methanol) for various heat flux input. The collected data are shown in Appendix-A. Using these data boiling curves for various evaporator surfaces and working fluids, are plotted. Rohsenow correlation and Stephan and Abdelsalam correlation are also plotted to make a comparison with the present experimental data. All the graphs are clearly explained and analyzed in this chapter. CHF values for three different fluids at the same working condition are calculated by Kutateladze correlation and plotted in these graphs.

4.2 Boiling Curves (q vs ΔT)

Boiling curves of plain surface (HRO) with Acetone as the working fluid for three experiments are shown in the Figure 4.1. The dotted line indicates the heat Stephan and Abdelsalam correlation, dashed line indicates Rohsenow correlation and solid line indicates Kutateladze correlation for Critical Heat Flux (CHF). About 25°C -wall superheat, the heat flux found 0.10 MW/m^2 . At this point heat flux from Stephan and Abdelsalam correlation is 0.19 MW/m^2 and from Rohsenow correlation is 0.11 MW/m^2 . At the point 18°C wall superheat, heat flux from Stephan and Abdelsalam correlation is the same of this experimental value and at the point 22°C wall superheat the heat flux from Rohsenow correlation is the same of the experimental value.

Boiling curves for the surface HRI with Acetone as the working fluid are shown in figure 4.2. In this case the results from three experiments are almost same. At the point 26°C wall superheat, heat flux found 0.24 MW/m^2 . At this point heat flux from Stephan and Abdelsalam correlation is found by calculation 0.22 MW/m^2 and from Rohsenow correlation is found 0.12 MW/m^2 . These values are also less than the value which is found from the experiment. At the point about 20°C wall superheat flux from Stephan and Abdelsalam correlation is the same of the experimental value.

Boiling curves for the surface of HR+ with Acetone for three sets of experiment are shown in figure 4.3. In this case the results from three experiments are almost same. At the point $\Delta T \sim 25^{\circ}\text{C}$, heat flux is found 0.20 MW/m^2 . At this point heat flux from Stephan and Abdelsalam correlation is 0.20 MW/m^2 which is same as the result obtained in the present experiment and heat flux from Rohsenow correlation is 0.12 MW/m^2 which is less than the experimental result.

Boiling curves for the plain surface HRO with Ethanol as the working fluid for three experiments are shown in figure 4.4. At 20°C wall superheat value, heat flux is found from 1st experiment is 0.19 MW/m^2 . At this point heat flux from Rohsenow correlation is 0.14 MW/m^2 and from Stephan & Abdelsalam correlation is 0.15 MW/m^2 . The experimental result is higher than from both correlation.

Boiling curves for the surface HRI with respect to Ethanol for three experiments are shown in figure 4.5. At the point of 20°C wall superheat, the heat flux is found from the experiment is 0.25 MW/m^2 . From Rohsenow correlation this value is 0.14 MW/m^2 and from Stephan and Abdelsalam correlation this value is 0.15 MW/m^2 . The heat flux values which are found from the present experiment are about two times higher than the calculated values from the correlation, because these correlation are for plain evaporator surface.

Boiling curves for evaporator surface HR+ with Ethanol are given in the figure 4.6. In this figure the results of three experiments are almost same. Heat flux at the point of 14°C wall superheat is found 0.28 MW/m^2 . From Rohsenow correlation this value is about 0.05 MW/m^2 and from Stephan and Abdelsalam correlation this value is 0.054 MW/m^2 . In this case experimental value is about 5 times higher than the calculated heat flux from the correlations.

Boiling curves for Methanol with evaporator surface HRO are shown in figure 4.7. At 20°C wall superheat i.e. at the 85°C wall temperature, heat flux is found 0.1 MW/m². At this point heat flux from Rohsenow correlation is 0.23 MW/m² and from Stephan and Abdelsalam correlation is 0.12 MW/m². Hence the heat flux of plain surface with Methanol is about 50% of the Rohsenow correlation and almost same as Stephan and Abdelsalam correlation.

Boiling curves for the evaporator surface (HRI) with Methanol are shown in the figure 4.8. At the point 16°C wall superheat the heat flux is found from the experiment 0.23 MW/m². At the same point heat flux from Rohsenow correlation is 0.12 MW/m² and from Stephan and Abdelsalam correlation is 0.06 MW/m². The heat flux from experiment is about 2 times higher than the value found from Rohsenow correlation and 4 times higher than the value found from Stephan and Abdelsalam correlation.

Pool boiling curves for the evaporator surface HR+ with Methanol as working fluid are shown in figure 4.9. At the point of wall superheat 15°C, the heat flux is found 0.17 MW/m². The heat flux from Rohsenow correlation at this point is 0.1 MW/m² and from Stephan and Abdelsalam correlation is 0.05 MW/m². Hence heat flux found from the experiment is about 1.7 times higher than that Rohsenow correlation and 3.4 times higher than that of Stephan and Abdelsalam correlation.

4.3 Effect of Evaporator Surface on Boiling Curves

Boiling curves for three types of evaporator surfaces, HRO, HRI and HR+ with Acetone as working fluid are given in the figure 4.10. In this curves higher heat flux is obtained for the surface HR+. At the point $\Delta T = 20^\circ\text{C}$ the heat flux for HR+ is 0.11 MW/m². For the surface HRI this value is approximate same of the value for HR+. For the surface HRO this value is 0.8 MW/m². Critical heat flux for Acetone from Kutateladze is found 0.412 MW/m² and is shown by the solid line.

Boiling curves for three types of evaporator surfaces HRO, HRI and HR+ with Ethanol as working fluid are given in the figure 4.11. In these curves higher heat flux is obtained for surface HR+. At the point $\Delta T = 14.6^\circ\text{C}$, the heat flux for HR+ is 0.27 MW/m², for the surface

HRI this value is 0.17 MW/m^2 and for the plain surface (HRO) the value is $\sim 0.09 \text{ MW/m}^2$. Critical heat flux CHF for Ethanol from Kutateladze correlation is found 0.624 MW/m^2 and is shown by the solid line.

Boiling curves for three types of Evaporator surfaces with Methanol as working fluid are given in the Figure 4.12. Highest heat flux is obtained for the surface HRI and lowest is obtained for the surface HRO. At the point of 17°C wall superheat the heat flux for HRO is 0.09 MW/m^2 , this value at the same point for HR+ is 0.22 MW/m^2 and for the surface HRI is 0.26 MW/m^2 . Critical Heat Flux (CHF) for Methanol from Kutateladze Correlation is found 0.667 MW/m^2 .

4.4 Effects of Working Fluid on Boiling Curves

Boiling Curves for three different fluids on the same evaporator surface HRO are given in the Figure 4.13. The highest heat flux is found for this surface with Ethanol. At the point $\Delta T \sim 20^\circ\text{C}$ the Heat Flux is found 0.18 MW/m^2 for Ethanol; 0.13 MW/m^2 for Methanol and 0.08 MW/m^2 for Acetone. Among these three fluids Ethanol gives the best performance for plain surface. At this point heat flux from Stephan and Abdelsalam correlation is 0.10 MW/m^2 and from Rohsenow correlation is 0.045 MW/m^2 .

Boiling curves for three types of working fluids with the evaporator surface (HRI) are given in the figure 4.14. The highest heat flux is found for this geometry with Methanol and lowest heat flux is found for Acetone. At the point of 85°C wall temperature for Methanol heat flux is 0.30 MW/m^2 , for Actone that value is 0.13 MW/m^2 and for Ethanol that value is 0.23 MW/m^2 .

Boiling curves for three types of working fluids with the evaporator surface HR+ are shown in figure 4.15. In this case Ethanol belongs to highest performance. At the point of $\Delta T = 15^\circ\text{C}$ the heat flux is found for Ethanol 0.275 MW/m^2 , for Methanol 0.18 MW/m^2 , for Acetone 0.06 MW/m^2 . Heat flux for Ethanol on the surface HR+ is about 1.5 times higher than of Methanol and about 4.5 times higher than of Acetone at the point of $\Delta T = 15^\circ\text{C}$.

4.5 Boiling Curves (h vs. ΔT)

Variation of heat transfer coefficient, h for three evaporator surfaces with the effect of three working fluids are shown in the Fig. 4.16 – 4.24. In Fig. 4.16 and 4.18 effect of HRO surface HR+ surface with and with Acetone on boiling are shown. The heat transfer coefficient increased with the increase of wall superheat. But in Fig. 4.17 for HRI surface heat transfer and then it increased with the increase of wall superheat. Figure 4.21 shows Ethanol with HRI surface, heat transfer coefficient decreased with the increasing of wall super heat. But the rate of increase of heat flux is less than the rate of increase of wall superheat. Fig. 4.23 shows the effect of HRO surface and Methanol on heat transfer coefficient h . Heat transfer coefficient decreased up to $\Delta T = 20^\circ\text{C}$. In Fig. 4.23 heat transfer coefficient decreases from the beginning to the end of the experiment but rate of variations are not always same. In Figure 4.24 variation of heat transfer coefficient, h for HR+ surface and Methanol is shown. For the 1st reading heat transfer coefficient decreases from 0.015 to 0.012 $\text{MW/m}^2 \text{ }^\circ\text{C}$ in between $\Delta T = 5.6 - 11^\circ\text{C}$, and then increases and again decreases and the reason is not yet understood. The 2nd and 3rd also show the same characteristics.

4.6 Effect of Evaporator Surface on h :

Effects of evaporator surface on heat transfer coefficient, h for three working fluids are given in Fig. 4.25 – 4.27. In Fig. 4.25 shows that for the surface HRI and working fluid Acetone, heat transfer coefficient, h falls from h falls from $0.0087 \text{ MW/m}^2 \text{ }^\circ\text{C}$ to $0.0053 \text{ MW/m}^2 \text{ }^\circ\text{C}$ for the increase of ΔT from 6.7°C to 19.5°C . Beyond this, h starts to rise up to $0.0096 \text{ MW/m}^2 \text{ }^\circ\text{C}$ for $\Delta T = 28.7^\circ\text{C}$. HRI surface for Acetone shows higher heat transfer coefficient. In Fig. 4.26 shows that the surface HR+ with Ethanol gives higher heat transfer coefficient. HRO surface for Ethanol shows lower value of heat transfer coefficient than HR+ surface. In Fig. 4.27 higher heat transfer coefficient is obtained for HRI surface than the HRO surface. The rate of change of heat transfer coefficient with respect of ΔT is always changed.



4.7 Effect of Working Fluid on h:

Effects of working fluids on heat transfer coefficient h for evaporator surface HRO, HRI and HR+ are given in the Fig. 4.28 – 4.30. In Fig. 4.28 Ethanol shows the highest heat transfer coefficient. Methanol shows the middle heat transfer coefficient and Acetone shows the lowest performance. All the cases h increased with the increasing wall super heat. Figure 4.29 shows that the surface HRI with Methanol, gives high heat transfer coefficient. At the point 15°C wall superheat h for Methanol is $0.015 \text{ MW/m}^2 \text{ }^{\circ}\text{C}$, for Ethanol $0.011 \text{ MW/m}^2 \text{ }^{\circ}\text{C}$ For Acetone $0.005 \text{ MW/m}^2 \text{ }^{\circ}\text{C}$. Effects of working fluids on surface HR+ are shown in the Figure 4.30. In this Figure Ethanol shows higher heat transfer coefficient.

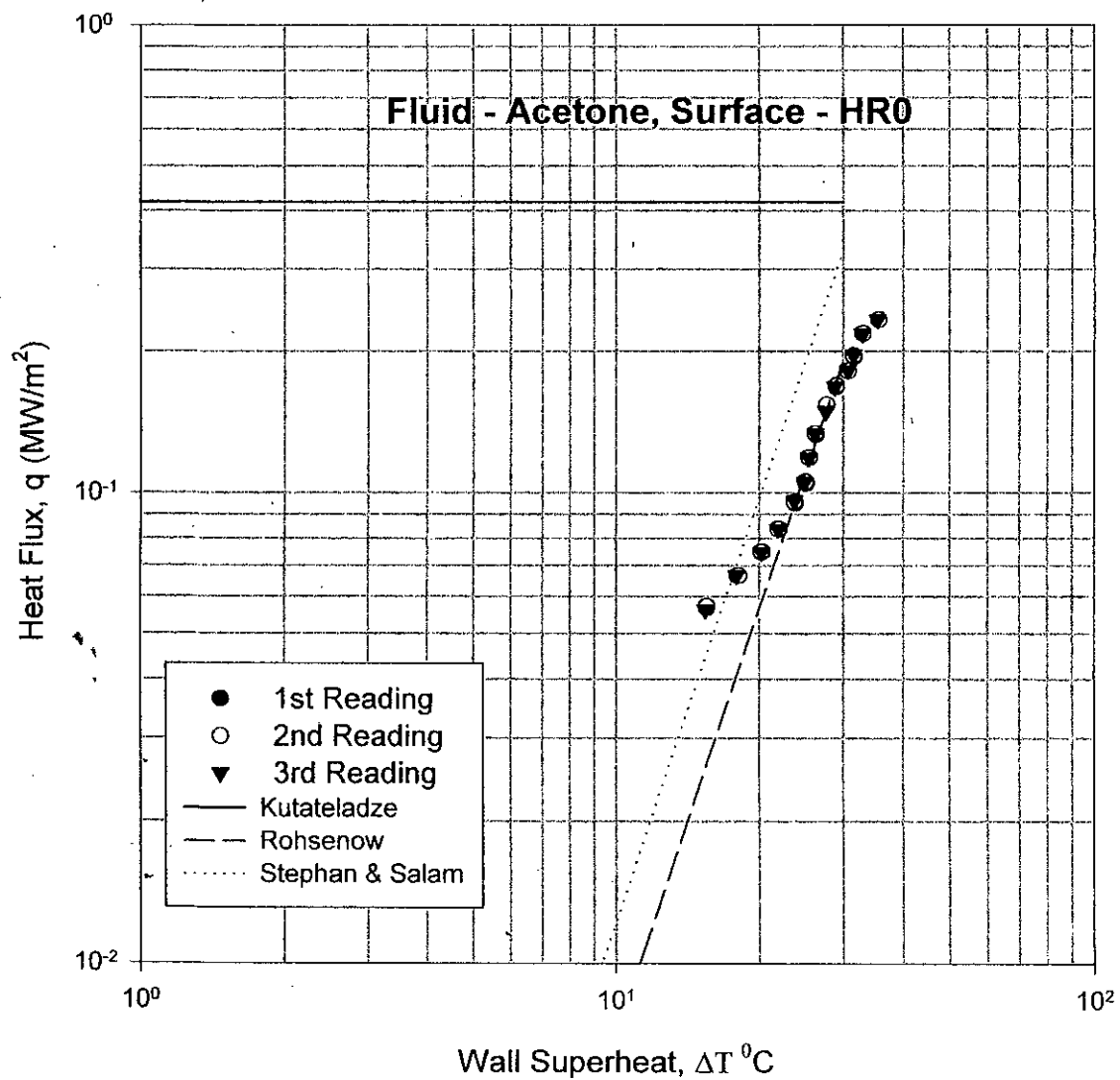


Fig. 4.1 Boiling Curves for HR0 - Acetone

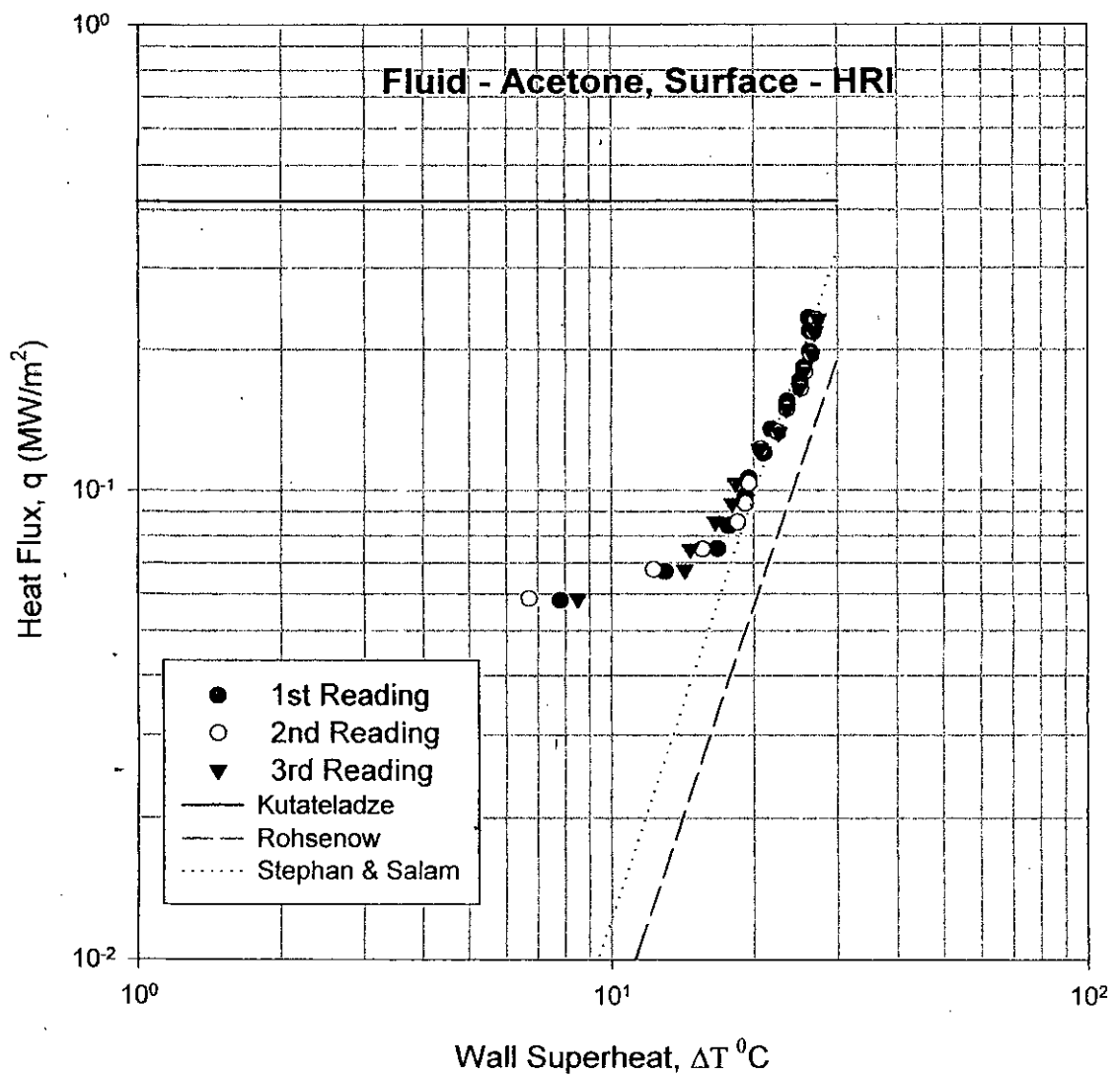


Fig. 4.2 Boiling Curves for HRI - Acetone

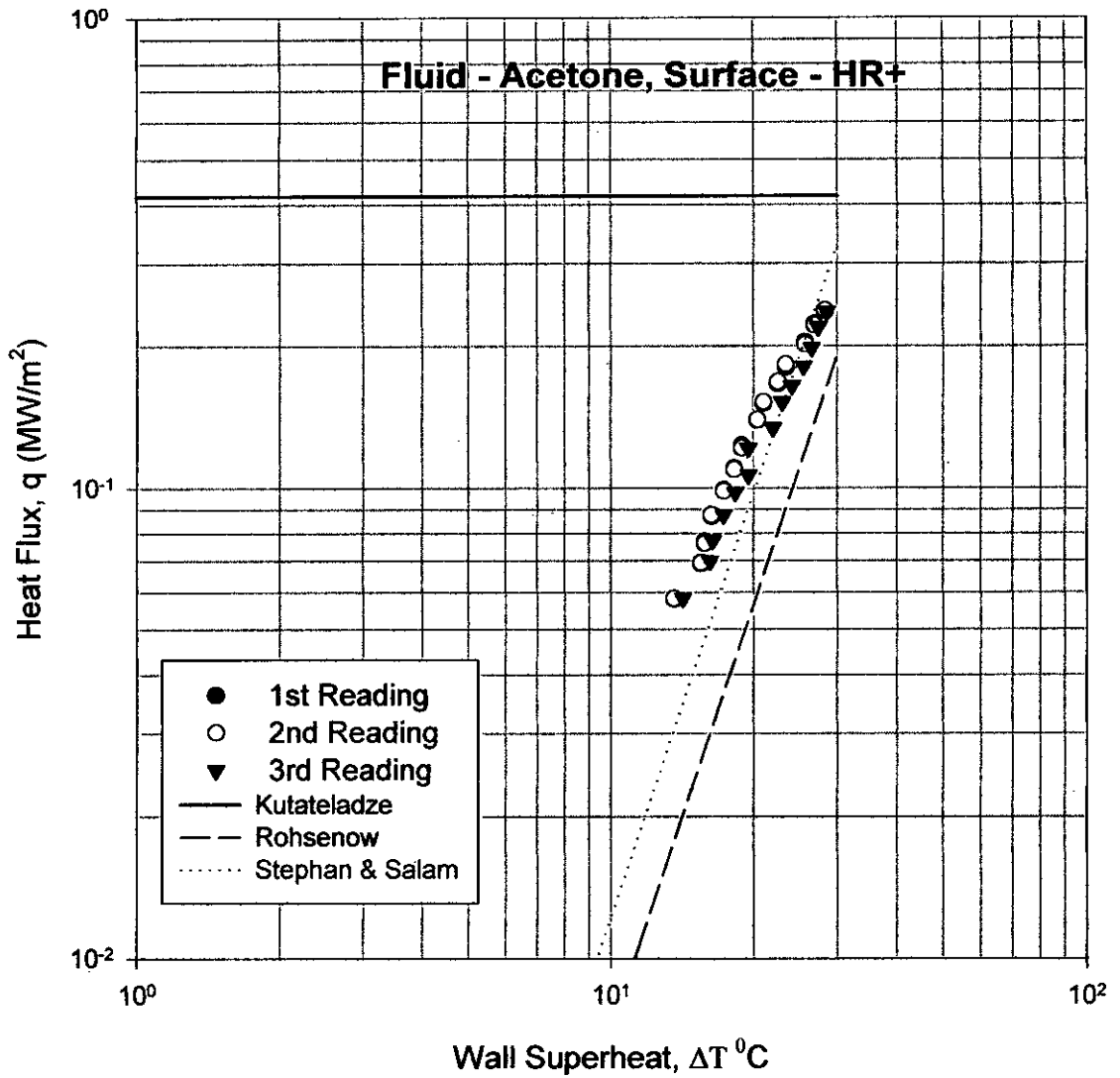


Fig. 4.3 Boiling Curves for HR+ - Acetone

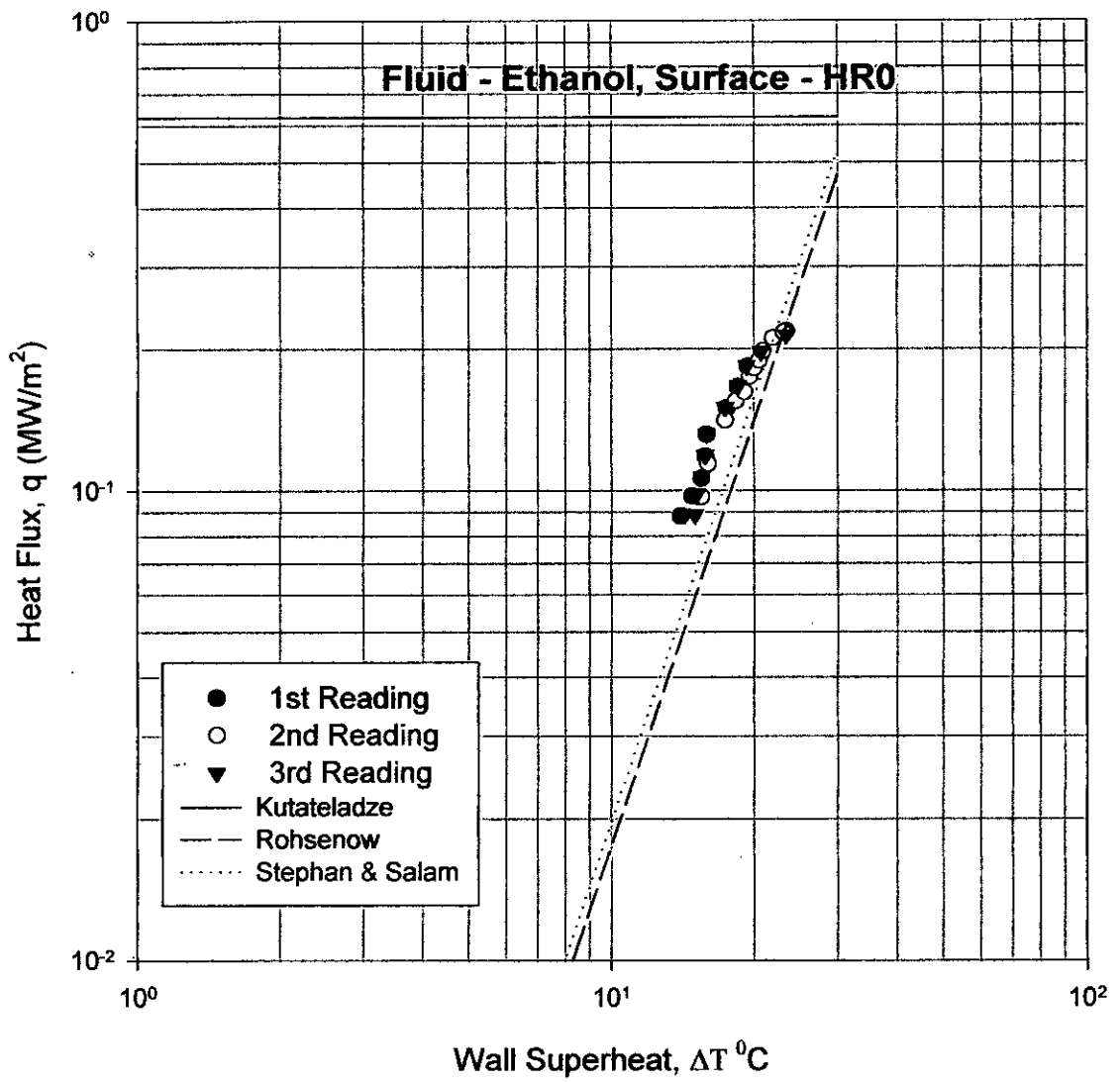


Fig. 4.4 Boiling Curves for HR0 - Ethanol

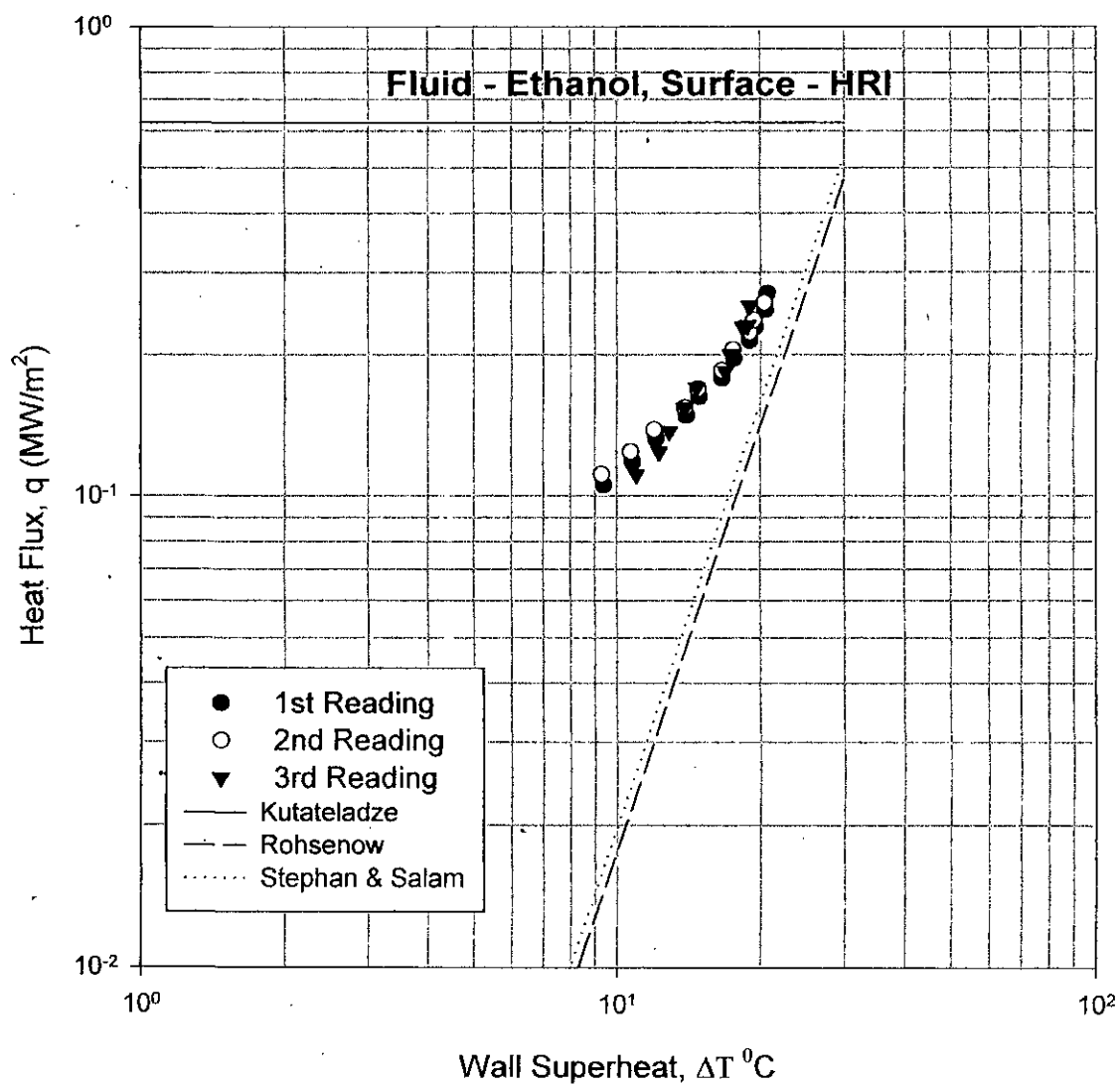


Fig. 4.5 Boiling Curves for HRI - Ethanol

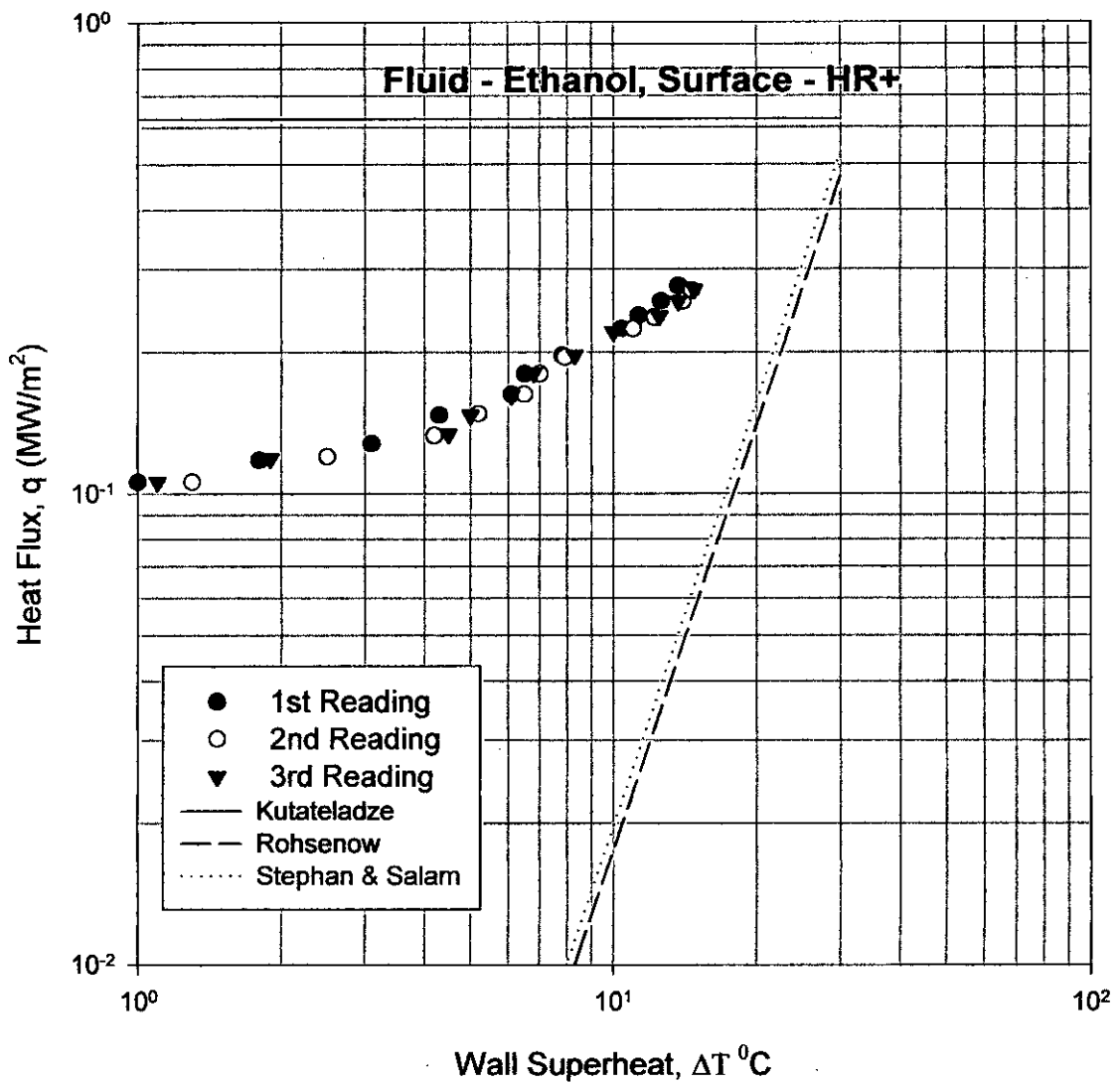


Fig. 4.6 Boiling Curves for HR+ - Ethanol

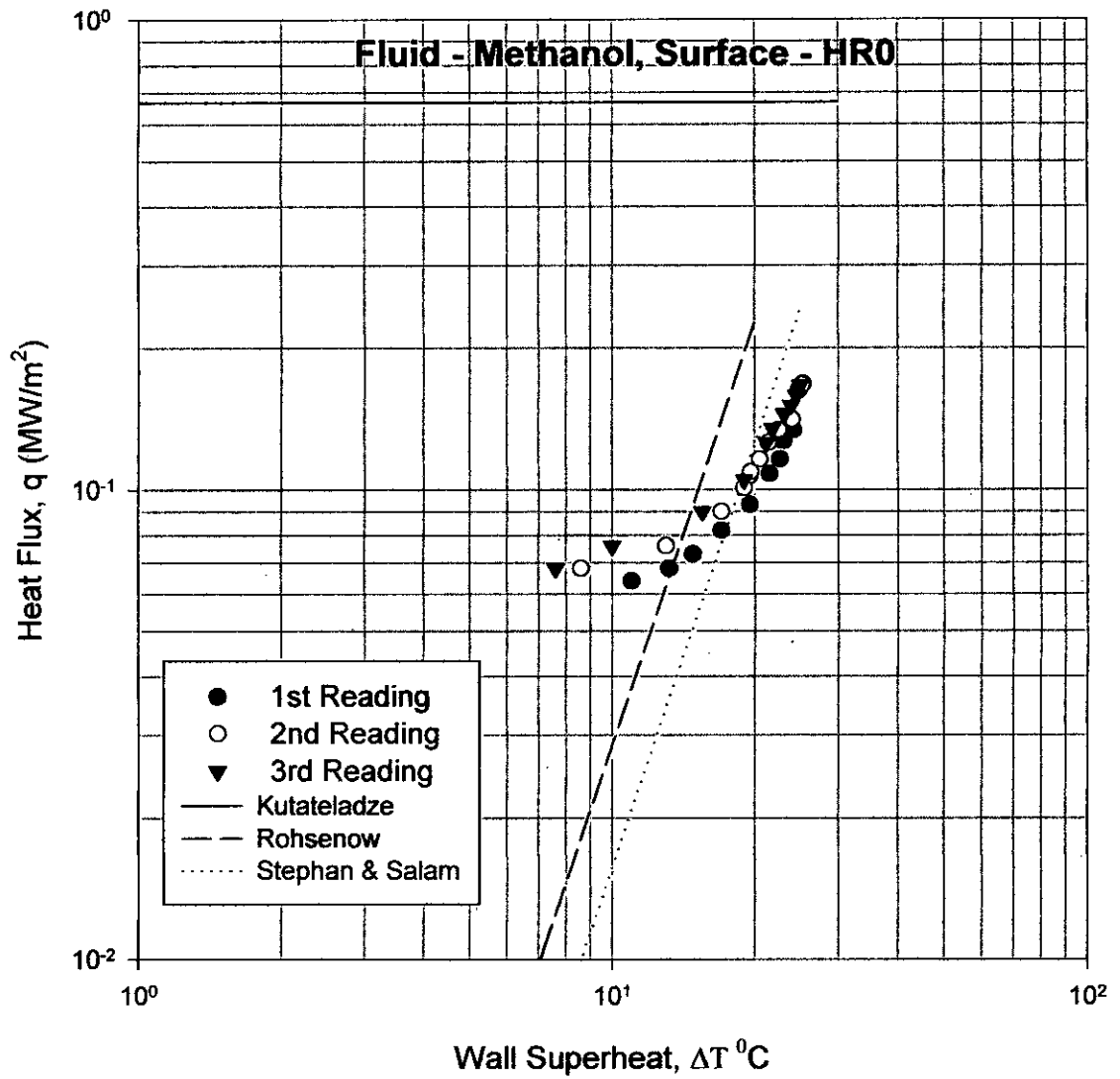


Fig. 4.7 Boiling Curves for HR0 - Methanol

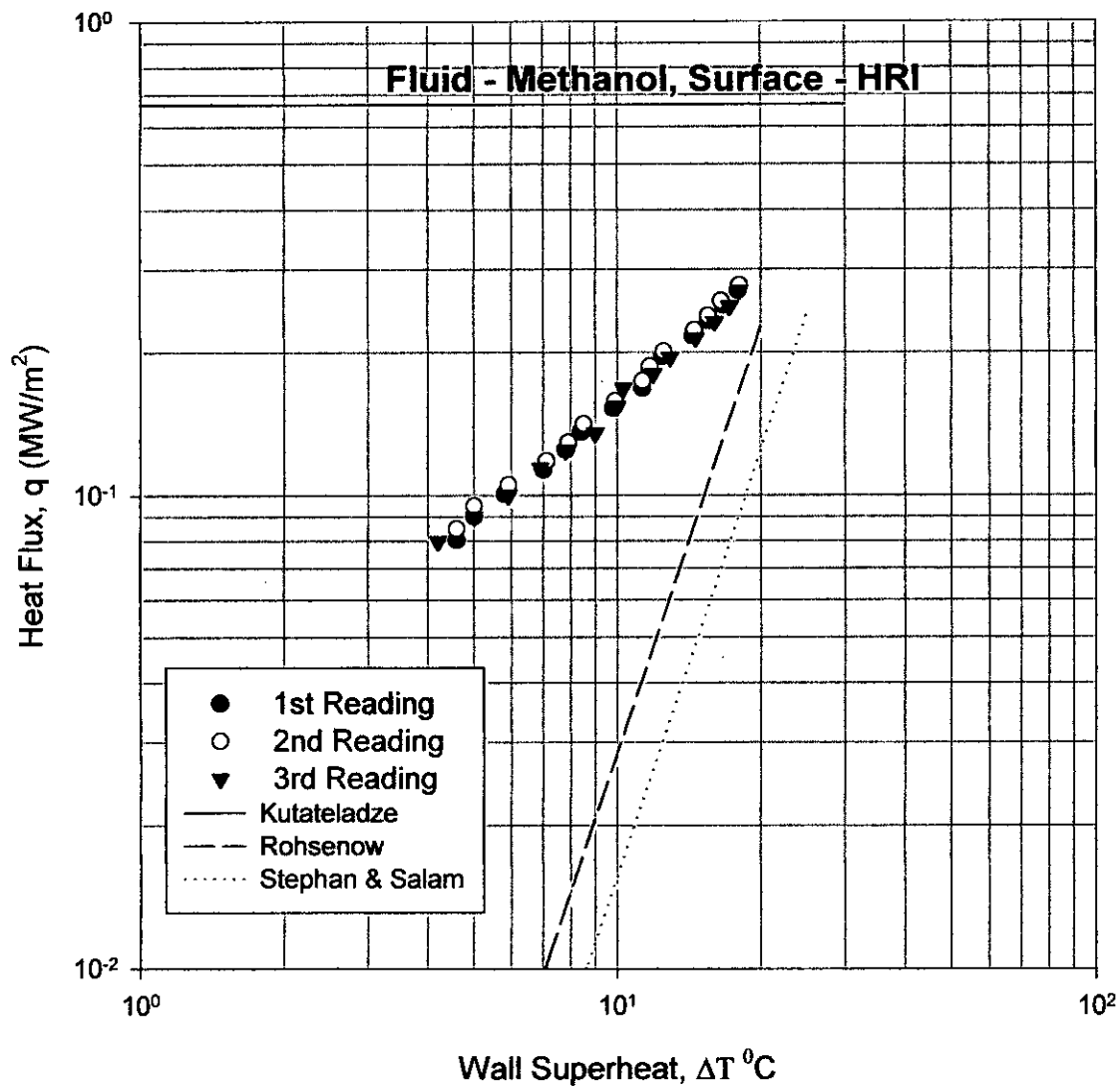


Fig. 4.8 Boiling Curves for HRI - Methanol

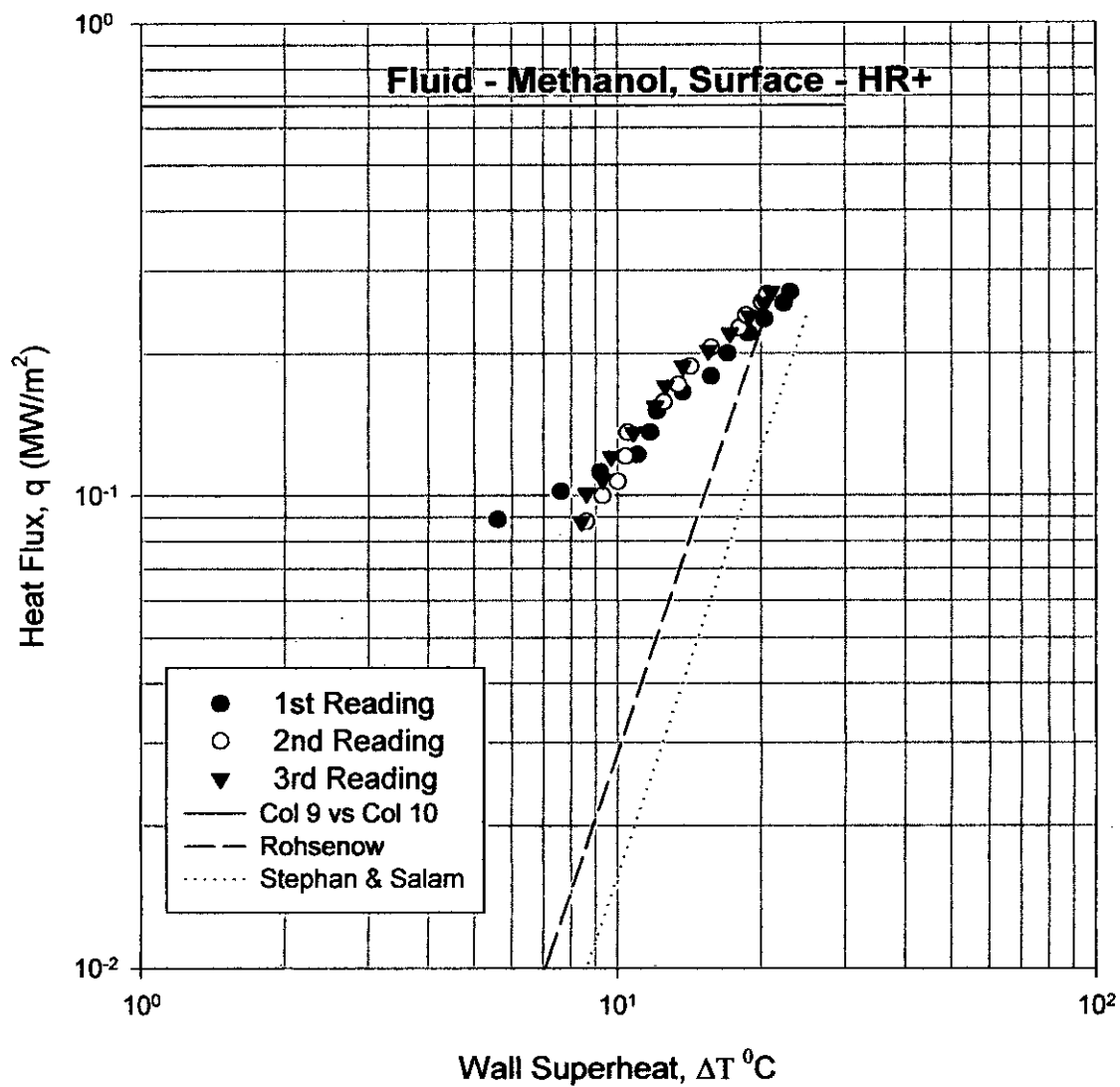


Fig. 4.9 Boiling Curves for HR+ - Methanol

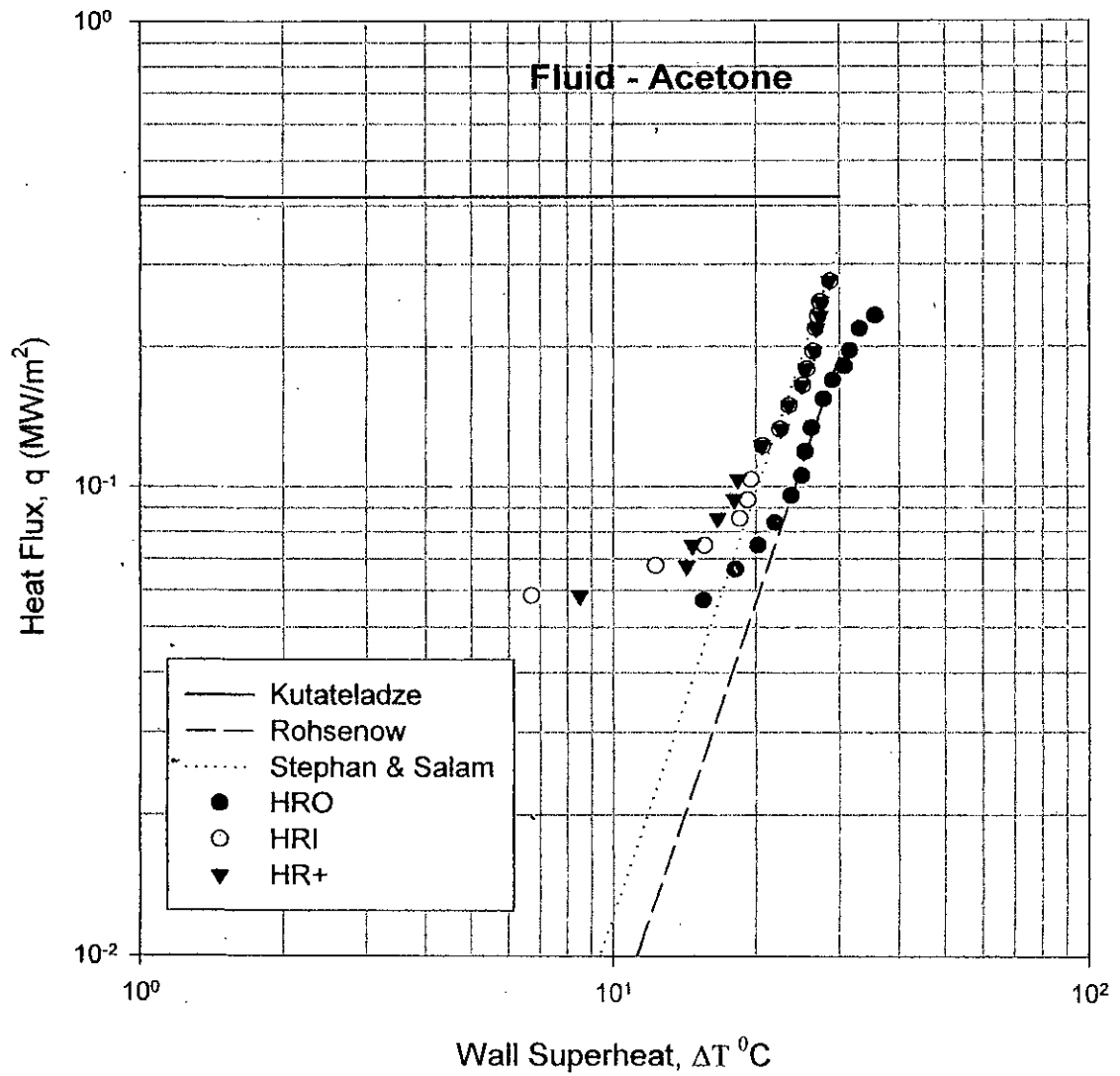


Fig. 4.10 Effects of Evaporator Surface on the boiling Curves for Acetone

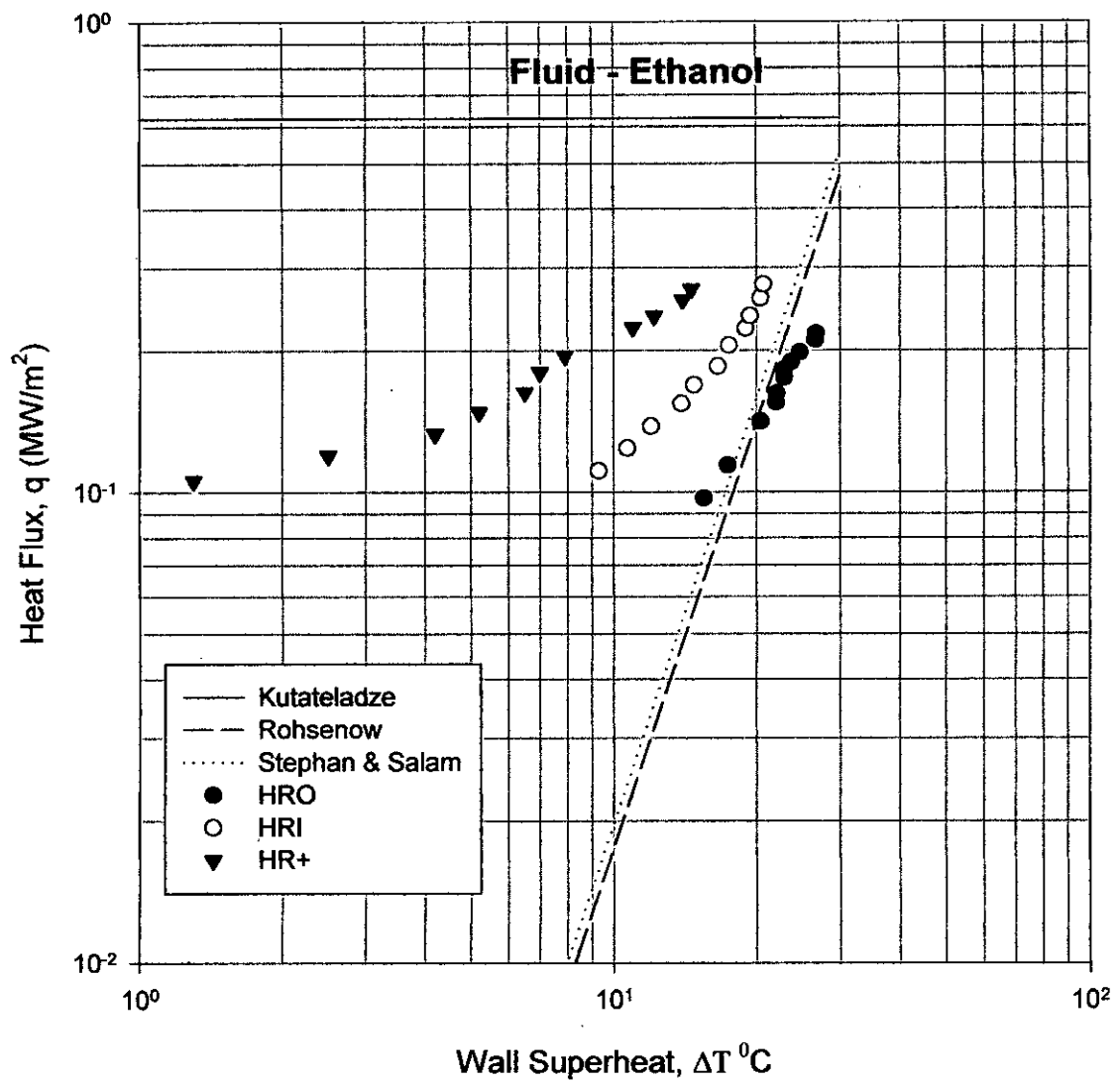


Fig. 4.11 Effects of Evaporator Surface on the boiling Curves for Ethanol

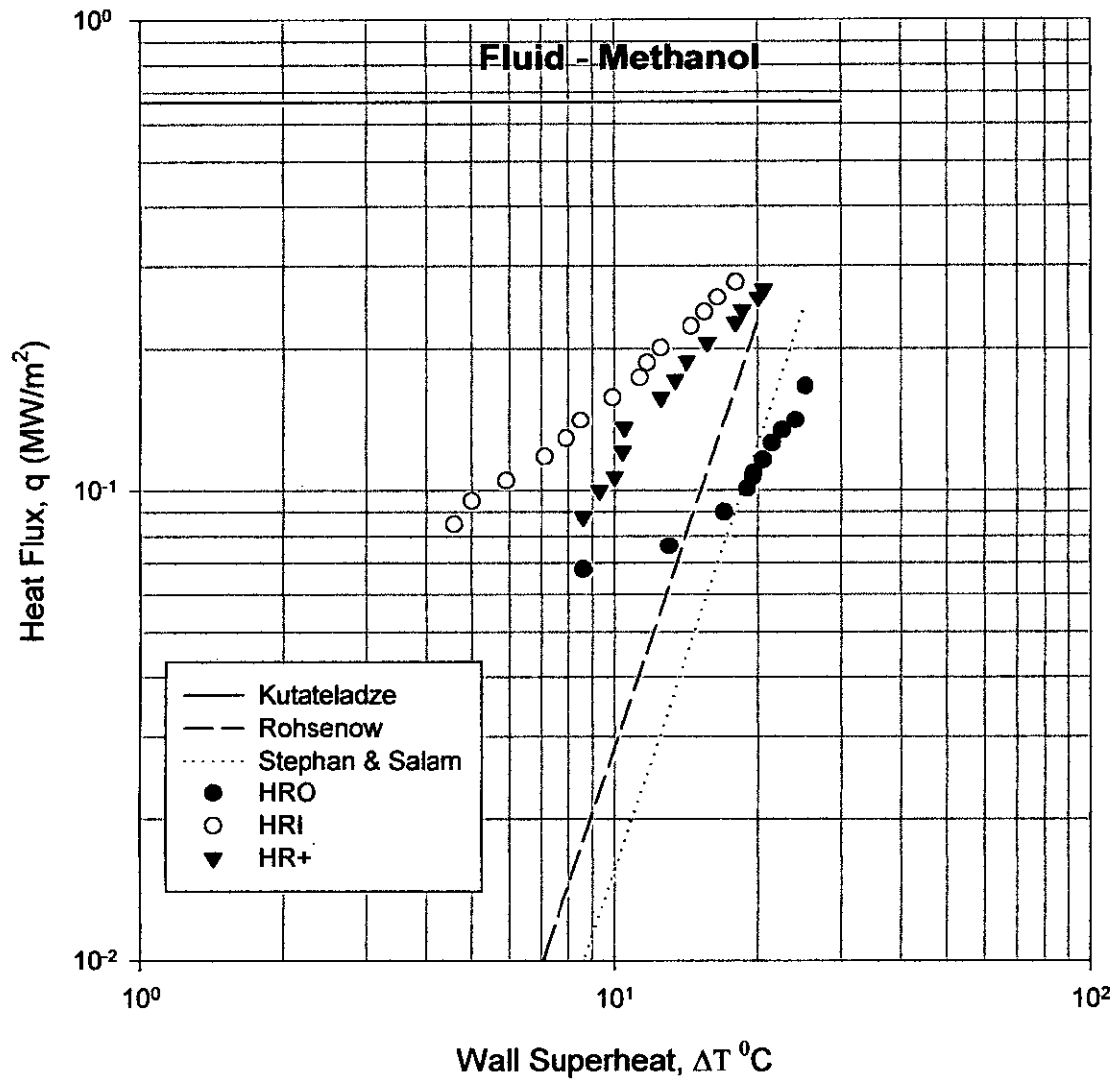


Fig. 4.12 Effects of Evaporator Surface on the boiling Curves for Methanol

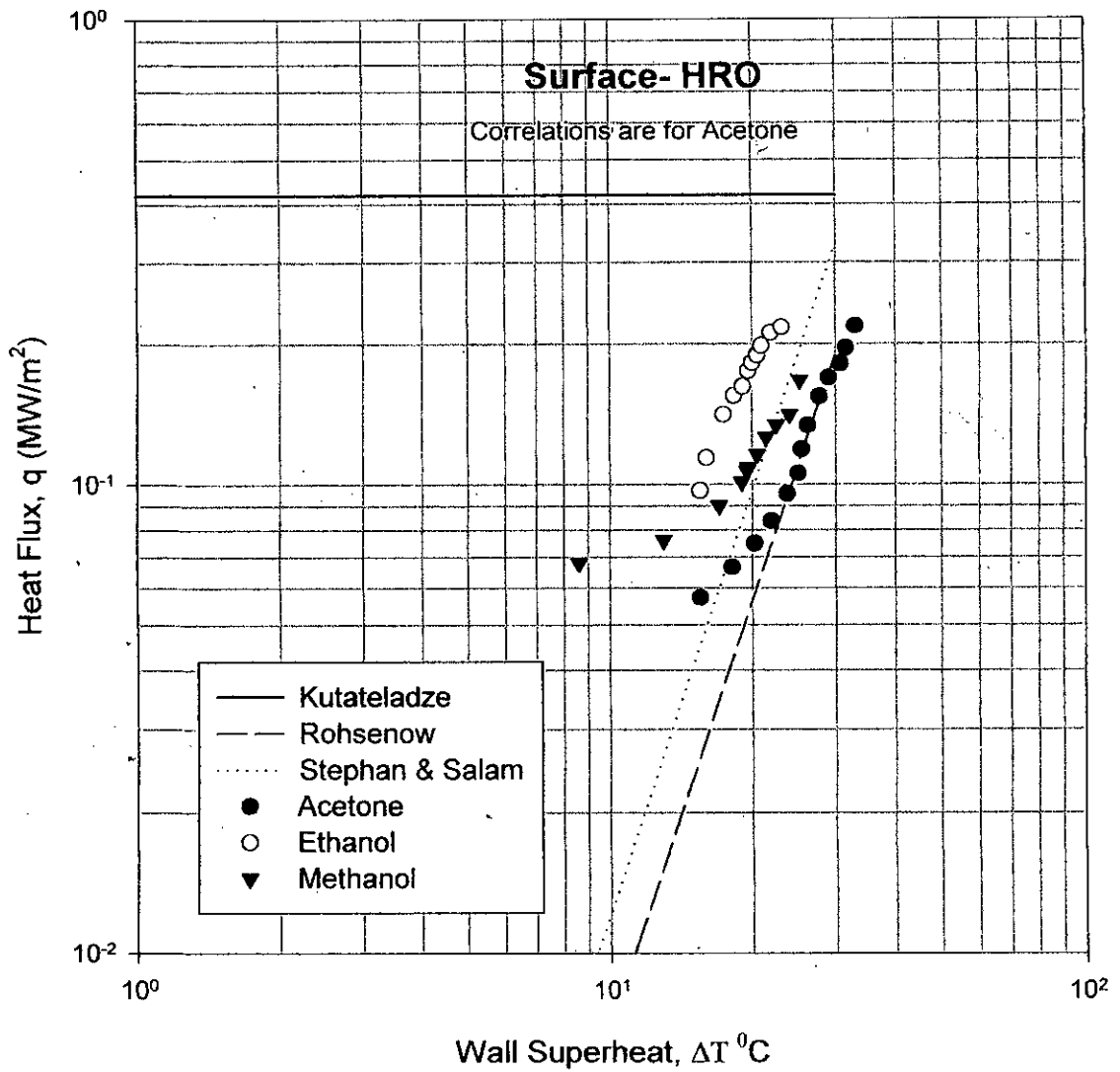


Fig. 4.13 Effects of Working Fluids on the boiling Curves for HR0

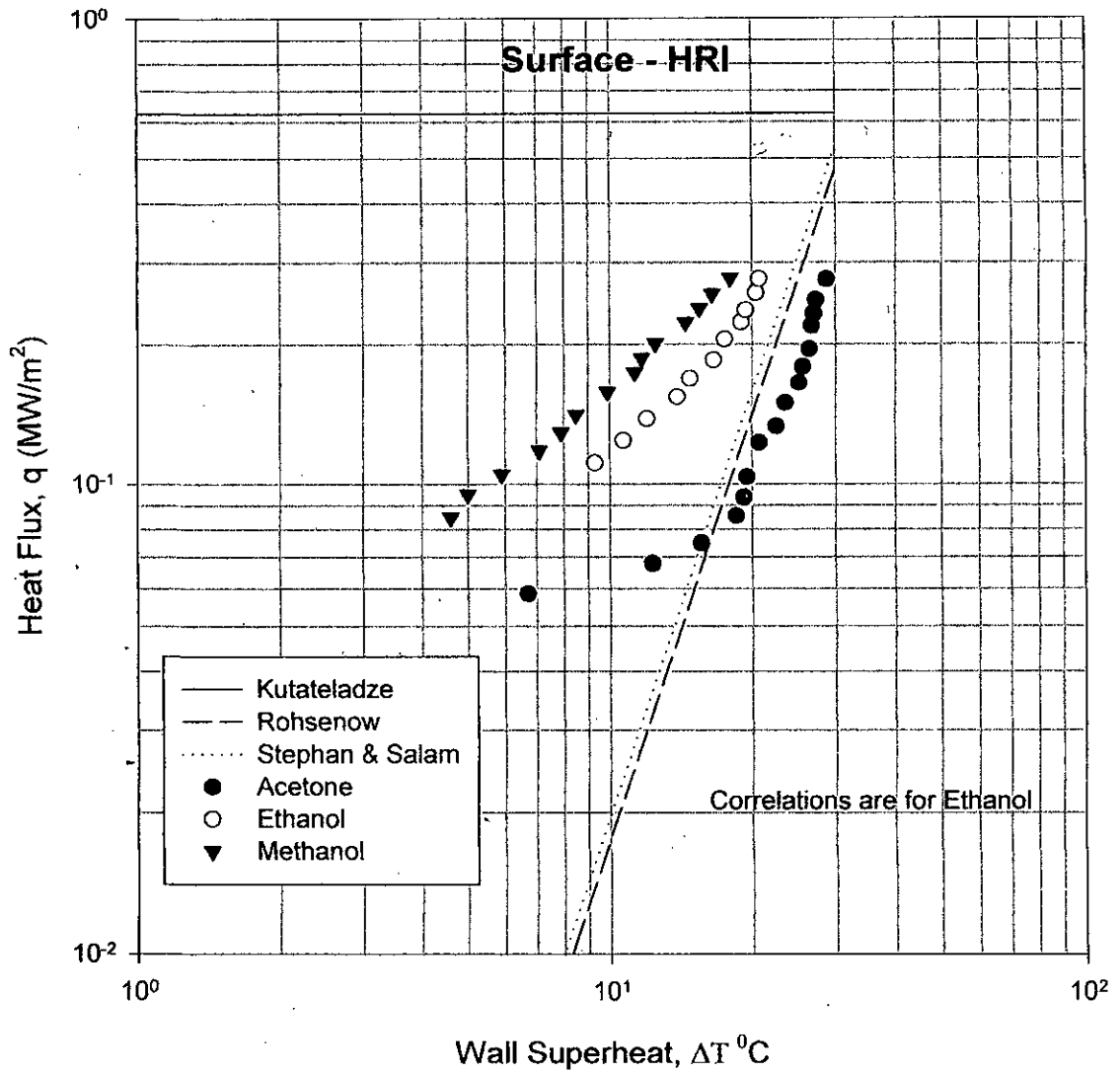


Fig. 4.14 Effects of Working Fluids on the boiling Curves for HRI

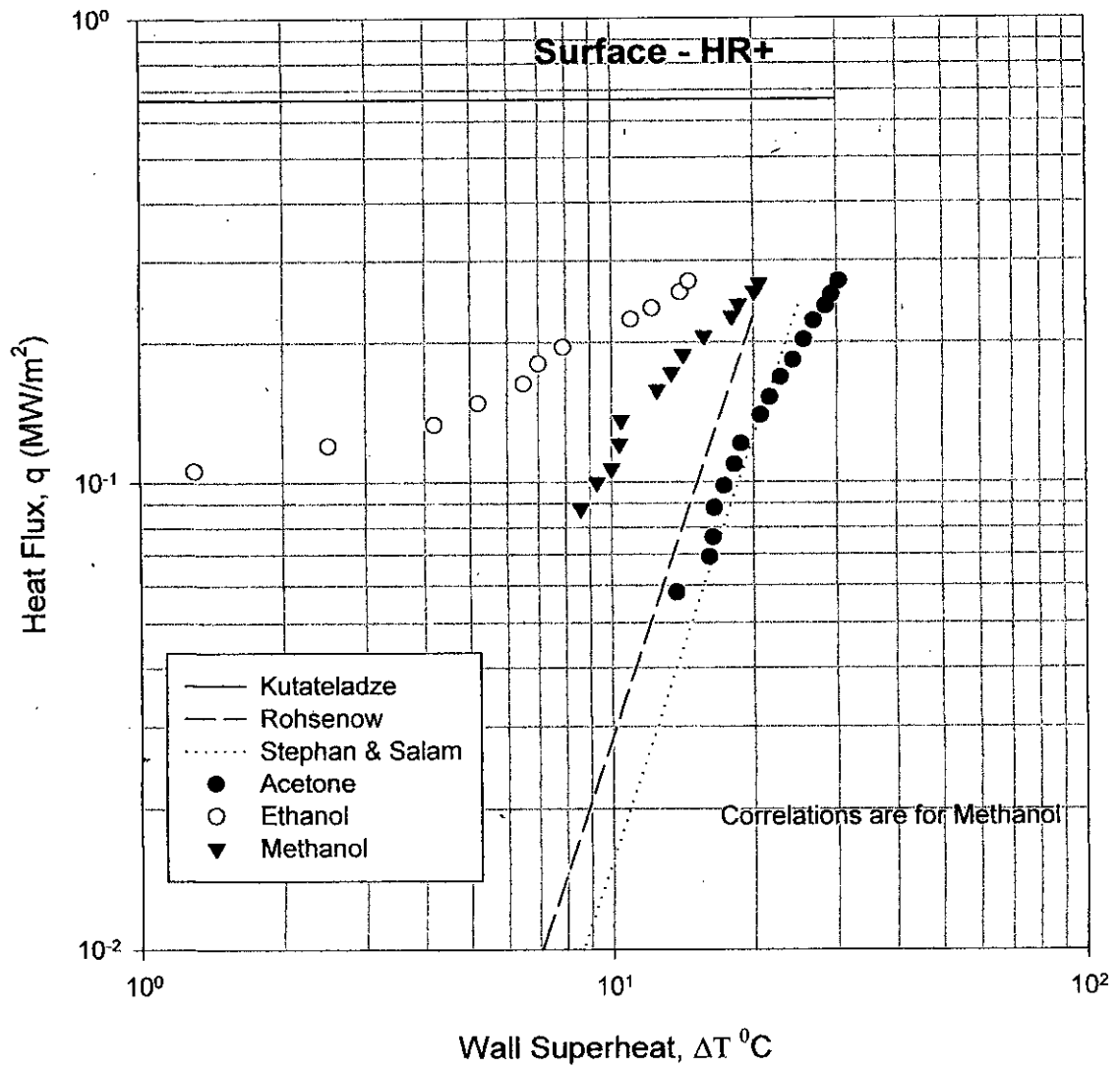


Fig. 4.15 Effects of Working Fluids on the boiling Curves for HR+

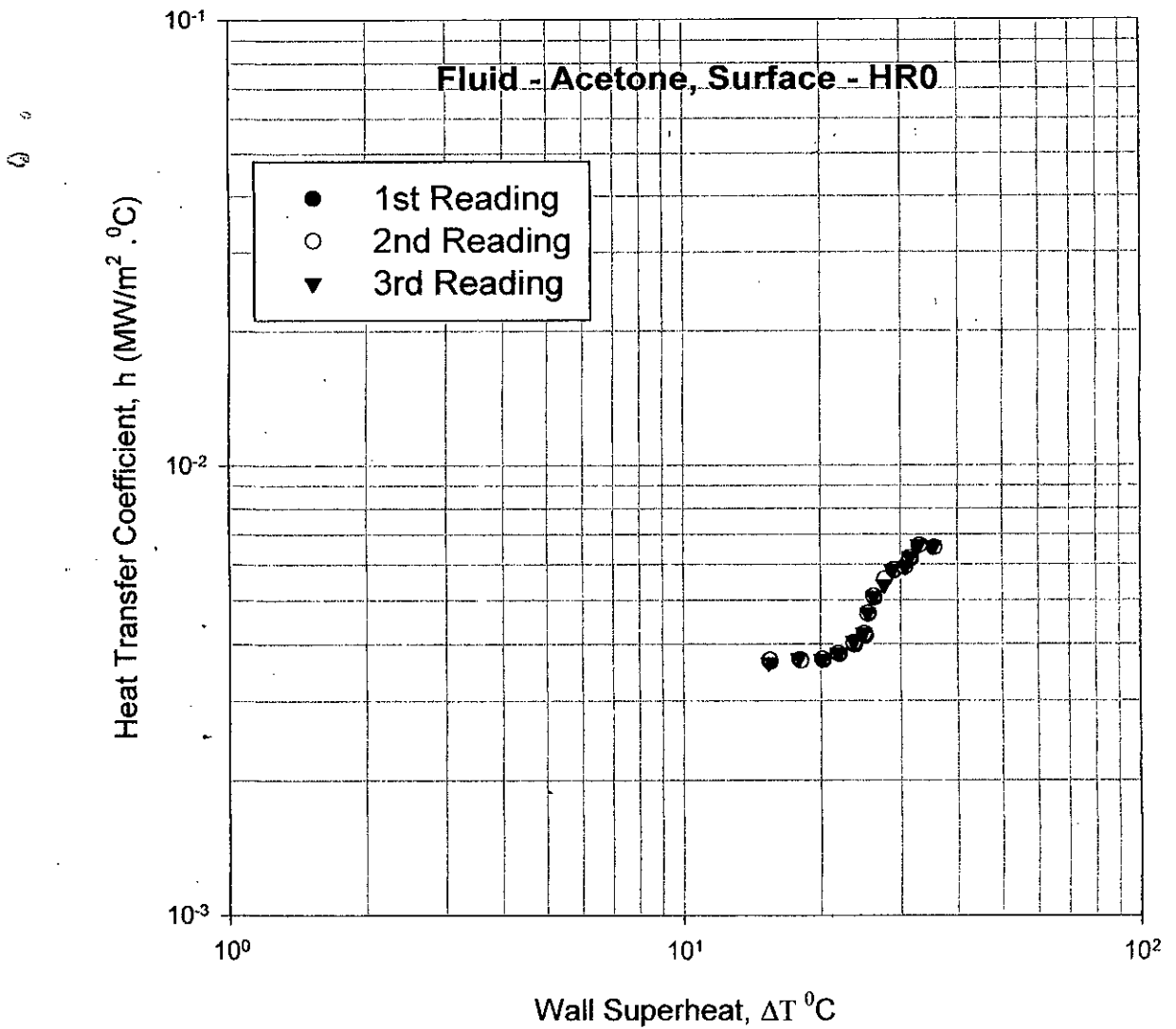


Fig. 4.16 Variation of Heat Transfer Coefficient, h for HR0 - Acetone

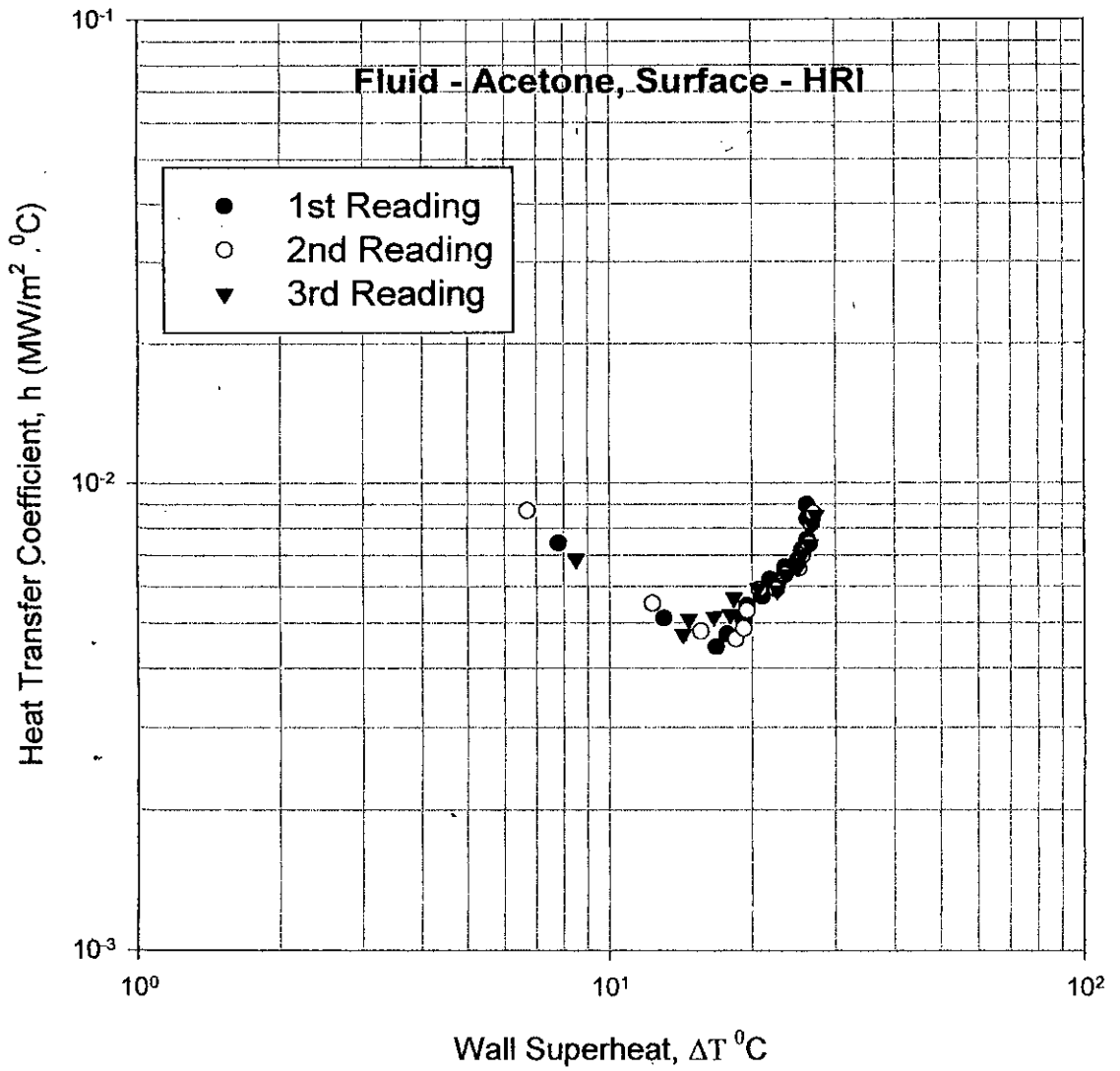


Fig. 4.17 Variation of Heat Transfer Coefficient, h for HRI - Acetone

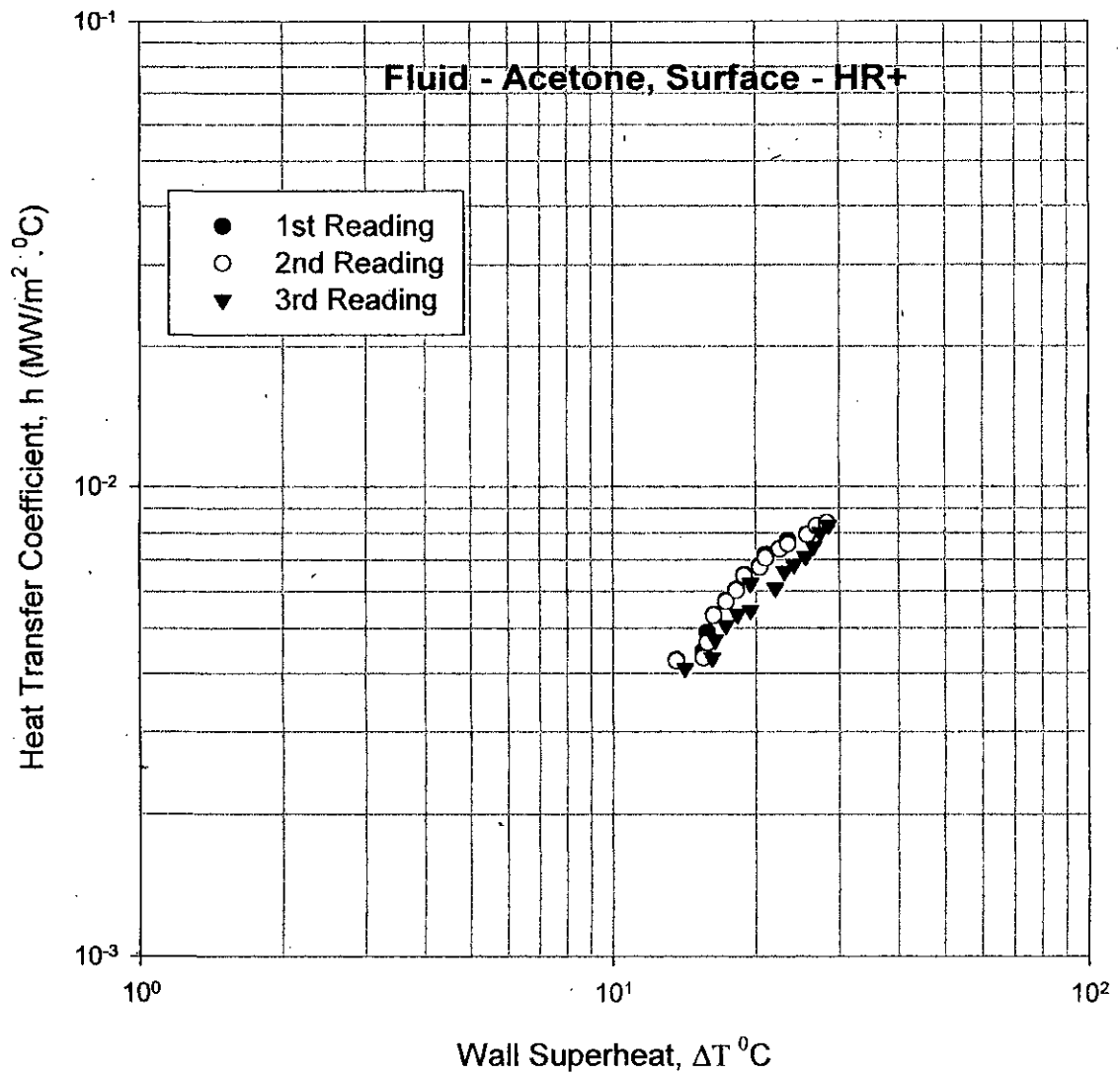
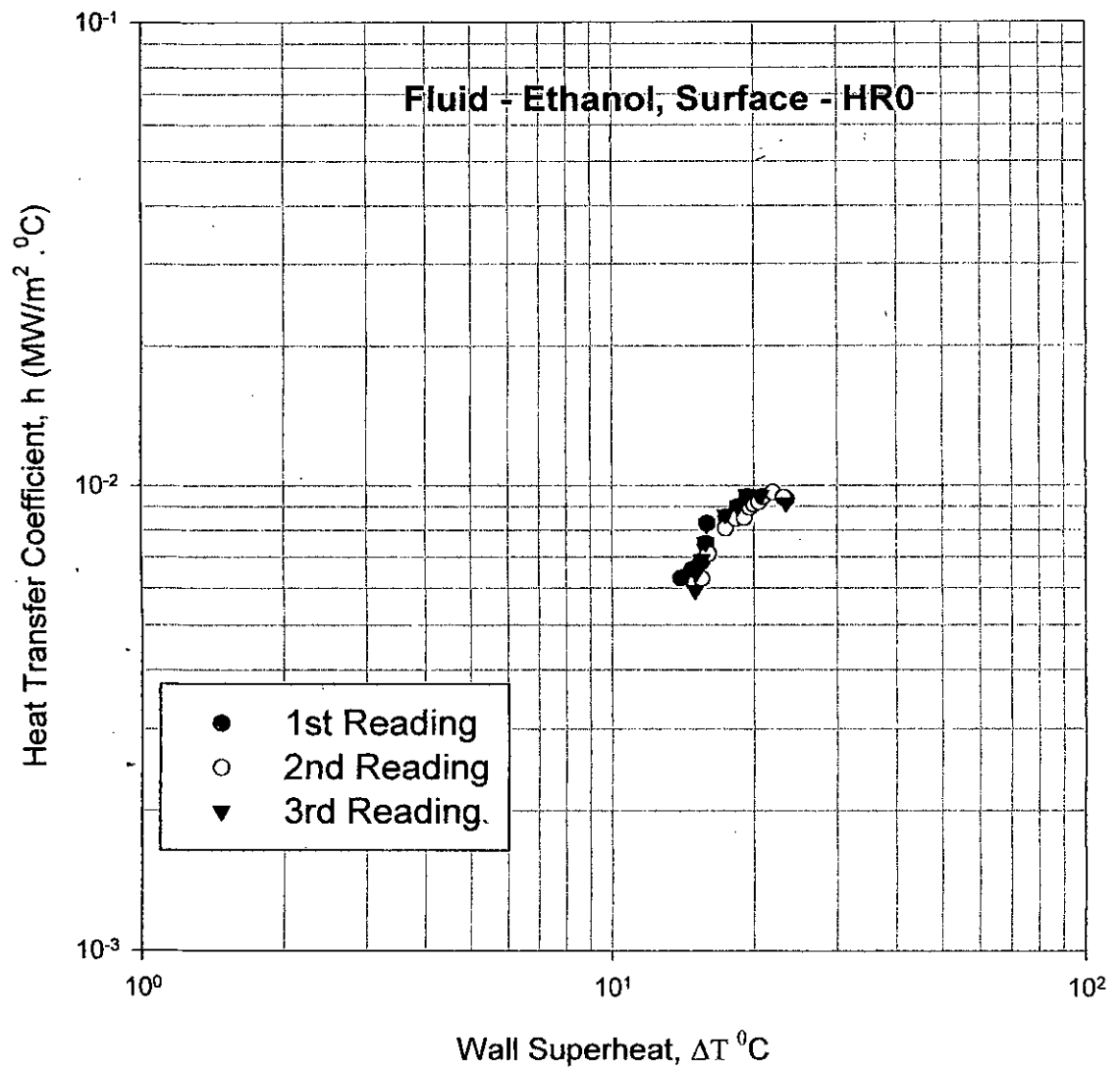


Fig. 4.18 Variation of Heat Transfer Coefficient, h for HR+ - Acetone



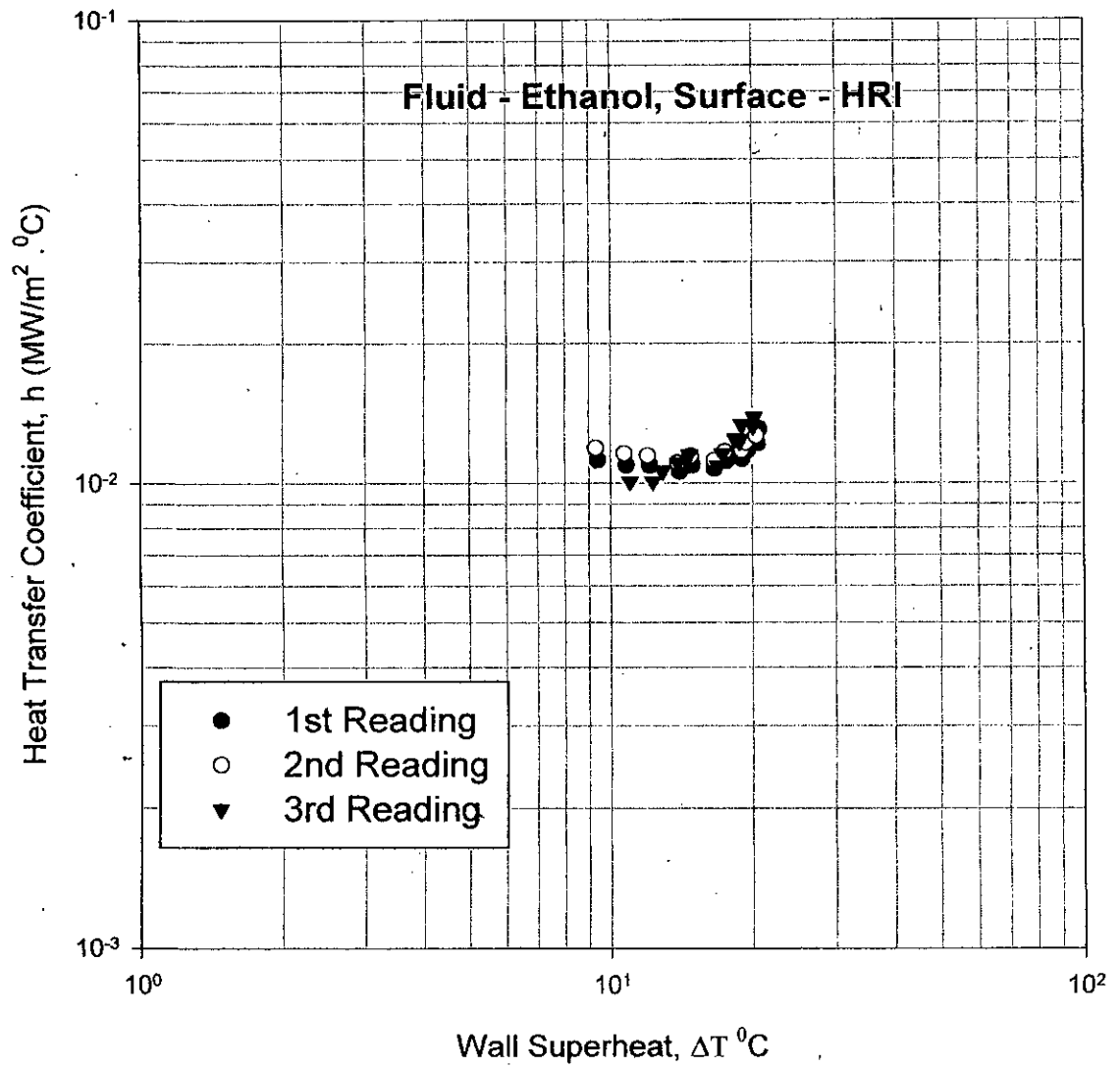


Fig. 4.20 Variation of Heat Transfer Coefficient, h for HRI - Ethanol

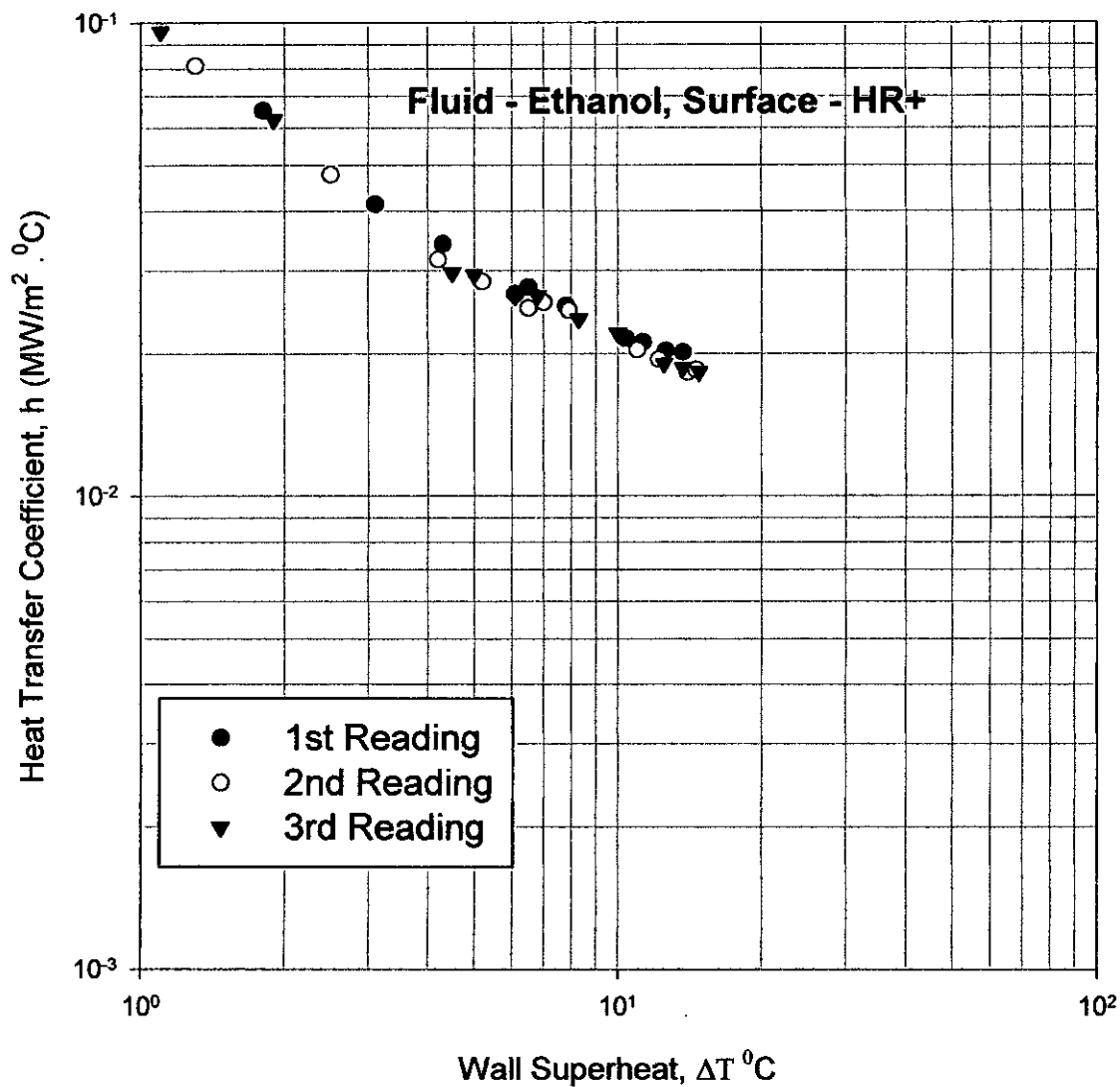


Fig. 4.21 Variation of Heat Transfer Coefficient, h for HR+ - Ethanol

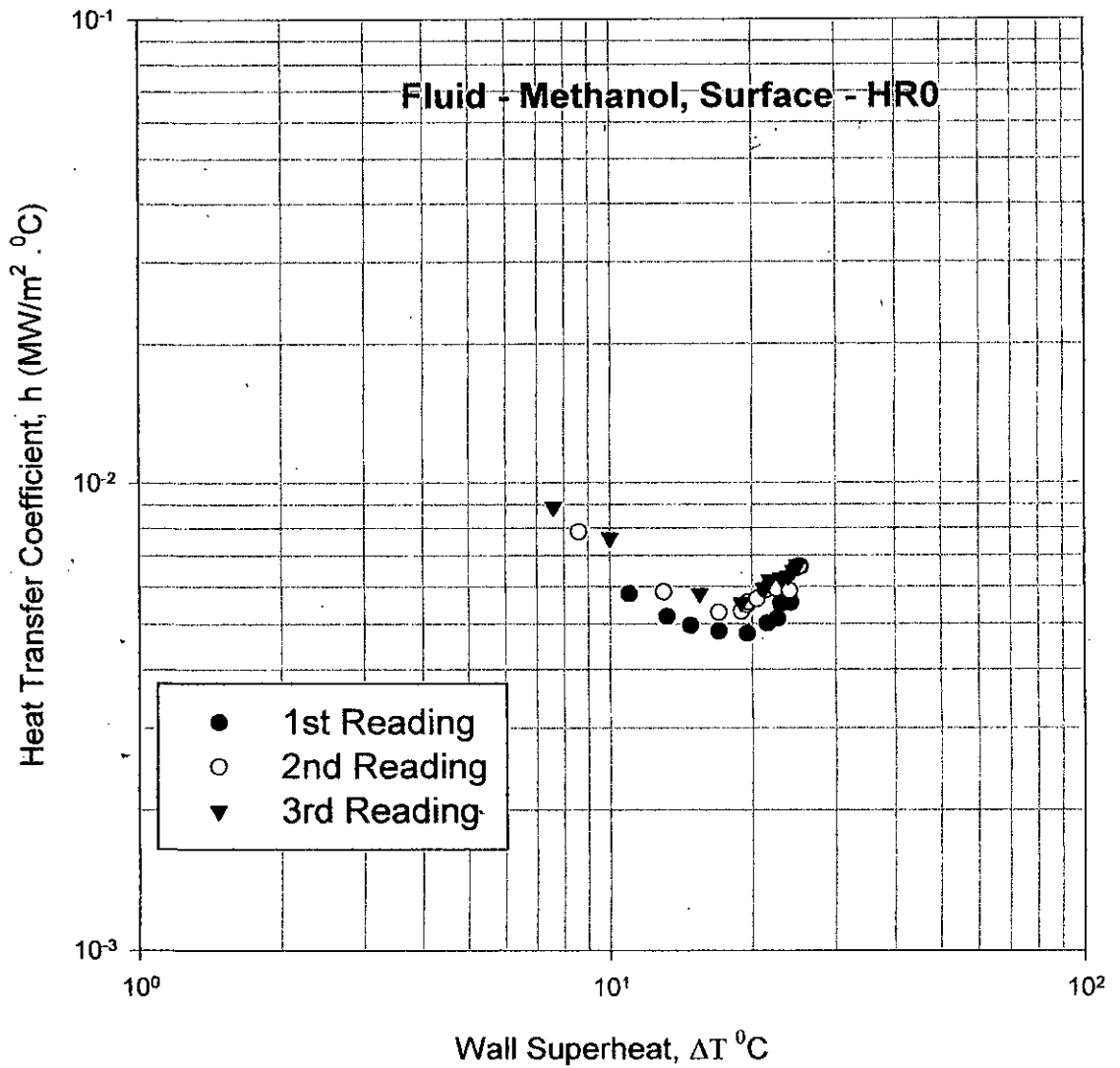


Fig. 4.22 Variation of Heat Transfer Coefficient, h for HR0 - Methanol

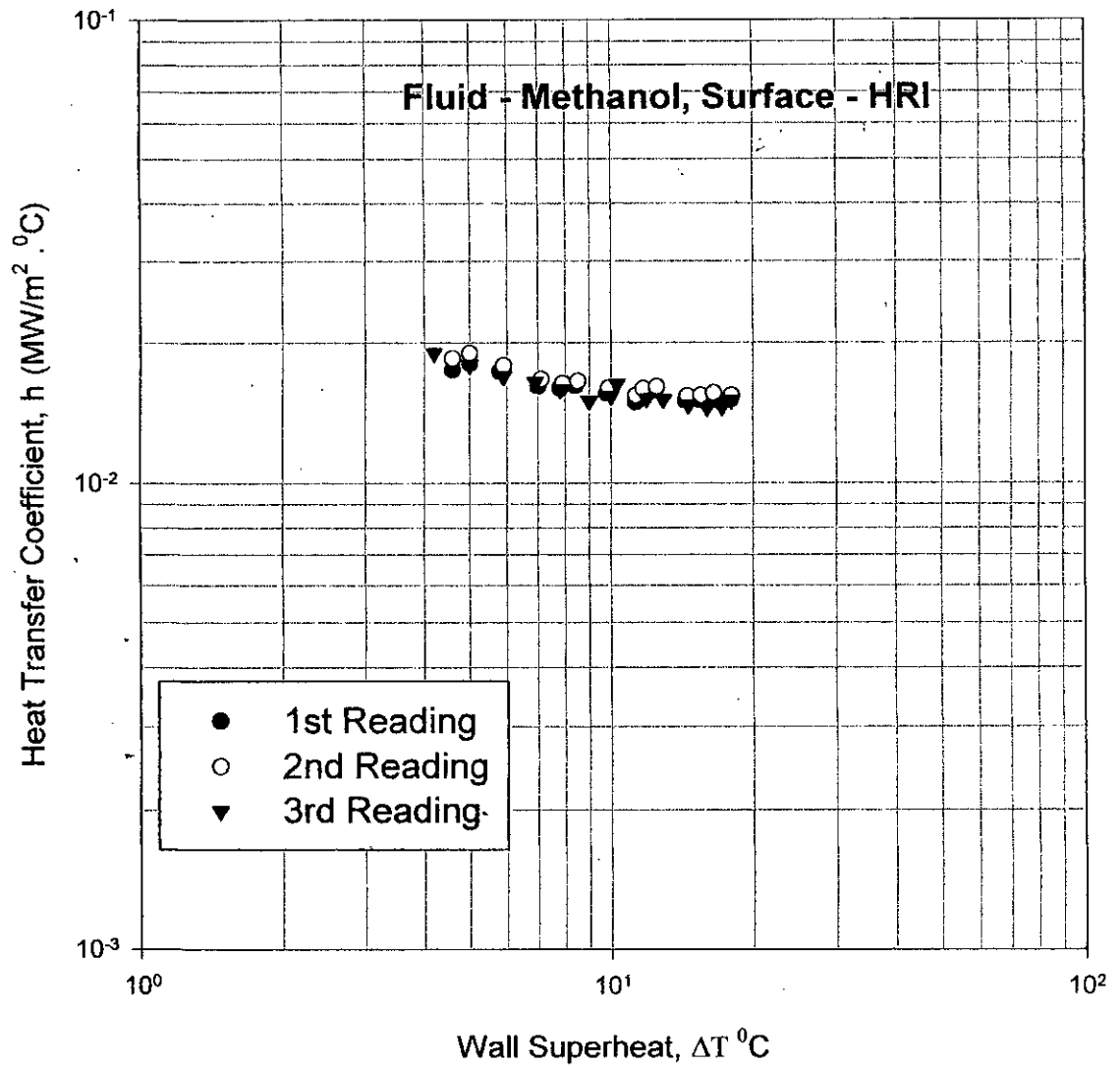


Fig. 4.23 Variation of Heat Transfer Coefficient, h for HRI - Methanol

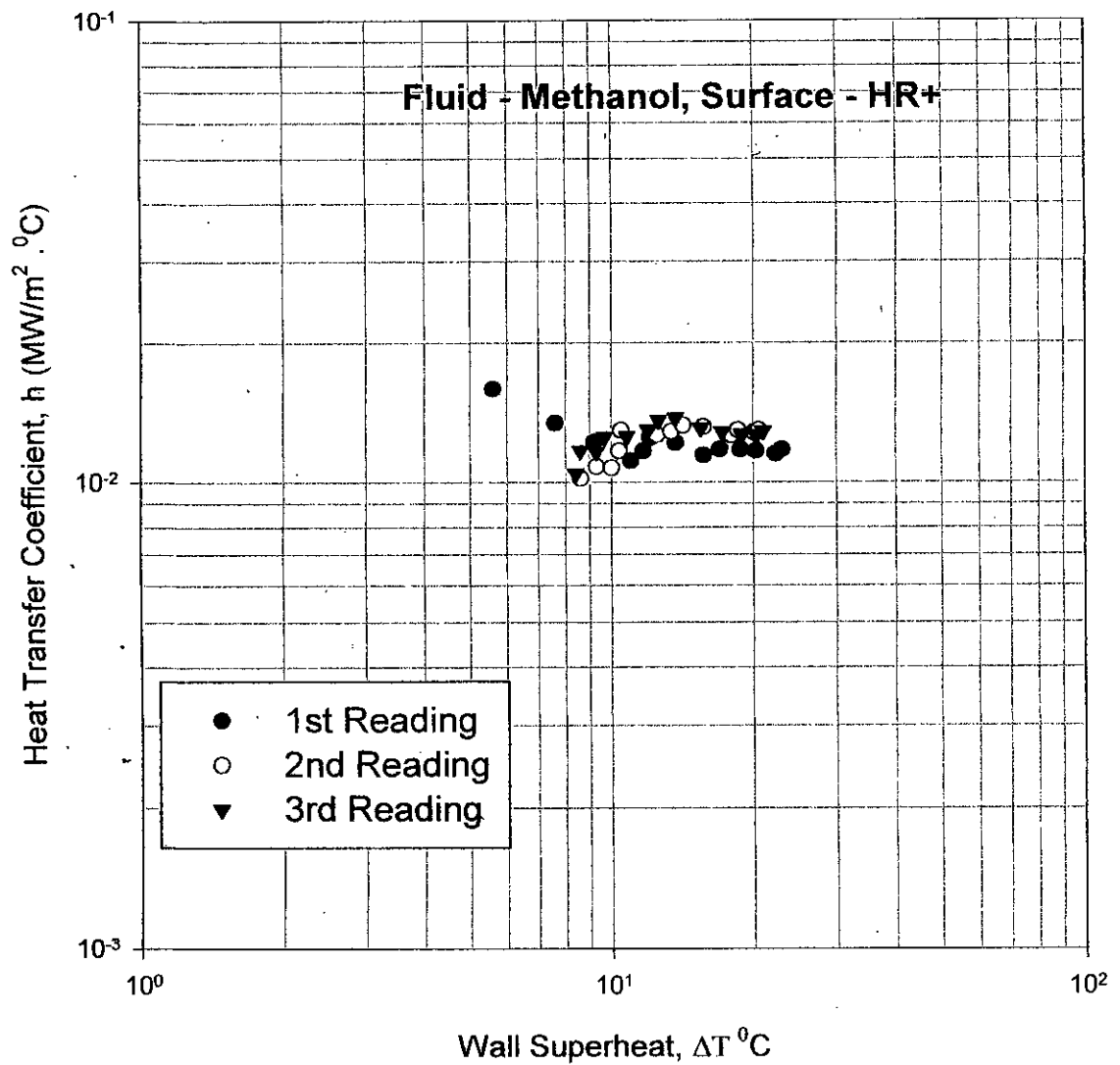


Fig. 4.24 Variation of Heat Transfer Coefficient, h for HR+ - Methanol

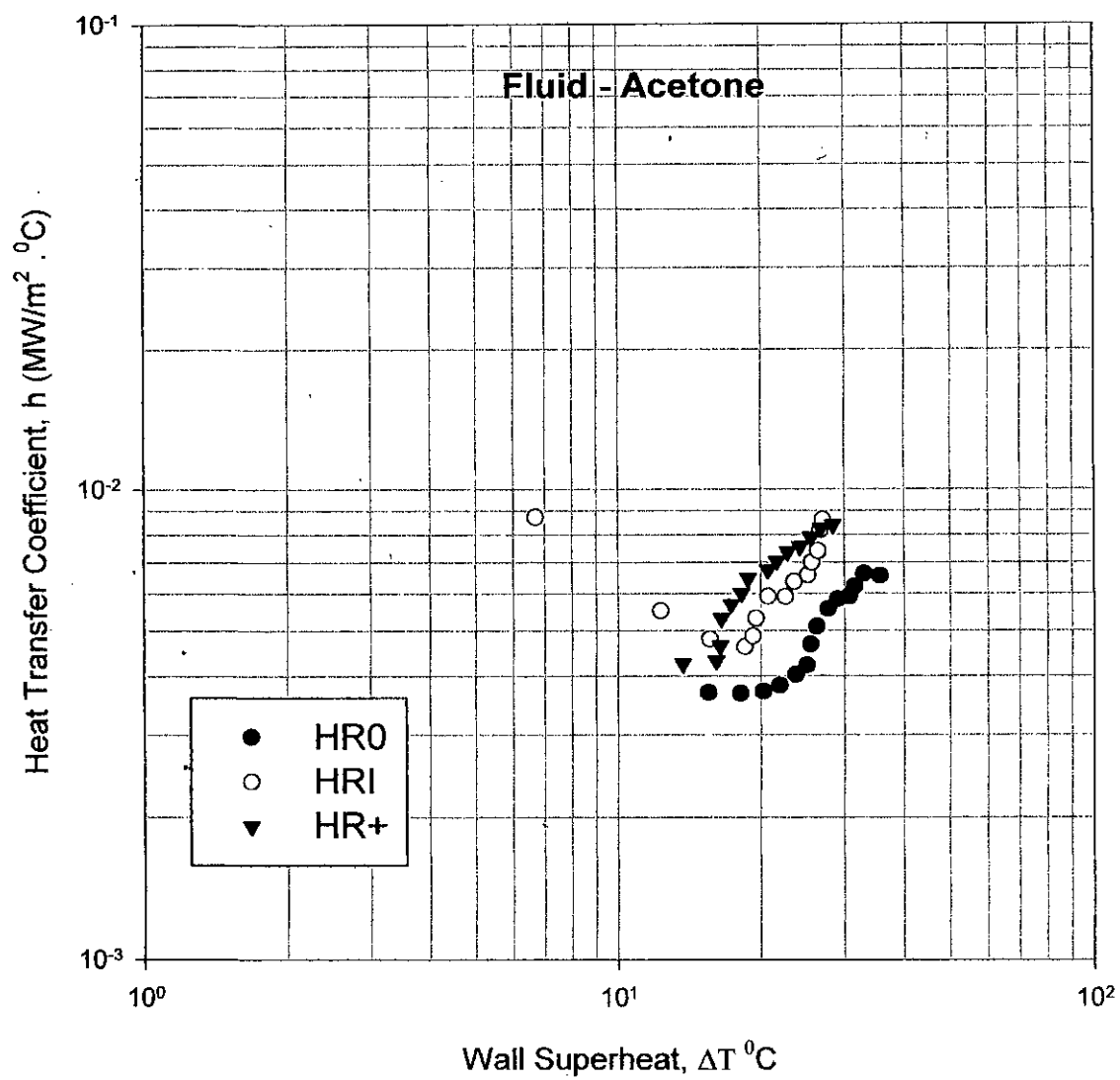


Fig. 4.25 Effects of Evaporator surface on Heat Transfer Coefficient, h for Acetone

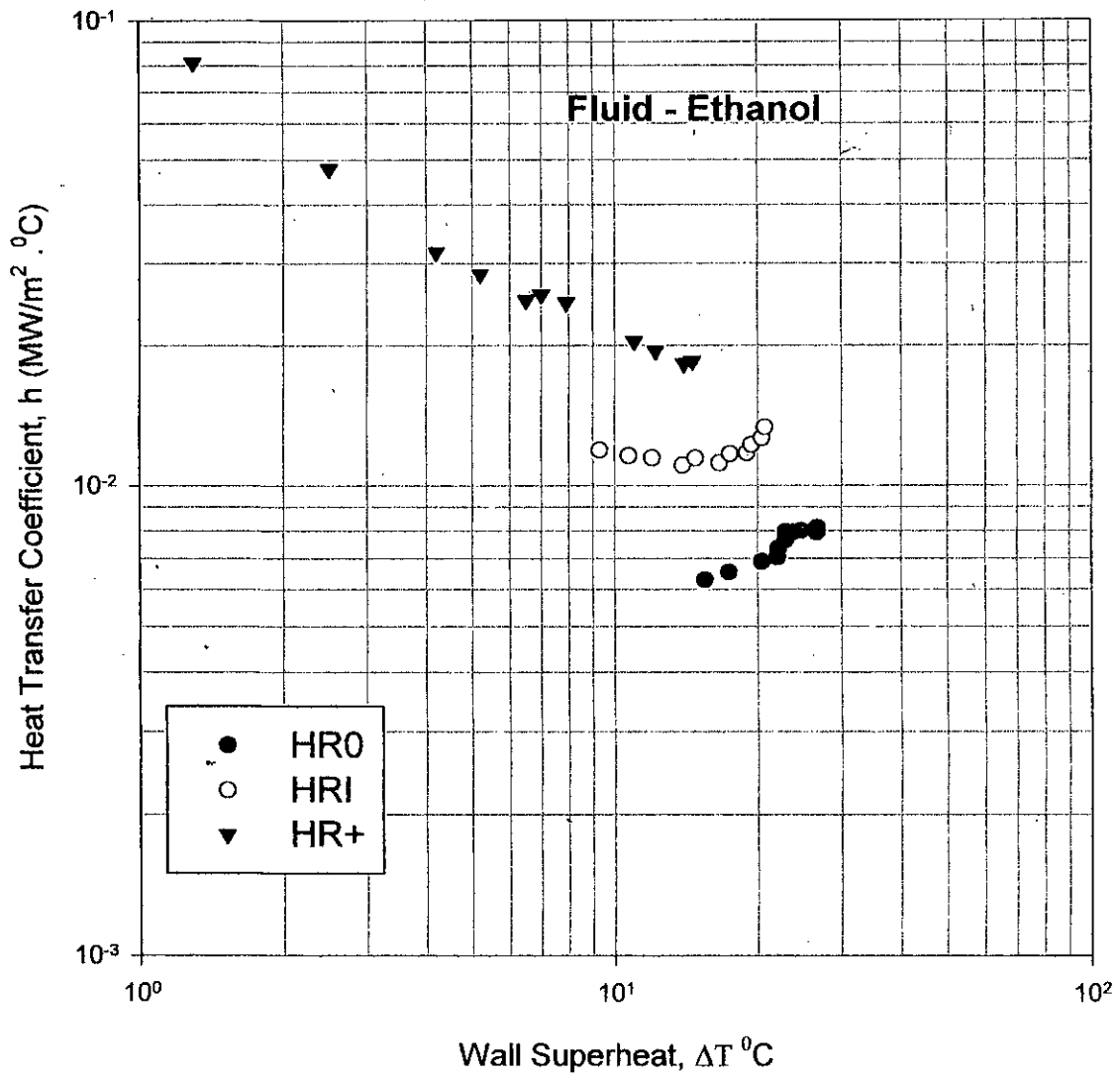


Fig. 4.26 Effects of Evaporator surface on Heat Transfer Coefficient, h for Ethanol

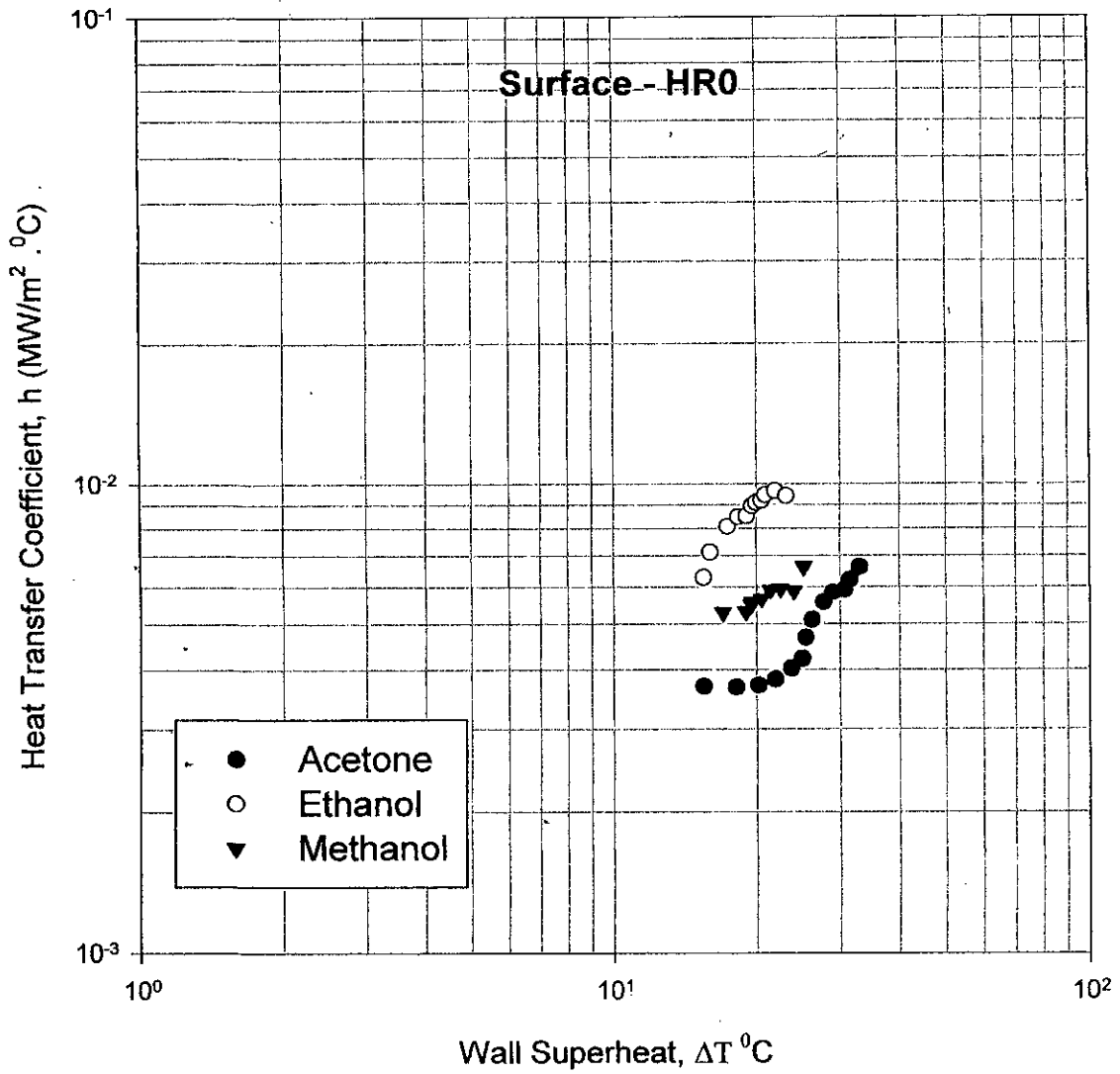


Fig. 4.28 Effects of Working Fluids on Heat Transfer Coefficient, h for HR0

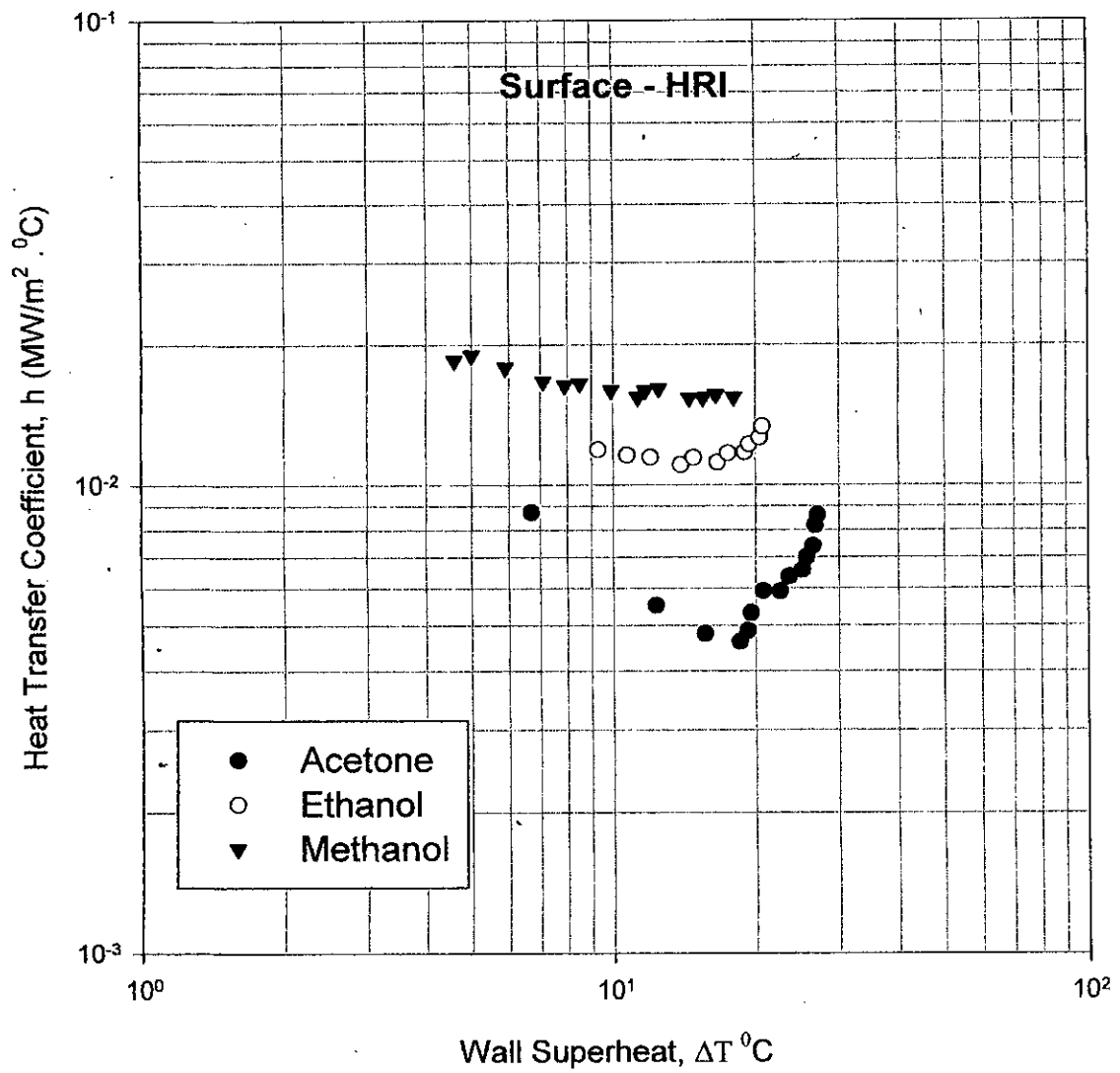


Fig. 4.29 Effects of Working Fluids on Heat Transfer Coefficient, h for HRI

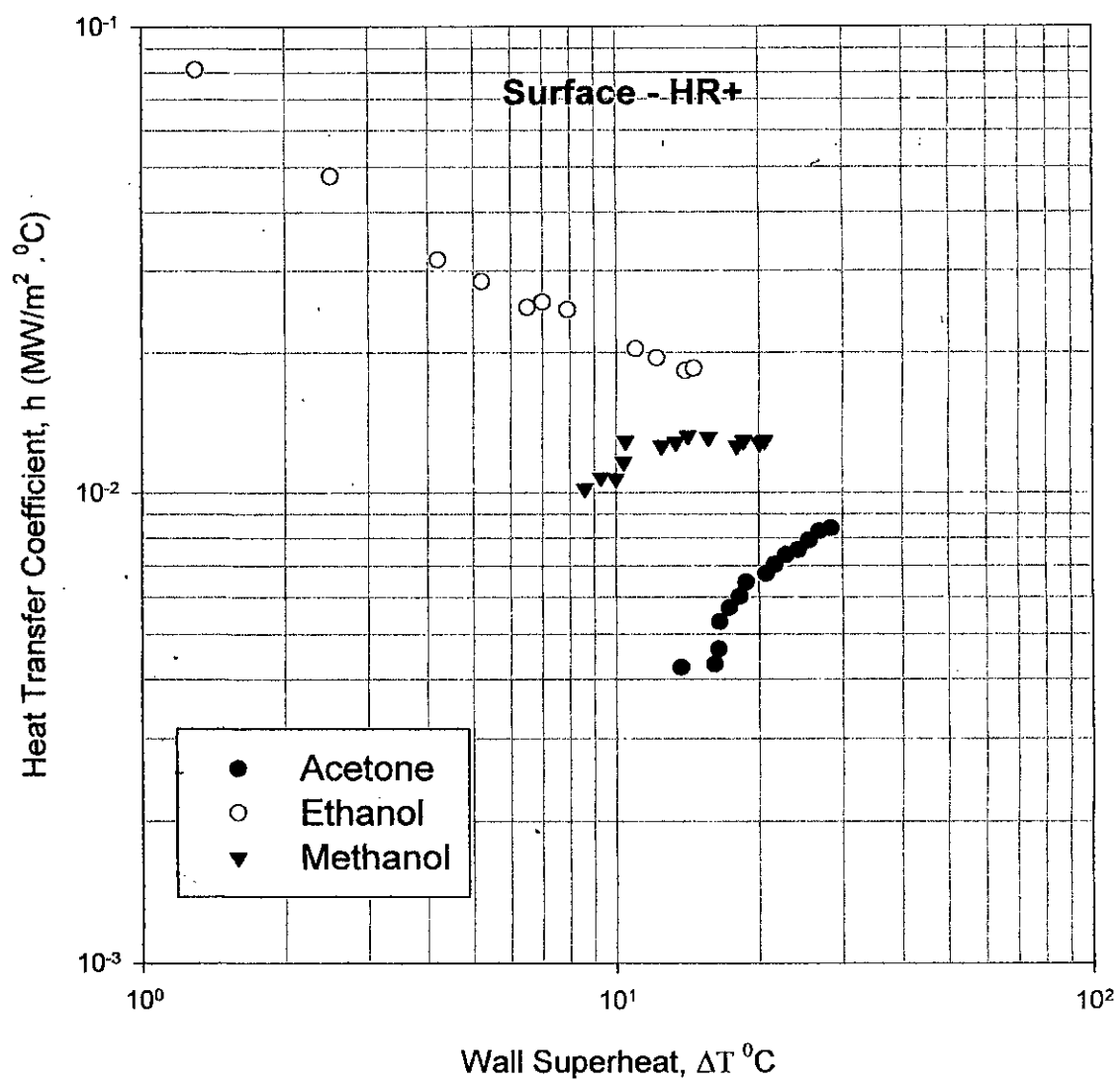


Fig. 4.30 Effects of Working Fluids on Heat Transfer Coefficient, h for HR+

CONCLUSIONS

5.1 Conclusions

This study demonstrates the performance evaluation of a two-phase thermosyphon with enhanced heat transfer surfaces in the evaporator. Better thermal performance achieved in this study can make the thermosyphon an attractive alternative for cooling of high heat flux electronic components. From the data presentation and analysis the following conclusions can be made:

1. The temperature very close to evaporator surface was as high as 99°C to transfer heat flux of 28 W/cm². These temperatures were 88, 99 and 85°C for Methanol, Ethanol, and Acetone respectively. The respective heat fluxes were 27.5, 28, 27.5 W/cm².
2. Enhanced surface can transfer more heat compared to the surface without it. The enhanced structure, HR+ can transfer a heat flux of 27.5 W/cm² boiling Methanol and keeping evaporator surface temperature very close to 85°C.
3. For Ethanol, the performance of surface HR+ shows the best and the surface HRI shows middle result. At the point Wall superheat values 15°C the heat flux for HRI is doubled and for HR+ is tripled than that of the plain surface HRO. For the case Methanol the performance of the surface HRI is the best. The dissipated heat flux through surface HRI is about three times than that of plain surface, and through surface, HR+ is about 2.5 times than that of plain surface at the point of 17°C wall superheat.
4. The heat transfer coefficient in this study was as high as $9 \times 10^4 \text{ W/m}^2 \text{ } ^\circ\text{C}$

5.2 Recommendations

For further study, the following recommendations may be made.

1. Further detailed numerical and experimental studies are needed to accurately predict the behavior of the loop thermosyphon.
2. Methanol is identified as the best working fluid than Acetone or Ethanol; however Optimum Charging and proper degassing may improve the quality of Acetone and Ethanol as working fluid.
3. Evaporator with integrated rectangular fins (HRI) with Methanol as working fluids shows better result. The heat dissipation rates may be increased with the increasing the depth of channel while keeping the channel width and pitch constant.
4. The heat flux may be high if this study perform with dielectric fluid (FC-72 or FC-87).
5. Water/liquid cooled condenser or air-cooled condenser with fan (Forced convection) may increase the performance of thermosyphon.
6. During the experiment power supply fluctuation can be minimized by using a voltage stabilizer.

REFERENCE

A. E., Bergles and A. Bar-Cohen, "Direct Liquid Cooling of Microelectronic Components", *Advances in Thermal Modeling of Electronic Components and Systems*, Vol. 2, Eds. A. Bar-Cohen and A. D. Kraas, ASME Press, NY, pp. 241-250, 1990.

Aniruddha Pal and Yogendra Joshi, "Design and Performance Evaluation of a Compact Thermosyphon", Woodruff School of Mechanical Engineering, Georgia Institute of Technology, Atlanta, Georgia.

Bar-Cohen, A., "Thermal Management of Electronic Components with Dielectric Liquids", *International Journal of JSME*, Ser. B., Vol. 36, no, pp. 1-25, 1993.

Bhavnani, S. H., Tasi, C. P., Jaeger, R. C. and Eison, D. L., "An Integral Heat Sink for Cooling Microelectronic Components", *ASME Journal of Electronic Packaging*, Vol. 115, pp. 284-291, 1993.

C. Ramaswamy, Y. Joshi, W. Nakayama and W. Johnson, "Performance of a Compact Two-Phase Two-Chamber Thermosyphon: Effect of Evaporator Confinement and Suddenly Applied Loads", Submitted for Publication in the Proceedings of AIAA/ASME Joint Heat Transfer and Thermophysics Conference at Albuquerque, NM, 1998.

Farber. E.A., and E.I Scoria: *Heat Transfer to Water Boiling Under pressure*, Trans ASME. vol. 70. p369, (book, Holman, 1997), 1948

I. Mudawar and T. M. Anderson, "High Flux Electronic Cooling by Means of Pool Boiling-Part-I: Parametric Investigation of the Effects of Coolant Variation, Pressurization, Sub-Cooling and Surface Augmentation", *Heat Transfer in Electronics*, ASME HTD-Vol. III, Ed. R. K. Shah, pp. 25-34, 1989.

Incropera, F. P., "Liquid Immersion Cooling of Electronic Components", Heat Transfer in Electronic and Microelectronic Equipment, A. E. Bergles, Ed., Hemisphere Publishing Corporation, Washington D.C., pp. 407-444, 1990.

Katto, Y., Yokoya, Y. and Teraoka, K., "Nucleate and Transition Boiling in a Narrow Space Between Two Horizontal, Parallel Disc Plates", Bulletin of the JSME, Vol. 20, pp. 98-107, 1977.

Kutateladze, S. S., "On the Transition to Film Boiling under Natural Convection", *Kotloturbostroenil*, No. 3, p. 10, (Book, Carey, 1994) 1948.

Lang Yuan, Joshi, Y. and Nakayama, W., "Effects of Condenser Location and Tubing Length on the Performance of a Compact Two-Phase Thermosyphon", Proceedings of 2001 International Mechanical Engineering Congress and Exposition, ASME 11-16, 2001, New York, NY, 2001.

99679 Miller, W. J., "Boiling and Visualization from Microconfigured Surfaces", M. S. Thesis, University of Pennsylvania, Philadelphia, P. A., 1991.

Mudawar and T. M. Anderson, "Optimization of Enhanced Surfaces for High Flux Chip Cooling by Pool Boiling", *Trans ASME. J. electronic Packaging*, V. 115, pp. 89-100, 1993.

Nakayama, W. and Bergles, A. E., "Cooling of Electronic EquipmentL Past, Present and Future", Heat Transfer in electronic and Microelectronic Equipment, A. E. Bergles, Ed., Hemisphere Publishing Corporation, Washington D.C., pp. 3-39, 1990.

Nowell, R. M., Bhavnani, S. H. and Jaedar, R. C., "Effect of Channel Width on Pool Boiling from a Microconfigured Heat Sink", Proceedings of the Intersociety Conference on Thermal Phenomena in Electronic System (I-THERM-IV), pp. 163-168, 1994.

Palm, B. and Tengblad, N., "Cooling of Electronics by Heat Pipes and Thermosyphons. A Review of Methods and Possibilities", Proceedings of the 31st National Heat Transfer Conference, ASME, HTD-Vol. 329, Vol. 7, pp. 97-108, 1996.

R. L. Judd, H. Merte, J. and M.E. Ulucakli, "Variation of Superheat with Sub-Cooling in Nucleate Pool Boiling", *Trans. ASME J. Heat Transfer*, Vol. 113, No. 1, pp. 201-208, 1991.

Ramasawamy, C., Joshi, Y., Nakayama, W. and Johnson, W., "Thermal Performance of a Two-Phase Thermosyphon: Response to Evaporator Confinement and Transient Loads", *Journal of enhanced Heat Transfer*, Vol. 6, No. 2-4, pp. 279-288, 1999.

Ramaswamy, C., Joshi, Y., Nakayama, W. and Johnson, W. B., "Performance of a Compact Two Chamber Two-Phase Thermosyphon: Effect of Evaporator Inclination, Liquid fill Volume and Contact Resistance", *Proceedings of the International Heat Transfer Conference*, Kyongju, South Korea, 1998.

Ramaswamy, C., Joshi, Y., Nakayama, W. and Johnson, W. B., "Compact Thermosyphons Employing Microfabricated Components", *Microscale Thermophysical Engineering*, Vol. 3, pp. 273-282, 1999.

Ramaswamy, C., Joshi, Y., Nakayama, W. and Johnson, W., "Performance of a Compact Two-Chamber Two-Phase Thermosyphon: Effect of Confinement and Suddenly Applied Loads", Submitted for Publication in the *Proceedings of AIAA/ASME Joint Thermophysics and Heat Transfer Conference at Albuquerque, New Mexico*, 1997.

Rohsenow, W. M., "A Method of Correlating Heat Transfer Data for surface Boiling Liquids", *Trans. ASME*, Vol. 74, p. 969, (Book, Holman,1997) 1952.

Stephan, K. and Abdelsalam, M., "Heat Transfer Correlation for Natural Convection Boiling", *International Journal of Heat Mass Transfer*, Vol. 23, pp. 73-87, (Book, Carey,1994) 1980.

Sunil S. Murthy, Yogendra K. Joshi, Wataru, Nakayama, "Single Chamber Compact Thermosyphons with Microfabricated Components" *Proceedings on the 7th Intersociety Conference on Thermal and Thermochemical Phenomena in Electronic Systems*, Las Vegas, NV, 2000.

W. Nakayama, T. Nakajima and S. Hirasawa, "Heat Sink Studs Having Enhanced Boiling Surfaces for Cooling Microelectronic Component", ASME Paper No. 84, WA/HT-89, 1984.

Webb, R. L., Gilley, M. D. and Zarnescu, V., "Advanced heat Exchange Technology for Thermoelectronic Cooling Devices", Proceedings of the 31st National Heat Transfer Conference, ASME, HTD-Vol. 329, Vol. 7, pp. 125-133, 1996.

Appendix-A

Experimental Data

Table-A.1: Collected data during the experiment, HRO-Acetone

Experiment No: 1

Working Fluid : Acetone , Surface: HRO

Here, V= Supply Voltage (Volt)

I=Line Current (Ampere)

T_{sat} =Saturated Temperature of Fluid ($^{\circ}\text{C}$)

T_{x_1} = Temperature at the point 1 of evaporator geometry ($^{\circ}\text{C}$)

T_{x_2} = Temperature at the point 2 of evaporator geometry ($^{\circ}\text{C}$)

T_{x_3} =Temperature at the point 3 of evaporator geometry ($^{\circ}\text{C}$)

T_{x_4} =Temperature at the point 4 of evaporator geometry ($^{\circ}\text{C}$)

Q = Total Heat Input (W)

$\Delta T = T_{x_4} - T_{sat}$ ($^{\circ}\text{C}$)

q = Heat Flux Per unit Area After deducting Heat loss (MW/m^2)

h = Boiling heat transfer coefficient ($\text{MW}/\text{m}^2 \cdot ^{\circ}\text{C}$)

$$T_{sat} = 56.5^{\circ}\text{C}$$

Obs. No.	V	I	T_{x_1}	T_{x_2}	T_{x_3}	T_{x_4}	Q(W)	$\Delta T^{\circ}\text{C}$	q(MW/m^2)	h($\text{MW}/\text{m}^2 \cdot ^{\circ}\text{C}$)
1.	116	0.30	81.10	75.90	74.00	72.00	29.58	15.50	0.056648	0.003655
2.	127	0.32	84.10	78.10	76.50	74.50	34.54	18.00	0.066549	0.003697
3.	134	0.34	87.00	80.00	78.50	76.80	38.73	20.30	0.074863	0.003688
4.	141	0.36	89.20	81.30	79.60	78.50	43.15	22.00	0.083712	0.003805
5.	151	0.38	93.00	83.50	81.70	80.30	48.77	23.80	0.094907	0.003988
6.	158	0.40	96.50	85.60	83.30	81.60	53.72	25.10	0.104737	0.004173
7.	170	0.42	97.00	86.00	83.00	82.00	60.69	25.50	0.118901	0.004663
8.	181	0.44	100.10	87.70	85.00	82.80	67.69	26.30	0.132951	0.005055
9.	200	0.46	104.30	90.20	87.00	84.20	78.20	27.70	0.154057	0.005562
10.	209	0.48	107.40	92.40	88.40	85.50	85.27	29.00	0.168245	0.005802
11.	216	0.50	110.00	94.70	90.20	87.20	91.80	30.70	0.18136	0.005907
12.	223	0.52	113.10	95.70	92.00	88.10	98.57	31.60	0.194924	0.006168
13.	240	0.54	116.00	98.00	93.10	89.50	110.16	33.00	0.218338	0.006616
14.	247	0.56	119.60	111.10	96.40	92.10	117.57	35.60	0.233184	0.00655

Table-A.2: Collected data during the experiment, HRO-Acetone

Experiment No: 2

Working Fluid : Acetone , Surface: HRO

Here, V= Supply Voltage (Volt)

I=Line Current (Ampere)

 T_{sat} =Saturated Temperature of Fluid ($^{\circ}\text{C}$) T_{x_1} = Temperature at the point 1 of evaporator geometry ($^{\circ}\text{C}$) T_{x_2} = Temperature at the point 2 of evaporator geometry ($^{\circ}\text{C}$) T_{x_3} =Temperature at the point 3 of evaporator geometry ($^{\circ}\text{C}$) T_{x_4} =Temperature at the point 4 of evaporator geometry ($^{\circ}\text{C}$)

Q = Total Heat Flux (W)

 $\Delta T = T_{x_4} - T_{sat}$ ($^{\circ}\text{C}$)q = Heat Flux Per unit Area After deducting Heat loss (MW/m²)q R= Heat Flux Found From Rohsenow Correlation (MW/m²)qs = Heat Flux Found From Stephan and Abdelsalam Correlation (MW/m²)h = Boiling heat transfer coefficient (MW/m². $^{\circ}\text{C}$)

$$T_{sat} = 56.5^{\circ}\text{C}$$

Obs. No.	V	I	T_{x_1}	T_{x_2}	T_{x_3}	T_{x_4}	Q(W)	$\Delta T^{\circ}\text{C}$	q(MW/m ²)	qR(MW/m ²)	qs(MW/m ²)	h(MW/m ² . $^{\circ}\text{C}$)
1.	117	0.30	81.00	76.00	74.10	72.00	29.835	15.50	0.05717	0.026253	0.045308	0.003689
2.	127	0.32	84.00	78.10	76.60	74.60	34.544	18.10	0.06656	0.041805	0.072147	0.003677
3.	134	0.34	87.00	80.10	78.60	76.70	38.726	20.20	0.07486	0.058109	0.100285	0.003706
4.	141	0.36	89.40	81.30	79.70	78.40	43.146	21.90	0.08370	0.074049	0.127796	0.003822
5.	152	0.38	93.00	83.60	81.70	80.20	49.096	23.70	0.09556	0.09385	0.161968	0.004032
6.	159	0.40	96.60	85.70	83.30	81.50	54.060	25.00	0.10542	0.110156	0.190109	0.004217
7.	170	0.42	97.00	86.00	83.00	81.90	60.690	25.40	0.11890	0.115529	0.199381	0.004681
8.	182	0.44	100.10	87.70	85.00	82.70	68.068	26.20	0.13371	0.126792	0.21882	0.005104
9.	200	0.46	104.20	90.20	87.00	84.20	78.200	27.70	0.15406	0.14984	0.258597	0.005562
10.	210	0.48	107.60	92.40	88.50	85.50	85.680	29.00	0.16906	0.171942	0.296741	0.00583
11.	216	0.50	110.00	94.80	90.30	87.20	91.800	30.70	0.18136	0.203988	0.352045	0.005907
12.	224	0.52	113.20	95.80	92.10	88.00	99.008	31.50	0.19582	0.220354	0.38029	0.006216
13.	240	0.54	116.00	98.00	93.20	89.50	110.160	33.00	0.21834	0.253356	0.437245	0.006616
14.	247	0.56	120.60	101.20	96.50	92.10	117.572	35.60	0.23311	0.318082	0.548951	0.006548

Table-A.3: Collected data during the experiment, HRO-Acetone**Experiment No: 3**

Working Fluid : Acetone , Surface : HRO

Here, V = Supply Voltage (Volt) I = Line Current (Ampere) T_{sat} = Saturated Temperature of Fluid ($^{\circ}\text{C}$) T_{x_1} = Temperature at the point 1 of evaporator geometry ($^{\circ}\text{C}$) T_{x_2} = Temperature at the point 2 of evaporator geometry ($^{\circ}\text{C}$) T_{x_3} = Temperature at the point 3 of evaporator geometry ($^{\circ}\text{C}$) T_{x_4} = Temperature at the point 4 of evaporator geometry ($^{\circ}\text{C}$) Q = Total Heat Flux (W) q = Heat Flux Per unit Area After deducting Heat loss (MW/m^2) q_R = Heat Flux Found From Rohsenow Correlation (MW/m^2) q_s = Heat Flux Found From Stephan and Abdelsalam Correlation (MW/m^2) h = Boiling heat transfer coefficient ($\text{MW}/\text{m}^2\cdot^{\circ}\text{C}$)

$$T_{sat} = 56.5^{\circ}\text{C}$$

Obs. No.	V	I	T_{x_1}	T_{x_2}	T_{x_3}	T_{x_4}	Q(W)	$\Delta T^{\circ}\text{C}$	$q(\text{MW}/\text{m}^2)$	$h(\text{MW}/\text{m}^2\cdot^{\circ}\text{C})$
1.	115	0.30	81.00	75.80	73.80	71.90	29.325	15.40	0.05614	0.003645
2.	127	0.32	84.00	78.00	76.40	74.40	34.544	17.90	0.06656	0.003718
3.	134	0.34	86.90	80.00	78.40	76.70	38.726	20.20	0.07487	0.003706
4.	141	0.36	89.10	81.30	79.50	78.40	43.146	21.90	0.08372	0.003823
5.	153	0.38	92.90	83.50	81.50	80.20	49.419	23.70	0.09623	0.00406
6.	159	0.40	96.30	85.50	83.20	81.40	54.060	24.90	0.10544	0.004235
7.	170	0.42	97.00	86.00	83.00	81.90	60.690	25.40	0.11890	0.004681
8.	182	0.44	100.00	87.60	84.90	82.70	68.068	26.20	0.13372	0.005104
9.	199	0.46	164.20	90.10	86.80	84.10	77.809	27.60	0.14903	0.005399
10.	209	0.48	107.40	92.30	88.20	85.30	85.272	28.80	0.16824	0.005842
11.	217	0.50	110.00	94.60	90.00	87.20	92.225	30.70	0.18223	0.005936
12.	225	0.52	113.00	95.60	92.00	88.00	99.450	31.50	0.19673	0.006245
13.	240	0.54	116.00	98.00	92.90	89.40	110.160	32.90	0.21834	0.006636
14.	247	0.56	119.50	111.00	96.00	91.90	117.572	35.40	0.23319	0.006587

Table-A.4: Collected data during the experiment, HRI-Acetone**Experiment No: 1**

Working Fluid : Acetone, Surface : HRI

Here, V= Supply Voltage (Volt)

I=Line Current (Ampere)

 T_{sat} =Saturated Temperature of Fluid ($^{\circ}\text{C}$) T_{x1} = Temperature at the point 1 of evaporator geometry ($^{\circ}\text{C}$) T_{x2} = Temperature at the point 2 of evaporator geometry ($^{\circ}\text{C}$) T_{x3} =Temperature at the point 3 of evaporator geometry ($^{\circ}\text{C}$) T_{x4} =Temperature at the point 4 of evaporator geometry ($^{\circ}\text{C}$)

Q = Total Heat Flux (W)

 $\Delta T = T_{x4} - T_{sat}$ ($^{\circ}\text{C}$)q = Heat Flux Per unit Area After deducting Heat loss (MW/m^2)q R= Heat Flux Found From Rohsenow Correlation (MW/m^2)qs = Heat Flux Found From Stephan and Abdelsalam Correlation (MW/m^2)h = Boiling heat transfer coefficient ($\text{MW}/\text{m}^2 \cdot ^{\circ}\text{C}$) $T_{sat} = 56.5^{\circ}\text{C}$

Obs. No.	V	I	T_{x1}	T_{x2}	T_{x3}	T_{x4}	Q(W)	$\Delta T^{\circ}\text{C}$	q(MW/m^2)	qR(MW/m^2)	qS(MW/m^2)	h($\text{MW}/\text{m}^2 \cdot ^{\circ}\text{C}$)
1.	117	0.300	69.300	68.600	67.200	64.300	29.835	7.800	0.058	0.003	0.00577	0.00744
2.	126	0.320	75.500	74.600	73.000	69.500	34.272	13.000	0.067	0.015	0.02672	0.00512
3.	133	0.340	80.000	79.900	77.000	73.300	38.437	16.800	0.075	0.033	0.05766	0.00445
4.	140	0.360	81.000	79.800	77.800	74.200	42.840	17.700	0.084	0.039	0.06743	0.00473
5.	153	0.380	83.400	82.000	79.600	75.700	49.419	19.200	0.097	0.050	0.08607	0.00505
6.	159	0.400	84.200	82.600	80.000	76.000	54.060	19.500	0.106	0.052	0.09016	0.00545
7.	170	0.420	86.800	85.000	82.000	77.500	60.690	21.000	0.120	0.065	0.11261	0.00570
8.	183	0.440	88.400	86.300	83.000	78.300	68.442	21.800	0.135	0.073	0.12598	0.00621
9.	200	0.460	92.500	89.600	85.400	80.000	78.200	23.500	0.155	0.091	0.15781	0.00659
10.	211	0.480	94.600	92.000	87.600	81.500	86.088	25.000	0.171	0.110	0.19000	0.00683
11.	217	0.500	96.000	93.300	88.400	82.000	92.225	25.500	0.183	0.117	0.20163	0.00718
12.	225	0.520	97.100	94.200	89.000	82.700	99.450	26.200	0.198	0.127	0.21869	0.00755
13.	240	0.540	101.000	95.200	89.100	82.700	110.160	26.200	0.219	0.127	0.21869	0.00837
14.	247	0.560	101.000	95.400	89.300	82.600	117.572	26.100	0.234	0.125	0.21620	0.00898
15.	256	0.580	192.500	97.500	91.000	83.000	126.208	26.500	0.246	0.131	0.22629	0.00927
16.	258	0.590	102.600	97.600	91.200	83.100	129.387	26.600	0.258	0.133	0.22886	0.00972

Table-A.5: Collected data during the experiment, HRI-Acetone**Experiment No: 2**

Working Fluid : Acetone

Here, V= Supply Voltage (Volt)

I=Line Current (Ampere)

 T_{sat} =Saturated Temperature of Fluid ($^{\circ}\text{C}$) T_{x1} = Temperature at the point 1 of evaporator geometry ($^{\circ}\text{C}$) T_{x2} = Temperature at the point 2 of evaporator geometry ($^{\circ}\text{C}$) T_{x3} =Temperature at the point 3 of evaporator geometry ($^{\circ}\text{C}$) T_{x4} =Temperature at the point 4 of evaporator geometry ($^{\circ}\text{C}$) $\Delta T = T_{x4} - T_{sat}$ ($^{\circ}\text{C}$)

Q = Total Heat Flux (W)

q = Heat Flux Per unit Area After deducting Heat loss (MW/m^2)q R= Heat Flux Found From Rohsenow Correlation (MW/m^2)h = Boiling heat transfer coefficient ($\text{MW}/\text{m}^2 \cdot ^{\circ}\text{C}$)

$$T_{sat} = 56.5^{\circ}\text{C}$$

Obs. No.	V	I	T_{x1}	T_{x2}	T_{x3}	T_{x4}	Q(W)	$\Delta T^{\circ}\text{C}$	q(MW/m^2)	qR(MW/m^2)	h($\text{MW}/\text{m}^2 \cdot ^{\circ}\text{C}$)
1.	118	0.300	69.100	68.600	67.200	63.200	30.090	6.700	0.05854	0.00212	0.00874
2.	128	0.320	75.000	74.100	72.600	68.800	34.816	12.300	0.06775	0.01312	0.00551
3.	133	0.340	78.700	77.700	76.000	72.100	38.437	15.600	0.07486	0.02676	0.00480
4.	143	0.360	82.000	81.500	78.500	75.000	43.758	18.500	0.08547	0.04464	0.00462
5.	148	0.380	83.700	82.300	80.000	75.700	47.804	19.200	0.09359	0.04990	0.00487
6.	155	0.400	85.100	83.500	80.900	76.000	52.700	19.500	0.10347	0.05227	0.00531
7.	174	0.420	86.600	84.800	82.000	77.200	62.118	20.700	0.12255	0.06253	0.00592
8.	180	0.440	90.000	87.900	84.400	79.000	67.320	22.500	0.13290	0.08030	0.00591
9.	193	0.460	91.800	89.500	85.700	80.000	75.463	23.500	0.14936	0.09149	0.00636
10.	204	0.480	94.800	92.300	88.000	81.600	83.232	25.100	0.16498	0.11148	0.00657
11.	212	0.500	96.300	93.700	88.900	82.100	90.100	25.600	0.17886	0.11828	0.00699
12.	222	0.520	97.900	95.000	90.000	82.900	98.124	26.400	0.19510	0.12972	0.00739
13.	239	0.540	101.300	98.000	92.700	83.200	109.701	26.700	0.21844	0.13419	0.00818
14.	245	0.560	102.300	98.700	91.000	83.500	116.620	27.000	0.23247	0.13877	0.00861
15.	253	0.580	102.400	98.500	91.900	83.800	124.729	27.300	0.24898	0.14344	0.00912
16.	266	0.610	104.100	99.700	93.200	85.200	137.921	28.700	0.27573	0.16666	0.00961

Table-A.6: Collected data during the experiment, HRI-Acetone**Experiment No: 3**

Working Fluid : Acetone , Surface: HRI

Here, V= Supply Voltage (Volt)

I=Line Current (Ampere)

 T_{sat} =Saturated Temperature of Fluid ($^{\circ}\text{C}$) T_{x_1} = Temperature at the point 1 of evaporator geometry ($^{\circ}\text{C}$) T_{x_2} = Temperature at the point 2 of evaporator geometry ($^{\circ}\text{C}$) T_{x_3} =Temperature at the point 3 of evaporator geometry ($^{\circ}\text{C}$) T_{x_4} =Temperature at the point 4 of evaporator geometry ($^{\circ}\text{C}$)

Q = Total Heat Flux (W)

 $\Delta T = T_{x_4} - T_{sat}$ ($^{\circ}\text{C}$)q = Heat Flux Per unit Area After deducting Heat loss (MW/m^2)q R= Heat Flux Found From Rohsenow Correlation (MW/m^2)h = Boiling heat transfer coefficient ($\text{MW}/\text{m}^2 \cdot ^{\circ}\text{C}$) $T_{sat} = 56.5^{\circ}\text{C}$

Obs. No.	V	I	T_{x_1}	T_{x_2}	T_{x_3}	T_{x_4}	Q(W)	$\Delta T^{\circ}\text{C}$	q(MW/m^2)	qR(MW/m^2)	h($\text{MW}/\text{m}^2 \cdot ^{\circ}\text{C}$)
1.	118	0.300	71.000	70.400	69.100	65.000	30.090	8.500	0.05840	0.00433	0.00687
2.	128	0.320	76.300	75.300	74.700	70.800	34.816	14.300	0.06765	0.02062	0.00473
3.	133	0.340	78.000	76.600	74.500	71.200	38.437	14.700	0.07491	0.02239	0.00510
4.	143	0.360	79.900	78.000	75.700	73.100	43.758	16.600	0.08562	0.03225	0.00516
5.	148	0.380	80.900	79.000	76.400	74.500	47.804	18.000	0.09379	0.04112	0.00521
6.	155	0.400	82.500	80.800	76.900	74.800	52.700	18.300	0.10365	0.04321	0.00566
7.	174	0.420	86.300	84.500	82.200	77.100	62.118	20.600	0.12257	0.06163	0.00595
8.	180	0.440	90.100	87.800	84.300	79.100	67.320	22.600	0.13290	0.08138	0.00588
9.	193	0.460	91.700	89.500	85.600	80.000	75.463	23.500	0.14937	0.09149	0.00636
10.	204	0.480	94.700	92.200	88.100	81.500	83.232	25.000	0.16499	0.11016	0.00660
11.	212	0.500	96.200	93.600	88.700	82.000	90.100	25.500	0.17887	0.11690	0.00701
12.	222	0.520	98.000	95.100	90.100	83.000	98.124	26.500	0.19509	0.13120	0.00736
13.	239	0.540	101.200	98.100	92.600	83.300	109.701	26.800	0.21845	0.13570	0.00815
14.	245	0.560	102.400	98.700	91.000	83.800	116.620	27.300	0.23246	0.14344	0.00852
15.	253	0.580	102.500	98.900	91.900	83.900	124.729	27.400	0.24897	0.14502	0.00909
16.	266	0.610	104.200	99.700	93.200	85.100	137.921	28.600	0.27573	0.16493	0.00964

Table-A.7: Collected data during the experiment, HR+-Acetone**Experiment No: 1**

Working Fluid : Acetone , Surface : HR+

Here, V= Supply Voltage (Volt)

I=Line Current (Ampere)

 T_{sat} =Saturated Temperature of Fluid ($^{\circ}\text{C}$) T_{x1} = Temperature at the point 1 of evaporator geometry ($^{\circ}\text{C}$) T_{x2} = Temperature at the point 2 of evaporator geometry ($^{\circ}\text{C}$) T_{x3} =Temperature at the point 3 of evaporator geometry ($^{\circ}\text{C}$) T_{x4} =Temperature at the point 4 of evaporator geometry ($^{\circ}\text{C}$) $\Delta T = T_{x4} - T_{sat}$ ($^{\circ}\text{C}$)

Q = Total Heat input,(W)

q = Heat Flux Per unit Area After deducting Heat loss (MW/m^2)q R= Heat Flux Found From Rohsenow Correlation (MW/m^2)qs = Heat Flux Found From Stephan and Abdelsalam Correlation (MW/m^2)h = Boiling heat transfer coefficient ($\text{MW}/\text{m}^2.\text{^{\circ}\text{C}}$) $T_{sat} = 56.5^{\circ}\text{C}$

Obs. No.	V	I	T_{x1}	T_{x2}	T_{x3}	T_{x4}	Q(W)	$\Delta T^{\circ}\text{C}$	q(MW/m^2)	qR(MW/m^2)	qs(MW/m^2)	h($\text{MW}/\text{m}^2.\text{^{\circ}\text{C}}$)
1	118	0.300	72.900	71.900	71.000	70.100	30.090	13.600	0.058	0.017734	0.030588	0.00428
2	131	0.320	75.700	74.500	73.100	72.000	35.632	15.500	0.069	0.0262533	0.045282	0.00447
3	137	0.340	76.200	74.800	73.400	72.300	39.593	15.800	0.077	0.0278074	0.047963	0.00490
4	145	0.360	77.400	75.800	74.000	72.800	44.370	16.300	0.087	0.0305318	0.052662	0.00534
5	156	0.380	79.000	77.100	75.100	73.800	50.388	17.300	0.099	0.0365029	0.062961	0.00573
6	164	0.400	80.500	78.400	76.100	74.700	55.760	18.200	0.110	0.0425014	0.073307	0.00605
7	174	0.420	81.800	79.500	77.000	75.400	62.118	18.900	0.123	0.0475964	0.082095	0.00650
8	187	0.440	84.600	81.800	78.700	76.900	69.938	20.400	0.139	0.0598521	0.103234	0.00679
9	194	0.460	85.800	82.800	79.500	77.500	75.854	21.000	0.151	0.0652901	0.112614	0.00717
10	205	0.480	88.400	85.000	81.200	79.000	83.640	22.500	0.166	0.0803039	0.13851	0.00739
11	213	0.500	90.100	86.400	82.300	79.900	90.525	23.400	0.180	0.090331	0.155805	0.00770
12	232	0.520	94.400	90.100	85.200	82.200	102.544	25.700	0.204	0.1196709	0.206411	0.00795
13	243	0.540	96.300	91.800	86.500	83.400	111.537	26.900	0.223	0.137229	0.236696	0.00827
14	250	0.560	98.600	93.900	88.200	84.800	119.000	28.300	0.238	0.1597896	0.275609	0.00839
15	256	0.580	99.900	95.000	89.200	85.700	126.208	29.200	0.252	0.1755245	0.302749	0.00864
16	266	0.600	101.500	96.500	90.600	87.000	135.660	30.500	0.271	0.20003	0.345011	0.00890

Table-A.8: Collected data during the experiment, HR+-Acetone.**Experiment No: 2**

Working Fluid : Acetone , Surface : HR+

Here, V= Supply Voltage (Volt)

I=Line Current (Ampere)

 T_{sat} =Saturated Temperature of Fluid ($^{\circ}\text{C}$) T_{x_1} = Temperature at the point 1 of evaporator geometry ($^{\circ}\text{C}$) T_{x_2} = Temperature at the point 2 of evaporator geometry ($^{\circ}\text{C}$) T_{x_3} =Temperature at the point 3 of evaporator geometry ($^{\circ}\text{C}$) T_{x_4} =Temperature at the point 4 of evaporator geometry ($^{\circ}\text{C}$) $\Delta T = T_{x_4} - T_{sat}$ ($^{\circ}\text{C}$)

Q = Total Heat Flux (W)

q = Heat Flux Per unit Area After deducting Heat loss (MW/m^2)q R= Heat Flux Found From Rohsenow Correlation (MW/m^2)h = Boiling heat transfer coefficient ($\text{MW}/\text{m}^2 \cdot ^{\circ}\text{C}$)

$$T_{sat} = 56.5^{\circ}\text{C}$$

Obs. No.	V	I	T_{x_1}	T_{x_2}	T_{x_3}	T_{x_4}	Q(W)	$\Delta T^{\circ}\text{C}$	q(MW/m^2)	qR(MW/m^2)	h($\text{MW}/\text{m}^2 \cdot ^{\circ}\text{C}$)
1	118	0.300	72.800	71.800	71.000	70.200	30.090	13.700	0.058	0.01813	0.00425
2	131	0.320	75.900	74.500	73.200	72.600	35.632	16.100	0.069	0.02942	0.00431
3	135	0.340	76.400	74.900	73.800	72.900	39.015	16.400	0.076	0.0311	0.00465
4	146	0.360	77.800	76.000	74.200	73.000	44.676	16.500	0.088	0.03167	0.00531
5	155	0.380	79.500	77.600	75.200	73.800	50.065	17.300	0.098	0.0365	0.00569
6	163	0.400	80.600	78.600	76.100	74.700	55.420	18.200	0.109	0.0425	0.00601
7	172	0.420	81.700	79.400	76.900	75.300	61.404	18.800	0.121	0.04684	0.00646
8	188	0.440	84.700	81.900	79.000	77.200	70.312	20.700	0.139	0.06253	0.00673
9	196	0.460	86.300	83.500	79.700	78.100	76.636	21.600	0.152	0.07105	0.00704
10	207	0.480	88.600	85.400	81.900	79.300	84.456	22.800	0.168	0.08356	0.00736
11	216	0.500	90.500	87.300	83.200	80.700	91.800	24.200	0.183	0.09992	0.00755
12	229	0.520	94.000	90.100	85.100	82.000	101.218	25.500	0.202	0.1169	0.00791
13	242	0.540	96.200	91.700	86.500	83.300	111.078	26.800	0.222	0.1357	0.00827
14	251	0.560	98.700	94.000	88.400	84.900	119.476	28.400	0.239	0.16149	0.00840
15	257	0.580	99.800	95.200	89.200	85.700	126.701	29.200	0.253	0.17552	0.00867
16	265	0.600	101.000	96.000	90.500	86.800	135.150	30.300	0.270	0.19612	0.00892

Table-A.9: Collected data during the experiment, HR+-Acetone**Experiment No: 3**

Working Fluid : Acetone , Surface : HR+

Here, V= Supply Voltage (Volt)

I=Line Current (Ampere)

 T_{sat} =Saturated Temperature of Fluid ($^{\circ}\text{C}$) T_{x1} = Temperature at the point 1 of evaporator geometry ($^{\circ}\text{C}$) T_{x2} = Temperature at the point 2 of evaporator geometry ($^{\circ}\text{C}$) T_{x3} =Temperature at the point 3 of evaporator geometry ($^{\circ}\text{C}$) T_{x4} =Temperature at the point 4 of evaporator geometry ($^{\circ}\text{C}$) $\Delta T = T_{x4} - T_{sat}$ ($^{\circ}\text{C}$)

Q = Total Heat Flux (W)

q = Heat Flux Per unit Area After deducting Heat loss (MW/m^2)q R= Heat Flux Found From Rohsenow Correlation (MW/m^2)h = Boiling heat transfer coefficient ($\text{MW}/\text{m}^2 \cdot ^{\circ}\text{C}$) $T_{sat} = 56.5^{\circ}\text{C}$

Obs. No.	V	I	T_{x1}	T_{x2}	T_{x3}	T_{x4}	Q(W)	$\Delta T^{\circ}\text{C}$	q(MW/m^2)	qR(MW/m^2)	h($\text{MW}/\text{m}^2 \cdot ^{\circ}\text{C}$)
1	118	0.300	73.100	72.300	71.400	70.700	30.090	14.200	0.058	0.020186	0.00410
2	132	0.320	75.800	74.500	73.200	72.700	35.904	16.200	0.070	0.029973	0.00432
3	137	0.340	76.700	74.900	73.400	72.900	39.593	16.400	0.077	0.031097	0.00472
4	146	0.360	77.900	76.100	74.300	73.800	44.676	17.300	0.088	0.036503	0.00507
5	154	0.380	79.100	77.500	75.900	74.800	49.742	18.300	0.098	0.043206	0.00535
6	159	0.400	80.700	79.000	77.100	76.000	54.060	19.500	0.107	0.052275	0.00546
7	172	0.420	82.200	80.500	78.100	76.000	61.404	19.500	0.121	0.052275	0.00623
8	181	0.440	84.800	82.600	80.100	78.500	67.694	22.000	0.134	0.075068	0.00609
9	196	0.460	86.500	83.700	81.500	79.500	76.636	23.000	0.152	0.085777	0.00661
10	203	0.480	89.200	86.000	82.600	80.600	82.824	24.100	0.165	0.098683	0.00683
11	214	0.500	91.200	87.800	84.100	82.000	90.950	25.500	0.181	0.116899	0.00710
12	225	0.520	94.000	90.800	85.900	83.000	99.450	26.500	0.198	0.131198	0.00747
13	240	0.540	95.900	91.700	86.600	83.900	110.160	27.400	0.220	0.145024	0.00802
14	249	0.560	99.000	93.800	88.700	85.000	118.524	28.500	0.237	0.163201	0.00830
15	255	0.580	100.600	95.800	90.000	86.200	125.715	29.700	0.251	0.184696	0.00846
16	262	0.600	101.600	96.600	91.500	87.500	133.620	31.000	0.267	0.210027	0.00862

Table-A.10: Collected data during the experiment, HRO-Ethanol

Experiment No: 1

Working Fluid : Ethanol , Surface : HRO

Here, V= Supply Voltage (Volt)

I=Line Current (Ampere)

 T_{sat} =Saturated Temperature of Fluid ($^{\circ}\text{C}$) T_{x_1} = Temperature at the point 1 of evaporator geometry ($^{\circ}\text{C}$) T_{x_2} = Temperature at the point 2 of evaporator geometry ($^{\circ}\text{C}$) T_{x_3} =Temperature at the point 3 of evaporator geometry ($^{\circ}\text{C}$) T_{x_4} =Temperature at the point 4 of evaporator geometry ($^{\circ}\text{C}$)

Q = Total Heat Input(W)

 $\Delta T = T_{x_4} - T_{sat}$ ($^{\circ}\text{C}$)q = Heat Flux Per unit Area After deducting Heat loss (MW/m^2)h = Boiling heat transfer coefficient ($\text{MW}/\text{m}^2 \cdot ^{\circ}\text{C}$)

$$T_{sat} = 78^{\circ}\text{C}$$

Obs. No.	V	I	T_{x_1}	T_{x_2}	T_{x_3}	T_{x_4}	Q	ΔT	q(MW/m^2)	h($\text{MW}/\text{m}^2 \cdot ^{\circ}\text{C}$)
1.	150	0.36	103.20	95.40	94.20	92.00	45.900	14.0	0.08833	.0063
2.	156	0.38	104.20	96.00	94.60	92.80	50.388	14.8	0.09741	.0065
3.	161	0.40	104.50	95.30	93.50	93.5	54.740	15.5	0.10625	.0068
4.	170	0.42	106.50	96.30	94.50	93.8	60.690	15.8	0.11823	.0074
5.	180	0.44	109.00	98.00	95.80	93.9	67.320	15.9	0.13156	.0082
6.	195	0.46	112.80	100.20	97.60	95.5	76.245	17.5	0.14947	.0085
7.	207	0.48	116.00	102.10	99.00	96.5	84.456	18.5	0.16597	.0089
8.	219	0.50	118.20	103.20	100.00	97.4	93.075	19.4	0.18338	.0094
9.	225	0.52	122.00	105.00	101.80	98.8	99.450	20.8	0.19610	.0094
10.	241	0.54	127.60	108.60	104.10	101.4	110.619	23.4	0.21845	.0094

Table-A.11: Collected data during the experiment, HRO-Ethanol**Experiment No: 2**

Working Fluid : Ethanol , Surface : HRO

Here, V= Supply Voltage (Volt)

I=Line Current (Ampere)

 T_{sat} =Saturated Temperature of Fluid ($^{\circ}\text{C}$) T_{x1} = Temperature at the point 1 of evaporator geometry ($^{\circ}\text{C}$) T_{x2} = Temperature at the point 2 of evaporator geometry ($^{\circ}\text{C}$) T_{x3} =Temperature at the point 3 of evaporator geometry ($^{\circ}\text{C}$) T_{x4} =Temperature at the point 4 of evaporator geometry ($^{\circ}\text{C}$)

Q = Total Heat Input(W)

 $\Delta T = T_{x4} - T_{sat}$ ($^{\circ}\text{C}$)q = Heat Flux Per unit Area After deducting Heat loss (MW/m^2)q R= Heat Flux Found From Rohsenow Correlation (MW/m^2)h = Boiling heat transfer coefficient ($\text{MW}/\text{m}^2 \cdot ^{\circ}\text{C}$)

$$T_{sat} = 78^{\circ}\text{C}$$

Obs. No.	V	I	T_{x1}	T_{x2}	T_{x3}	T_{x4}	Q	ΔT	q(MW/m^2)	qR(MW/m^2)	h($\text{MW}/\text{m}^2 \cdot ^{\circ}\text{C}$)
1.	152	0.390	103.400	96.000	94.600	93.500	50.388	15.500	0.097	0.065	0.00629
2.	164	0.420	107.400	98.500	96.800	94.000	58.548	16.000	0.114	0.072	0.00711
3.	188	0.450	114.700	103.000	100.500	95.400	71.910	17.400	0.141	0.092	0.00808
4.	198	0.470	118.200	105.200	102.300	96.300	79.101	18.300	0.155	0.107	0.00847
5.	203	0.480	118.200	105.400	102.500	97.100	82.824	19.100	0.162	0.122	0.00851
6.	210	0.500	121.600	106.900	103.600	97.600	89.250	19.600	0.175	0.132	0.00895
7.	218	0.500	122.800	107.400	103.900	98.000	92.650	20.000	0.182	0.140	0.00911
8.	221	0.510	124.100	108.400	104.700	98.500	95.804	20.500	0.189	0.151	0.00920
9.	227	0.520	127.400	110.100	106.100	98.900	100.334	20.900	0.198	0.160	0.00945
10.	238	0.530	131.000	112.400	108.000	99.900	107.219	21.900	0.211	0.184	0.00965
11.	240	0.540	131.400	112.500	108.200	101.100	110.160	23.100	0.217	0.216	0.00940

Table-A.12: Collected data during the experiment, HRO-Ethanol

Experiment No: 3

Working Fluid : Ethanol , Surface : HRO

Here, V= Supply Voltage (Volt)

I=Line Current (Ampere)

 T_{sat} =Saturated Temperature of Fluid ($^{\circ}\text{C}$) T_{x_1} = Temperature at the point 1 of evaporator geometry ($^{\circ}\text{C}$) T_{x_2} = Temperature at the point 2 of evaporator geometry ($^{\circ}\text{C}$) T_{x_3} =Temperature at the point 3 of evaporator geometry ($^{\circ}\text{C}$) T_{x_4} =Temperature at the point 4 of evaporator geometry ($^{\circ}\text{C}$)

Q = Total Heat Input(W)

 $\Delta T = T_{x_4} - T_{sat}$ ($^{\circ}\text{C}$)q = Heat Flux Per unit Area After deducting Heat loss (MW/m^2)q R= Heat Flux Found From Rohsenow Correlation (MW/m^2)h = Boiling heat transfer coefficient ($\text{MW}/\text{m}^2 \cdot ^{\circ}\text{C}$)

$$T_{sat} = 78^{\circ}\text{C}$$

Obs. No.	V	I	T_{x_1}	T_{x_2}	T_{x_3}	T_{x_4}	Q	ΔT	q(MW/m^2)	qR(MW/m^2)	h($\text{MW}/\text{m}^2 \cdot ^{\circ}\text{C}$)
1.	151	0.360	103.200	95.500	94.300	93.000	46.206	15.000	0.089	0.059	0.00593
2.	157	0.380	104.400	96.100	94.600	93.100	50.711	15.100	0.098	0.060	0.00649
3.	162	0.400	104.500	96.800	95.000	93.500	55.080	15.500	0.107	0.065	0.00690
4.	171	0.420	106.500	97.400	95.500	93.800	61.047	15.800	0.119	0.069	0.00753
5.	180	0.440	109.000	98.000	95.800	93.900	67.320	15.900	0.132	0.070	0.00827
6.	196	0.460	113.000	100.300	97.700	95.400	76.636	17.400	0.150	0.092	0.00864
7.	208	0.480	116.100	102.100	99.000	96.500	84.864	18.500	0.167	0.111	0.00902
8.	220	0.500	118.500	103.400	100.000	97.300	93.500	19.300	0.184	0.126	0.00955
9.	226	0.520	122.100	105.600	101.700	98.700	99.892	20.700	0.197	0.155	0.00952
10.	241	0.530	127.700	108.700	104.100	101.400	108.571	23.400	0.214	0.224	0.00916

Table-A.13: Collected data during the experiment, HRI-Ethanol**Experiment No: 1**

Working Fluid : Ethanol , Surface : HRI

Here, V= Supply Voltage (Volt)

I=Line Current (Ampere)

 T_{sat} =Saturated Temperature of Fluid ($^{\circ}\text{C}$) T_{x_1} = Temperature at the point 1 of evaporator geometry ($^{\circ}\text{C}$) T_{x_2} = Temperature at the point 2 of evaporator geometry ($^{\circ}\text{C}$) T_{x_3} =Temperature at the point 3 of evaporator geometry ($^{\circ}\text{C}$) T_{x_4} =Temperature at the point 4 of evaporator geometry ($^{\circ}\text{C}$)

Q = Total Heat Flux (W)

 $\Delta T = T_{x_4} - T_{sat}$ ($^{\circ}\text{C}$)q = Heat Flux Per unit Area After deducting Heat loss (MW/m^2)h = Boiling heat transfer coefficient ($\text{MW}/\text{m}^2 \cdot ^{\circ}\text{C}$) $T_{sat} = 78^{\circ}\text{C}$

Obs. No.	V	I	T_{x_1}	T_{x_2}	T_{x_3}	T_{x_4}	Q	ΔT	q(MW/m^2)	h($\text{MW}/\text{m}^2 \cdot ^{\circ}\text{C}$)
1.	159	0.4	97.7	96.5	92.4	87.4	54.06	9.4	0.105345	.0112
2.	169	0.42	98.3	96.9	93.4	88.8	60.333	10.8	0.118082	.0109
3.	180	0.44	99.3	97.7	94.7	90.1	67.32	13.1	0.132245	.0100
4.	192	0.46	102.2	100.2	96.9	92	75.072	14.0	0.147833	.0105
5.	202	0.48	105.3	102.9	99.2	92.9	82.416	14.9	0.162575	.0109
6.	212	0.5	107.2	104.5	100.3	94.6	90.1	16.6	0.178094	.0107
7.	224	0.52	109.3	106.5	101.7	95.6	99.008	17.6	0.196093	.0111
8.	235	0.54	112.7	109.4	104	97	107.865	19.0	0.213896	.01125
9.	242	0.56	113.5	110.9	104.4	97.5	115.192	19.5	0.228766	.01173
10.	254	0.58	116.2	112.2	106	98.5	125.222	20.5	0.249009	.0121
11.	266	0.6	116.9	113	106.4	98.7	135.66	20.7	0.270223	.0130

Table-A.14: Collected data during the experiment, HRI-Ethanol

Experiment No: 2

Working Fluid : Ethanol , Surface: HRI

Here, V= Supply Voltage (Volt)

I= Line Current (Ampere)

 T_{sat} = Saturated Temperature of Fluid ($^{\circ}\text{C}$) T_{x_1} = Temperature at the point 1 of evaporator geometry ($^{\circ}\text{C}$) T_{x_2} = Temperature at the point 2 of evaporator geometry ($^{\circ}\text{C}$) T_{x_3} = Temperature at the point 3 of evaporator geometry ($^{\circ}\text{C}$) T_{x_4} = Temperature at the point 4 of evaporator geometry ($^{\circ}\text{C}$)

Q = Total Heat Input (W)

 $\Delta T = T_{x_4} - T_{sat}$ ($^{\circ}\text{C}$)q = Heat Flux Per unit Area After deducting Heat loss (MW/m^2)qR = Heat Flux Found From Rohsenow Correlation (MW/m^2)h = Boiling heat transfer coefficient ($\text{MW}/\text{m}^2 \cdot ^{\circ}\text{C}$)

$$T_{sat} = 78^{\circ}\text{C}$$

Obs. No.	V	I	T_{x_1}	T_{x_2}	T_{x_3}	T_{x_4}	Q	ΔT	q(MW/m^2)	qR(MW/m^2)	h($\text{MW}/\text{m}^2 \cdot ^{\circ}\text{C}$)
1.	159	0.420	97.500	95.000	92.300	87.300	56.763	9.300	0.111	0.01408	0.01192
2.	169	0.440	98.200	95.700	93.200	88.700	63.206	10.700	0.124	0.02144	0.01158
3.	179	0.460	99.200	97.600	94.600	90.000	69.989	12.000	0.138	0.03024	0.01147
4.	191	0.480	102.100	100.100	96.900	91.900	77.928	13.900	0.154	0.04700	0.01105
5.	202	0.500	109.200	102.900	99.100	92.800	85.850	14.800	0.169	0.05673	0.01144
6.	212	0.520	107.000	104.400	100.200	94.600	93.704	16.600	0.185	0.08005	0.01117
7.	225	0.540	109.300	106.400	101.700	95.500	103.275	17.500	0.205	0.09379	0.01170
8.	236	0.560	112.700	109.300	104.000	97.000	112.336	19.000	0.223	0.12003	0.01174
9.	242	0.580	113.400	100.900	104.400	97.400	119.306	19.400	0.237	0.12777	0.01222
10.	254	0.600	116.200	112.200	106.000	98.400	129.540	20.400	0.258	0.14857	0.01264
11.	267	0.61	116.900	113.000	106.300	98.700	138.440	20.700	0.276	0.15522	0.01333

Table-A.15: Collected data during the experiment, HRI-Ethanol**Experiment No: 3**

Working Fluid : Ethanol , Surface :HRI

Here, V= Supply Voltage (Volt)

I=Line Current (Ampere)

 T_{sat} =Saturated Temperature of Fluid ($^{\circ}\text{C}$) T_{x_1} = Temperature at the point 1 of evaporator geometry ($^{\circ}\text{C}$) T_{x_2} = Temperature at the point 2 of evaporator geometry ($^{\circ}\text{C}$) T_{x_3} =Temperature at the point 3 of evaporator geometry ($^{\circ}\text{C}$) T_{x_4} =Temperature at the point 4 of evaporator geometry ($^{\circ}\text{C}$)

Q = Total Heat Input(W)

 $\Delta T = T_{x_4} - T_{sat}$ ($^{\circ}\text{C}$)q = Heat Flux Per unit Area After deducting Heat loss (MW/m^2)q R= Heat Flux Found From Rohsenow Correlation (MW/m^2)h = Boiling heat transfer coefficient ($\text{MW}/\text{m}^2 \cdot ^{\circ}\text{C}$) $T_{sat} = 78^{\circ}\text{C}$

Obs. No.	V	I	T_{x_1}	T_{x_2}	T_{x_3}	T_{x_4}	Q	ΔT	q(MW/m^2)	qR(MW/m^2)	h($\text{MW}/\text{m}^2 \cdot ^{\circ}\text{C}$)
1.	159	0.420	97.700	96.500	94.500	89.000	56.763	11.000	0.111	0.02329	0.01008
2.	169	0.440	98.400	96.900	94.300	90.300	63.206	12.300	0.124	0.03257	0.01008
3.	178	0.460	99.800	98.300	95.600	90.900	69.598	12.900	0.137	0.03757	0.01061
4.	191	0.480	101.900	100.000	96.800	91.900	77.928	13.900	0.154	0.04700	0.01106
5.	202	0.500	105.500	103.800	100.300	92.700	85.850	14.700	0.170	0.05559	0.01153
6.	210	0.520	106.400	104.000	100.100	94.900	92.820	16.900	0.184	0.08447	0.01087
7.	220	0.540	109.400	106.600	102.200	95.300	100.980	17.300	0.200	0.09061	0.01157
8.	242	0.560	110.000	106.700	101.500	96.400	115.192	18.400	0.229	0.10902	0.01245
9.	236	0.580	112.100	108.000	102.100	96.800	116.348	18.800	0.231	0.11628	0.01230
10.	250	0.600	113.200	109.400	103.600	97.000	127.500	19.000	0.254	0.12003	0.01336
11.	258	0.61	115.400	111.400	105.100	98.100	133.773	20.100	0.266	0.14211	0.01326
12.	266	0.620	117.000	113.000	105.800	98.200	140.182	20.200	0.279	0.14424	0.01383

Table-A.16: Collected data during the experiment, HR+-Ethanol**Experiment No: 1**

Working Fluid : Ethanol , Surface : HR+

Here, V= Supply Voltage (Volt)

I=Line Current (Ampere)

 T_{sat} =Saturated Temperature of Fluid ($^{\circ}\text{C}$) T_{x1} = Temperature at the point 1 of evaporator geometry ($^{\circ}\text{C}$) T_{x2} = Temperature at the point 2 of evaporator geometry ($^{\circ}\text{C}$) T_{x3} =Temperature at the point 3 of evaporator geometry ($^{\circ}\text{C}$) T_{x4} =Temperature at the point 4 of evaporator geometry ($^{\circ}\text{C}$)

Q = Total Heat Flux (W)

 $\Delta T = T_{x4} - T_{sat}$ ($^{\circ}\text{C}$)q = Heat Flux Per unit Area After deducting Heat loss (MW/m^2)q R= Heat Flux Found From Rohsenow Correlation (MW/m^2)qs = Heat Flux Found From Stephan and Abdelsalam Correlation (MW/m^2)h = Boiling heat transfer coefficient ($\text{MW}/\text{m}^2 \cdot ^{\circ}\text{C}$)

$$T_{sat} = 78^{\circ}\text{C}$$

Obs. No.	V	I	T_{x1}	T_{x2}	T_{x3}	T_{x4}	Q	ΔT	q(MW/m^2)	qR(MW/m^2)	qS(MW/m^2)	h($\text{MW}/\text{m}^2 \cdot ^{\circ}\text{C}$)
1.	158	0.400	84.200	82.300	80.300	79.000	53.720	1.000	0.106	0.00002	0.00002	0.10561
2.	167	0.420	85.600	83.400	81.100	79.800	59.619	1.800	0.118	0.00010	0.00011	0.06529
3.	174	0.440	87.900	85.300	82.700	81.100	65.076	3.100	0.128	0.00052	0.00059	0.04145
4.	190	0.460	90.000	87.100	84.000	82.300	74.290	4.300	0.147	0.00139	0.00156	0.03421
5.	202	0.480	93.400	90.000	86.200	84.100	82.416	6.100	0.163	0.00397	0.00447	0.02679
6.	213	0.500	94.100	90.600	86.700	84.500	90.525	6.500	0.180	0.00481	0.00540	0.02767
7.	224	0.520	96.500	92.700	88.200	85.800	99.008	7.800	0.197	0.00830	0.00934	0.02526
8.	245	0.540	100.800	96.300	91.400	88.400	112.455	10.400	0.224	0.01969	0.02214	0.02155
9.	252	0.560	102.400	97.600	92.500	89.300	119.952	11.300	0.239	0.02525	0.02840	0.02117
10.	260	0.580	104.400	99.300	93.900	90.600	128.180	12.600	0.256	0.03501	0.03937	0.02031
11.	271	0.600	106.600	101.000	95.200	91.700	138.210	13.700	0.276	0.04500	0.05060	0.02016

Table-A.17: Collected data during the experiment, HR+-Ethanol

Experiment No: 2

Working Fluid : Ethanol , Surface: Ethanol

Here, V= Supply Voltage (Volt)

I=Line Current (Ampere)

 T_{sat} =Saturated Temperature of Fluid ($^{\circ}\text{C}$) T_{x_1} = Temperature at the point 1 of evaporator geometry ($^{\circ}\text{C}$) T_{x_2} = Temperature at the point 2 of evaporator geometry ($^{\circ}\text{C}$) T_{x_3} =Temperature at the point 3 of evaporator geometry ($^{\circ}\text{C}$) T_{x_4} =Temperature at the point 4 of evaporator geometry ($^{\circ}\text{C}$)

Q = Total Heat Flux (W)

 $\Delta T = T_{x_4} - T_{sat}$ ($^{\circ}\text{C}$)q = Heat Flux Per unit Area After deducting Heat loss (MW/m^2)q R= Heat Flux Found From Rohsenow Correlation (MW/m^2)h = Boiling heat transfer coefficient ($\text{MW}/\text{m}^2 \cdot ^{\circ}\text{C}$)

$$T_{sat} = 78^{\circ}\text{C}$$

Obs. No.	V	I	T_{x_1}	T_{x_2}	T_{x_3}	T_{x_4}	Q	ΔT	q(MW/m^2)	qR(MW/m^2)	h($\text{MW}/\text{m}^2 \cdot ^{\circ}\text{C}$)
1.	158	0.400	84.300	82.400	80.300	79.300	53.720	1.300	0.106	0.00004	0.08123
2.	170	0.420	86.800	84.500	82.200	80.500	60.690	2.500	0.120	0.00027	0.04785
3.	180	0.440	88.700	86.400	84.000	82.200	67.320	4.200	0.133	0.00130	0.03167
4.	191	0.460	91.000	88.300	85.300	83.200	74.681	5.200	0.148	0.00246	0.02843
5.	201	0.480	93.300	90.000	86.500	84.500	82.008	6.500	0.163	0.00481	0.02501
6.	213	0.500	94.200	91.400	87.800	85.000	90.525	7.000	0.180	0.00600	0.02570
7.	222	0.520	96.500	93.800	88.500	85.900	98.124	7.900	0.195	0.00863	0.02471
8.	245	0.540	100.700	96.600	92.000	89.000	112.455	11.000	0.224	0.02329	0.02037
9.	250	0.560	103.100	98.300	93.500	90.200	119.000	12.200	0.237	0.03178	0.01945
10.	260	0.580	104.900	100.200	95.100	92.000	128.180	14.000	0.256	0.04802	0.01827
11.	265	0.600	106.500	101.300	96.000	92.600	135.150	14.600	0.270	0.05446	0.01849

Table-A.18: Collected data during the experiment, HR+-Ethanol**Experiment No: 3**

Working Fluid : Ethanol , Surface: Ethanol

Here, V= Supply Voltage (Volt)

I=Line Current (Ampere)

 T_{sat} =Saturated Temperature of Fluid ($^{\circ}\text{C}$) T_{x_1} = Temperature at the point 1 of evaporator geometry ($^{\circ}\text{C}$) T_{x_2} = Temperature at the point 2 of evaporator geometry ($^{\circ}\text{C}$) T_{x_3} =Temperature at the point 3 of evaporator geometry ($^{\circ}\text{C}$) T_{x_4} =Temperature at the point 4 of evaporator geometry ($^{\circ}\text{C}$)

Q = Total Heat Flux (W)

 $\Delta T = T_{x_4} - T_{sat}$ ($^{\circ}\text{C}$)q = Heat Flux Per unit Area After deducting Heat loss (MW/m^2)q R= Heat Flux Found From Rohsenow Correlation (MW/m^2)h = Boiling heat transfer coefficient ($\text{MW}/\text{m}^2 \cdot ^{\circ}\text{C}$) $T_{sat} = 78^{\circ}\text{C}$

Obs. No.	V	I	T_{x_1}	T_{x_2}	T_{x_3}	T_{x_4}	Q	ΔT	q(MW/m^2)	qR(MW/m^2)	h($\text{MW}/\text{m}^2 \cdot ^{\circ}\text{C}$)
1.	158	0.400	84.800	82.600	80.500	79.600	53.720	1.100	0.106	0.00002	0.09597
2.	169	0.420	86.600	84.400	81.900	80.400	60.333	1.900	0.119	0.00012	0.06258
3.	181	0.440	89.500	87.200	84.000	83.000	67.694	4.500	0.134	0.00159	0.02971
4.	190	0.460	91.000	88.100	85.100	83.500	74.290	5.000	0.147	0.00219	0.02941
5.	200	0.480	92.000	90.300	86.700	84.600	81.600	6.100	0.162	0.00397	0.02653
6.	214	0.500	93.100	91.000	87.500	85.300	90.950	6.800	0.181	0.00550	0.02659
7.	224	0.520	96.700	93.300	89.200	86.800	99.008	8.300	0.197	0.01001	0.02373
8.	242	0.540	99.900	96.000	91.500	88.500	111.078	10.000	0.221	0.01750	0.02213
9.	251	0.560	103.300	98.300	94.000	91.000	119.476	12.500	0.238	0.03418	0.01906
10.	260	0.580	105.600	100.600	95.300	92.200	128.180	13.700	0.256	0.04500	0.01867
11.	266	0.600	107.000	102.000	96.400	93.300	135.660	14.800	0.271	0.05673	0.01831

Table-A.19: Collected data during the experiment, HRO-Methanol

Experiment No: 1

Working Fluid : Methanol , Surface : HRO

Here, V= Supply Voltage (Volt)

I=Line Current (Ampere)

 T_{sat} =Saturated Temperature of Fluid ($^{\circ}\text{C}$) T_{x1} = Temperature at the point 1 of evaporator geometry ($^{\circ}\text{C}$) T_{x2} = Temperature at the point 2 of evaporator geometry ($^{\circ}\text{C}$) T_{x3} =Temperature at the point 3 of evaporator geometry ($^{\circ}\text{C}$) T_{x4} =Temperature at the point 4 of evaporator geometry ($^{\circ}\text{C}$)

Q = Total Heat Input (W)

 $\Delta T = T_{x4} - T_{sat}$ ($^{\circ}\text{C}$)q = Heat Flux Per unit Area After deducting Heat loss (MW/m^2)q R= Heat Flux Found From Rohsenow Correlation (MW/m^2)qs = Heat Flux Found From Stephan and Abdelsalam Correlation (MW/m^2)h = Boiling heat transfer coefficient ($\text{MW}/\text{m}^2 \cdot ^{\circ}\text{C}$) $T_{sat} = 65^{\circ}\text{C}$

Obs. No.	V	I	T_{x1}	T_{x2}	T_{x3}	T_{x4}	Q	ΔT	q(MW/m^2)	qR(MW/m^2)	qS(MW/m^2)	h($\text{MW}/\text{m}^2 \cdot ^{\circ}\text{C}$)
1.	125	0.310	78.500	78.300	77.000	76.000	32.938	11.000	0.064	0.040	0.02080	0.005788
2.	130	0.320	81.400	81.000	79.400	78.200	35.360	13.200	0.068	0.069	0.03594	0.005182
3.	135	0.330	82.600	82.200	80.900	79.800	37.868	14.800	0.073	0.097	0.05065	0.004961
4.	146	0.340	86.300	85.500	83.500	82.000	42.194	17.000	0.082	0.147	0.07677	0.004822
5.	160	0.350	88.000	87.500	85.700	84.500	47.600	19.500	0.093	0.222	0.11586	0.004763
6.	170	0.380	91.000	90.200	88.000	86.500	54.910	21.500	0.108	0.298	0.15529	0.005002
7.	178	0.390	91.600	91.000	89.000	87.600	59.007	22.600	0.116	0.346	0.18036	0.005126
8.	185	0.410	93.000	91.200	88.800	88.000	64.473	23.000	0.127	0.365	0.19011	0.005517
9.	190	0.420	94.600	92.900	91.200	89.100	67.830	24.100	0.134	0.419	0.21871	0.005544
10.	210	0.460	97.000	95.900	92.200	89.800	82.110	24.800	0.163	0.457	0.23833	0.006554
11.	212	0.470	98.500	96.200	93.100	90.300	84.694	25.300	0.168	0.485	0.25304	0.006628

Table-A.20: Collected data during the experiment, HRO-Methanol**Experiment No: 2**

Working Fluid : Methanol , Surface : HRO

Here, V= Supply Voltage (Volt)

I=Line Current (Ampere)

 T_{sat} =Saturated Temperature of Fluid ($^{\circ}\text{C}$) T_{x_1} = Temperature at the point 1 of evaporator geometry ($^{\circ}\text{C}$) T_{x_2} = Temperature at the point 2 of evaporator geometry ($^{\circ}\text{C}$) T_{x_3} =Temperature at the point 3 of evaporator geometry ($^{\circ}\text{C}$) T_{x_4} =Temperature at the point 4 of evaporator geometry ($^{\circ}\text{C}$)

Q = Total Heat Input(W)

 $\Delta T = T_{x_4} - T_{sat}$ ($^{\circ}\text{C}$)q = Heat Flux Per unit Area After deducting Heat loss (MW/m^2)q R= Heat Flux Found From Rohsenow Correlation (MW/m^2)h = Boiling heat transfer coefficient ($\text{MW}/\text{m}^2 \cdot ^{\circ}\text{C}$) $T_{sat} = 65^{\circ}\text{C}$

Obs. No.	V	I	T_{x_1}	T_{x_2}	T_{x_3}	T_{x_4}	Q	ΔT	q(MW/m^2)	qR(MW/m^2)	h($\text{MW}/\text{m}^2 \cdot ^{\circ}\text{C}$)
1.	132	0.310	76.200	75.900	74.500	73.600	34.782	8.600	0.068	0.019	0.00786
2.	144	0.320	83.000	81.500	80.600	78.000	39.168	13.000	0.076	0.066	0.00585
3.	155	0.350	86.500	85.200	83.300	82.000	46.113	17.000	0.090	0.147	0.00529
4.	164	0.370	88.700	87.700	85.600	84.000	51.578	19.000	0.101	0.205	0.00531
5.	169	0.380	89.500	88.300	86.100	84.500	54.587	19.500	0.107	0.222	0.00549
6.	172	0.380	90.600	89.000	86.300	84.600	55.556	19.600	0.109	0.226	0.00556
7.	178	0.390	91.700	90.000	87.400	85.500	59.007	20.500	0.116	0.258	0.00565
8.	184	0.410	93.300	91.500	88.600	86.400	64.124	21.400	0.126	0.294	0.00590
9.	190	0.420	94.500	92.800	89.900	87.500	67.830	22.500	0.134	0.341	0.00594
10.	196	0.430	96.900	94.900	91.700	89.000	71.638	24.000	0.141	0.414	0.00588
11.	211	0.470	98.500	96.300	93.000	90.200	84.295	25.200	0.167	0.479	0.00662

Table-A.21: Collected data during the experiment, HRO-Methanol**Experiment No: 3**

Working Fluid : Methanol , Surface : HRO

Here, V= Supply Voltage (Volt)

I=Line Current (Ampere)

 T_{sat} =Saturated Temperature of Fluid ($^{\circ}\text{C}$) T_{x_1} = Temperature at the point 1 of evaporator geometry ($^{\circ}\text{C}$) T_{x_2} = Temperature at the point 2 of evaporator geometry ($^{\circ}\text{C}$) T_{x_3} =Temperature at the point 3 of evaporator geometry ($^{\circ}\text{C}$) T_{x_4} =Temperature at the point 4 of evaporator geometry ($^{\circ}\text{C}$)

Q = Total Heat Input (W)

 $\Delta T = T_{x_4} - T_{sat}$ ($^{\circ}\text{C}$)q = Heat Flux Per unit Area After deducting Heat loss (MW/m^2)q R= Heat Flux Found From Rohsenow Correlation (MW/m^2)h = Boiling heat transfer coefficient ($\text{MW}/\text{m}^2 \cdot ^{\circ}\text{C}$)

$$T_{sat} = 65^{\circ}\text{C}$$

Obs. No.	V	I	T_{x_1}	T_{x_2}	T_{x_3}	T_{x_4}	Q	ΔT	q(MW/m^2)	qR(MW/m^2)	h($\text{MW}/\text{m}^2 \cdot ^{\circ}\text{C}$)
1.	132	0.310	75.100	74.900	73.700	72.600	34.782	7.600	0.068	0.01315	0.008904
2.	144	0.320	80.500	78.100	76.000	75.000	39.168	10.000	0.076	0.02996	0.007622
3.	155	0.350	85.500	84.600	82.700	80.500	46.113	15.500	0.090	0.11157	0.005808
4.	171	0.370	90.500	89.100	86.600	84.000	53.780	19.000	0.105	0.20550	0.005541
5.	184	0.410	93.400	91.600	88.500	86.200	64.124	21.200	0.126	0.28546	0.005951
6.	190	0.420	94.000	92.200	89.300	86.800	67.830	21.800	0.135	0.31039	0.006196
7.	196	0.440	96.700	93.900	90.700	88.100	73.304	23.100	0.145	0.36930	0.006261
8.	200	0.450	97.100	94.500	91.200	88.900	76.500	23.900	0.151	0.40901	0.006322
9.	206	0.460	97.800	95.500	91.900	89.500	80.540	24.500	0.159	0.44060	0.006501
10.	211	0.470	98.600	96.300	92.800	90.000	84.300	25.000	0.167	0.46813	0.006675

Table-A.22: Collected data during the experiment, HRI-Methanol

Experiment No: 1

Working Fluid : Methanol

Here, V= Supply Voltage (Volt)

I=Line Current (Ampere)

 T_{sat} =Saturated Temperature of Fluid ($^{\circ}\text{C}$) T_{x1} = Temperature at the point 1 of evaporator geometry ($^{\circ}\text{C}$) T_{x2} = Temperature at the point 2 of evaporator geometry ($^{\circ}\text{C}$) T_{x3} =Temperature at the point 3 of evaporator geometry ($^{\circ}\text{C}$) T_{x4} =Temperature at the point 4 of evaporator geometry ($^{\circ}\text{C}$)

Q = Total Heat Input(W)

 $\Delta T = T_{x4} - T_{sat}$ ($^{\circ}\text{C}$)q = Heat Flux Per unit Area After deducting Heat loss (MW/m²)h = Boiling heat transfer coefficient (MW/m². $^{\circ}\text{C}$) $T_{sat} = 65^{\circ}\text{C}$

Obs. No.	V	I	T_{x1}	T_{x2}	T_{x3}	T_{x4}	Q	ΔT	q(MW/m ²)	h(MW/m ² . $^{\circ}\text{C}$)
1.	142	0.34	74.90	73.70	71.60	69.60	41.038	4.60	0.08043	0.017484
2.	150	0.36	76.90	74.40	72.10	70.00	45.900	5.00	0.09019	0.018038
3.	158	0.38	77.10	75.00	73.00	70.80	51.034	5.80	0.10064	0.017351
4.	168	0.40	79.10	76.90	74.50	72.00	57.120	7.00	0.11289	0.016128
5.	176	0.42	80.90	78.90	75.60	72.80	62.832	7.80	0.12440	0.015949
6.	183	0.44	81.90	79.80	76.40	73.40	68.442	8.40	0.13576	0.016162
7.	196	0.46	84.60	82.20	78.50	74.80	76.636	9.80	0.15226	0.015537
8.	207	0.48	87.30	84.40	80.00	76.30	84.456	11.30	0.16800	0.014868
9.	214	0.50	88.20	85.30	80.70	76.70	90.950	11.70	0.18117	0.015485
10.	222	0.52	90.00	86.70	81.70	77.40	98.124	12.40	0.19566	0.015779
11.	236	0.54	93.80	90.20	84.10	79.40	108.324	14.40	0.21617	0.015012
12.	245	0.56	95.60	92.00	85.60	80.50	116.620	15.50	0.23294	0.015028
13.	255	0.58	98.00	94.00	86.40	81.70	125.715	16.70	0.25130	0.015048
14.	265	0.60	99.80	95.90	89.00	82.90	135.150	17.90	0.27039	0.015106

Table-A.23: Collected data during the experiment, HRI-Methanol**Experiment No: 2**

Working Fluid : Methanol , Surface : HRI

Here, V= Supply Voltage (Volt)

I=Line Current (Ampere)

 T_{sat} =Saturated Temperature of Fluid ($^{\circ}\text{C}$) T_{x1} = Temperature at the point 1 of evaporator geometry ($^{\circ}\text{C}$) T_{x2} = Temperature at the point 2 of evaporator geometry ($^{\circ}\text{C}$) T_{x3} =Temperature at the point 3 of evaporator geometry ($^{\circ}\text{C}$) T_{x4} =Temperature at the point 4 of evaporator geometry ($^{\circ}\text{C}$)

Q = Total Heat Input(W)

 $\Delta T = T_{x4} - T_{sat}$ ($^{\circ}\text{C}$)q = Heat Flux Per unit Area After deducting Heat loss (MW/m^2)q R= Heat Flux Found From Rohsenow Correlation (MW/m^2)h = Boiling heat transfer coefficient ($\text{MW}/\text{m}^2 \cdot ^{\circ}\text{C}$) $T_{sat} = 65^{\circ}\text{C}$

Obs. No.	V	I	T_{x1}	T_{x2}	T_{x3}	T_{x4}	Q	ΔT	q(MW/m^2)	qR(MW/m^2)	h($\text{MW}/\text{m}^2 \cdot ^{\circ}\text{C}$)
1.	141	0.340	75.000	73.700	71.600	69.200	40.749	4.200	0.080	0.00222	0.01901
2.	149	0.360	76.900	74.100	72.100	70.000	45.594	5.000	0.090	0.00375	0.01791
3.	157	0.380	77.100	75.000	69.000	67.200	50.711	2.200	0.100	0.00032	0.04544
4.	169	0.400	79.000	77.100	74.300	71.900	57.460	6.900	0.114	0.00984	0.01646
5.	175	0.420	80.400	78.400	75.470	72.800	62.475	7.800	0.124	0.01422	0.01586
6.	182	0.440	82.500	80.300	77.900	74.000	68.068	9.000	0.135	0.02184	0.01500
7.	198	0.460	84.900	82.300	78.400	75.000	77.418	10.000	0.154	0.02996	0.01538
8.	207	0.480	85.600	82.800	78.700	75.300	84.456	10.300	0.168	0.03274	0.01632
9.	213	0.500	88.600	85.500	80.800	76.900	90.525	11.900	0.180	0.05049	0.01515
10.	221	0.520	90.600	87.300	82.100	77.900	97.682	12.900	0.195	0.06431	0.01509
11.	234	0.540	93.700	90.000	84.300	79.600	107.406	14.600	0.214	0.09324	0.01468
12.	244	0.560	96.000	92.300	86.100	81.000	116.144	16.000	0.232	0.12272	0.01450
13.	254	0.580	98.100	94.200	87.600	82.200	125.222	17.200	0.250	0.15245	0.01455
14.	265	0.600	99.800	95.900	88.900	83.000	135.150	18.000	0.270	0.17473	0.01502

Table-A.24: Collected data during the experiment, HRI-Methanol**Experiment No: 3**

Working Fluid : Methanol , Surface : HRI

Here, V= Supply Voltage (Volt)

I=Line Current (Ampere)

 T_{sat} =Saturated Temperature of Fluid ($^{\circ}\text{C}$) T_{x_1} = Temperature at the point 1 of evaporator geometry ($^{\circ}\text{C}$) T_{x_2} = Temperature at the point 2 of evaporator geometry ($^{\circ}\text{C}$) T_{x_3} =Temperature at the point 3 of evaporator geometry ($^{\circ}\text{C}$) T_{x_4} =Temperature at the point 4 of evaporator geometry ($^{\circ}\text{C}$)

Q = Total Heat Input (W)

 $\Delta T = T_{x_4} - T_{sat}$ ($^{\circ}\text{C}$)q = Heat Flux Per unit Area After deducting Heat loss (MW/m^2)q R= Heat Flux Found From Rohsenow Correlation (MW/m^2)h = Boiling heat transfer coefficient ($\text{MW}/\text{m}^2 \cdot ^{\circ}\text{C}$) $T_{sat} = 65^{\circ}\text{C}$

Obs. No.	V	I	T_{x_1}	T_{x_2}	T_{x_3}	T_{x_4}	Q	ΔT	q(MW/m^2)	qR(MW/m^2)	h($\text{MW}/\text{m}^2 \cdot ^{\circ}\text{C}$)
1.	141	0.340	75.000	73.700	71.600	69.200	40.749	4.200	0.080	0.00222	0.01901
2.	149	0.360	76.900	74.100	72.100	70.000	45.594	5.000	0.090	0.00375	0.01791
3.	157	0.380	77.100	75.000	73.200	70.900	50.711	5.900	0.100	0.00615	0.01695
4.	169	0.400	79.000	77.100	74.300	71.900	57.460	6.900	0.114	0.00984	0.01646
5.	175	0.420	80.400	78.400	75.470	72.800	62.475	7.800	0.124	0.01422	0.01586
6.	182	0.440	82.500	80.300	77.900	74.000	68.068	9.000	0.135	0.02184	0.01500
7.	198	0.460	84.900	82.300	78.400	75.000	77.418	10.000	0.154	0.02996	0.01538
8.	207	0.480	85.600	82.800	78.700	75.300	84.456	10.300	0.168	0.03274	0.01632
9.	213	0.500	88.600	85.500	80.800	76.900	90.525	11.900	0.180	0.05049	0.01515
10.	221	0.520	90.600	87.300	82.100	77.900	97.682	12.900	0.195	0.06431	0.01509
11.	234	0.540	93.700	90.000	84.300	79.600	107.406	14.600	0.214	0.09324	0.01468
12.	244	0.560	96.000	92.300	86.100	81.000	116.144	16.000	0.232	0.12272	0.01450
13.	254	0.580	98.100	94.200	87.600	82.200	125.222	17.200	0.250	0.15245	0.01455
14.	265	0.600	99.800	95.900	88.900	83.000	135.150	18.000	0.270	0.17473	0.01502

Table-A.25: Collected data during the experiment, HR+-Methanol**Experiment No: 1**

Working Fluid : Methanol , Surface :HR+

Here, V= Supply Voltage (Volt)

I=Line Current (Ampere)

 T_{sat} =Saturated Temperature of Fluid ($^{\circ}\text{C}$) T_{x1} = Temperature at the point 1 of evaporator geometry ($^{\circ}\text{C}$) T_{x2} = Temperature at the point 2 of evaporator geometry ($^{\circ}\text{C}$) T_{x3} =Temperature at the point 3 of evaporator geometry ($^{\circ}\text{C}$) T_{x4} =Temperature at the point 4 of evaporator geometry ($^{\circ}\text{C}$)

Q = Total Heat Input(W)

 $\Delta T = T_{x4} - T_{sat}$ ($^{\circ}\text{C}$)q = Heat Flux Per unit Area After deducting Heat loss (MW/m^2)q R= Heat Flux Found From Rohsenow Correlation (MW/m^2)qs = Heat Flux Found From Stephan and Abdelsalam Correlation (MW/m^2)h = Boiling heat transfer coefficient ($\text{MW}/\text{m}^2 \cdot ^{\circ}\text{C}$) $T_{sat} = 65^{\circ}\text{C}$

Obs. No.	V	I	T_{x1}	T_{x2}	T_{x3}	T_{x4}	Q	ΔT	q(MW/m^2)	qR(MW/m^2)	qs(MW/m^2)	h($\text{MW}/\text{m}^2 \cdot ^{\circ}\text{C}$)
1.	148	0.360	75.200	73.600	71.700	70.600	45.288	5.600	0.089	0.00526	0.00274	0.0159
2.	160	0.380	78.200	76.200	74.000	72.600	51.680	7.600	0.102	0.01315	0.00686	0.0134
3.	167	0.400	80.000	77.600	76.100	74.200	56.780	9.200	0.112	0.02333	0.01217	0.01219
4.	173	0.420	82.700	80.200	77.700	76.000	61.761	11.000	0.122	0.03988	0.02080	0.0111
5.	184	0.440	84.100	81.400	78.400	76.700	68.816	11.700	0.136	0.04798	0.02503	0.01166
6.	194	0.460	85.300	82.300	79.000	77.100	75.854	12.100	0.151	0.05308	0.02768	0.01245
7.	205	0.480	88.200	84.700	81.000	78.700	83.640	13.700	0.166	0.07704	0.04018	0.01214
8.	212	0.500	90.900	87.200	83.100	80.700	90.100	15.700	0.179	0.11594	0.06047	0.01142
9.	227	0.520	93.500	89.900	84.700	82.000	100.334	17.000	0.200	0.14719	0.07677	0.01176
10.	241	0.540	96.700	92.300	83.900	83.800	110.619	18.800	0.221	0.19907	0.10382	0.01174
11.	249	0.560	98.700	94.300	88.600	85.300	118.524	20.300	0.237	0.25063	0.13071	0.01166
12.	260	0.580	102.100	97.000	91.000	87.300	128.180	22.300	0.256	0.33224	0.17327	0.01148
13.	265	0.600	103.600	98.200	92.400	88.000	135.150	23.000	0.270	0.36452	0.19011	0.01174

Table-A.26: Collected data during the experiment, HR+-Methanol**Experiment No: 2**

Working Fluid : Methanol ,Surface :HR+

Here, V= Supply Voltage (Volt)

I=Line Current (Ampere)

 T_{sat} =Saturated Temperature of Fluid ($^{\circ}\text{C}$) T_{x1} = Temperature at the point 1 of evaporator geometry ($^{\circ}\text{C}$) T_{x2} = Temperature at the point 2 of evaporator geometry ($^{\circ}\text{C}$) T_{x3} =Temperature at the point 3 of evaporator geometry ($^{\circ}\text{C}$) T_{x4} =Temperature at the point 4 of evaporator geometry ($^{\circ}\text{C}$)

Q = Total Heat Input (W)

 $\Delta T = T_{x4} - T_{sat}$ ($^{\circ}\text{C}$)q = Heat Flux Per unit Area After deducting Heat loss (MW/m^2)q R= Heat Flux Found From Rohsenow Correlation (MW/m^2)h = Boiling heat transfer coefficient ($\text{MW}/\text{m}^2 \cdot ^{\circ}\text{C}$) $T_{sat} = 65^{\circ}\text{C}$

Obs. No.	V	I	T_{x1}	T_{x2}	T_{x3}	T_{x4}	Q	ΔT	q(MW/m^2)	qR(MW/m^2)	h($\text{MW}/\text{m}^2 \cdot ^{\circ}\text{C}$)
1.	146	0.360	78.200	76.700	74.800	73.600	44.676	8.600	0.088	0.01906	0.010187
2.	158	0.380	79.600	77.700	75.600	74.300	51.034	9.300	0.100	0.02410	0.010802
3.	160	0.400	80.300	78.400	76.300	75.000	54.400	10.000	0.107	0.02996	0.010727
4.	172	0.420	81.500	79.300	76.900	75.400	61.404	10.400	0.121	0.03370	0.011678
5.	183	0.440	82.600	80.000	77.100	75.500	68.442	10.500	0.136	0.03468	0.012925
6.	203	0.460	86.600	83.400	79.700	77.500	79.373	12.500	0.158	0.05852	0.012616
7.	212	0.480	88.400	84.700	80.700	78.400	86.496	13.400	0.172	0.07209	0.012842
8.	222	0.500	90.100	86.500	81.800	79.200	94.350	14.200	0.188	0.08578	0.013237
9.	234	0.520	92.600	88.200	83.400	80.700	103.428	15.700	0.206	0.11594	0.013139
10.	248	0.540	96.500	92.000	86.300	83.000	113.832	18.000	0.227	0.17473	0.012622
11.	253	0.560	97.400	92.700	86.800	83.600	120.428	18.600	0.241	0.19279	0.012934
12.	261	0.580	99.900	94.900	88.700	85.100	128.673	20.100	0.257	0.24329	0.012796
13.	266	0.590	100.700	95.600	89.400	85.600	133.399	20.600	0.267	0.26190	0.01295

Table-A.27: Collected data during the experiment, HR+- Methanol**Experiment No: 3**

Working Fluid : Methanol , Surface ; HR+

Here, V= Supply Voltage (Volt)

I=Line Current (Ampere)

 T_{sat} =Saturated Temperature of Fluid ($^{\circ}\text{C}$) T_{x1} = Temperature at the point 1 of evaporator geometry ($^{\circ}\text{C}$) T_{x2} = Temperature at the point 2 of evaporator geometry ($^{\circ}\text{C}$) T_{x3} =Temperature at the point 3 of evaporator geometry ($^{\circ}\text{C}$) T_{x4} =Temperature at the point 4 of evaporator geometry ($^{\circ}\text{C}$)

Q = Total Heat Input(W)

 $\Delta T = T_{x4} - T_{sat}$ ($^{\circ}\text{C}$)q = Heat Flux Per unit Area After deducting Heat loss (MW/m²)qR= Heat Flux Found From Rohsenow Correlation (MW/m²)h = Boiling heat transfer coefficient (MW/m². $^{\circ}\text{C}$)

$$T_{sat} = 65^{\circ}\text{C}$$

Obs. No.	V	I	T_{x1}	T_{x2}	T_{x3}	T_{x4}	Q	ΔT	q(MW/m ²)	qR(MW/m ²)	h(MW/m ² . $^{\circ}\text{C}$)
1.	146	0.360	78.000	76.300	74.800	73.400	44.676	8.400	0.088	0.01776	0.010431
2.	158	0.380	78.900	77.100	75.000	73.600	51.034	8.600	0.101	0.01906	0.011687
3.	161	0.400	79.900	78.000	76.800	74.300	54.740	9.300	0.108	0.02410	0.011612
4.	172	0.420	81.200	78.000	76.900	74.700	61.404	9.700	0.121	0.02734	0.012523
5.	183	0.440	82.600	80.100	74.400	75.800	68.442	10.800	0.136	0.03774	0.012566
6.	200	0.460	85.000	82.100	79.000	77.000	78.200	12.000	0.155	0.05177	0.012952
7.	211	0.480	86.600	83.300	79.700	77.600	86.088	12.600	0.171	0.05993	0.013601
8.	222	0.500	88.500	85.000	81.000	78.700	94.350	13.700	0.188	0.07704	0.013728
9.	230	0.520	92.000	87.900	83.200	80.500	101.660	15.500	0.203	0.11157	0.013079
10.	241	0.540	94.700	90.300	85.200	82.200	110.619	17.200	0.221	0.15245	0.012836
11.	252	0.560	97.200	92.800	87.100	83.900	119.952	18.900	0.240	0.20227	0.012678
12.	260	0.580	99.700	94.800	88.900	85.300	128.180	20.300	0.256	0.25063	0.012621
13.	265	0.600	100.700	95.800	89.800	86.000	135.150	21.000	0.270	0.27746	0.012873

Appendix-B

Sample calculations of heat flux, correlation

Area of Heater Geometry:

In the present study Area of the heater geometry is calculated in the following way.

$$A = \pi r^2 \quad (B2)$$

Where, A = Area of the heater geometry, cm²
r = Radius of the heater geometry, cm

$$A = \pi (1.25)^2 = 4.9087\text{cm}^2 \quad (B3)$$

Heat losses are calculated by one dimensional heat conduction Analysis and is found

$$q_L = (T_{x1} - T_\alpha) * 0.0347 \text{ W/cm}^2 \quad (B4)$$

Where, T_{x1} = temperature at the point 1 of the heater assembly geometry, °C

T_α = Ambient Temperature, °C

q_L = Heat loss from heater assembly, °C

Which is about 1-2% of the total Heat supply

Total Heat Supply calculation

$$Q = V I \cos\theta \quad (B5)$$

Where, V = Voltage in volt

I = Current in ampere

$$\cos\theta = 0.85$$

Q = Total heat supply in watt

Resultant Heat Flux:

Resultant heat flux q is found by deducting the heat loss from total heat input

$$q = \{Q - (T_{x1} - T_\alpha) * 0.0347\} / 4.9087\text{W/cm}^2$$

$$q = \{Q - (T_{x1} - T_\alpha) * 0.0347\} / 490.87\text{MW/m}^2 \quad (B6)$$

Where, q = Heat Flux, MW/m²

Wall Superheat:(ΔT)

Wall superheat calculated for three different fluids, which are

$$\Delta T = T_{x_4} - 56.5^\circ\text{C} \quad (\text{for Acetone}) \quad (\text{B7})$$

$$\Delta T = T_{x_4} - 78^\circ\text{C} \quad (\text{for Ethanol}) \quad (\text{B8})$$

$$\Delta T_M = T_{x_4} - 65^\circ\text{C} \quad (\text{for Methanol}) \quad (\text{B9})$$

Rohsenow Correlation:

Heat Flux from Rohsenow correlation is calculated in the following way

$$\frac{C_l \Delta T_x}{h_{fg} Pr_l^s} = C_{sf} \left[\frac{qR}{\mu_l h_{fg}} \sqrt{\frac{g_c \sigma}{g(\rho_l - \rho_v)}} \right]^{0.33} \quad (\text{B10})$$

- where C_l = specific heat of saturated liquid, J/kg. $^\circ\text{C}$
 ΔT = temperature excess = $T_w - T_{sat}$, $^\circ\text{C}$
 h_{fg} = enthalpy of vaporization, J/kg
 Pr_l = Prandtl number of saturated liquid
 qR = heat flux per unit area, W/m 2 .
 μ_l = liquid viscosity, kg/m.s
 σ = surface tension of liquid-vapor interface, N/m
 g = gravitational acceleration, m/s 2
 ρ_l = density of saturated liquid, kg/m 3
 ρ_v = density of saturated vapor, kg/m 3
 C_{sf} = constant, determined from experimental data
 s = 1.0 for water and 1.7 for other liquids

For Methanol:

$$C_l = 2880 \text{ J/kg.}^\circ\text{C}$$

$$qR = ?$$

$$h_{fg} = 1101000 \text{ J/kg}$$

$$Pr_l = 5.13$$

$$\mu_l = 326 \cdot 10^{-6} \text{ kg/m.s}$$

$$C_{sf} = 0.0031$$

$$s = 1.7$$

$$\rho_l = 751.0 \text{ kg/m}^3$$

$$\rho_v = 1.222 \text{ kg/m}^3$$

$$\frac{2880\Delta T}{1101 \times 10^3 \times 5.13^{1.7}} = 0.0031 \left[\frac{qR}{326 \times 10^{-6} \times 1101 \times 10^3} \sqrt{\frac{18.75 \times 10^{-3}}{9.81(751 - 1.222)}} \right]^{0.33} \quad (\text{B11})$$

$$\begin{aligned} qR &= 28.36 (\Delta T)^3 \text{ W/m}^2 \\ &= 0.00002836 (\Delta T)^3 \text{ MW/m}^2 \end{aligned}$$

For Ethanol:

$$C_1 = 3000 \text{ J/kg} \cdot ^\circ\text{C}$$

$$qR = ?$$

$$h_{fg} = 963 \text{ kJ/kg}$$

$$Pr_l = 8.37$$

$$\mu_l = 428.7 \times 10^{-6} \text{ kg/m} \cdot \text{s}$$

$$C_{sf} = 0.002$$

$$s = 1.7$$

$$\rho_l = 757.0 \text{ kg/m}^3$$

$$\rho_v = 1.435 \text{ kg/m}^3$$

$$\frac{3000\Delta T}{963 \times 10^3 \times 8.37^{1.7}} = 0.002 \left[\frac{qR}{428.7 \times 10^{-6} \times 963 \times 10^3} \sqrt{\frac{17.7 \times 10^{-3}}{9.81(751 - 1.435)}} \right]^{0.33} \quad (\text{B12})$$

$$\begin{aligned} qR &= 17.5 (\Delta T)^3 \text{ W/m}^2 \\ &= 0.0000175 (\Delta T)^3 \text{ MW/m}^2 \end{aligned}$$

For Acetone:

$$C_1 = 2280 \text{ J/kg} \cdot ^\circ\text{C}$$

$$qR = ?$$

$$h_{fg} = 506 \text{ kJ/kg}$$

$$Pr_l = 3.77$$

$$\mu_l = 235 \times 10^{-6} \text{ kg/m} \cdot \text{s}$$

$$C_{sf} = 0.01$$

$$s = 1.7$$

$$\sigma = 18.4 \times 10^{-3} \text{ N/m}$$

$$\rho_l = 750.0 \text{ kg/m}^3$$

$$\rho_v = 2.33 \text{ kg/m}^3$$

$$\frac{2280\Delta T}{506 \times 10^3 \times 3.77^{1.7}} = 0.01 \left[\frac{qR}{235 \times 10^{-6} \times 506 \times 10^3} \sqrt{\frac{18.4 \times 10^{-3}}{9.81(750 - 2.23)}} \right]^{0.33} \quad (\text{B13})$$

$$\begin{aligned} qR &= 7.05 (\Delta T)^3 \text{ W/m}^2 \\ &= 0.00000705 (\Delta T)^3 \text{ MW/m}^2 \end{aligned}$$

Stephan and Abdelsalam Correlations

$$qS = \{C_2 (T_w - T_{sat})\}^{1/0.33}$$

where

$$qS = \text{heat flux, W/m}^2$$

$c_2 = \text{constant}$

For Methanol:

$$c_2 = 2.5$$

$$qS = \{2.5(T_w - T_{sat})\}^{1/0.33}$$

$$qS = \{2.5(\Delta T)\}^{1/0.33}$$

$$\begin{aligned} qS &= 15.625 (\Delta T)^3 \text{ W/m}^2 \\ &= 0.00001562 (\Delta T)^3 \text{ MW/m}^2 \end{aligned}$$

For Ethanol:

$$c_2 = 2.7$$

$$qS = \{2.7(T_w - T_{sat})\}^{1/0.33}$$

$$qS = \{2.7(\Delta T)\}^{1/0.33}$$

$$\begin{aligned} qS &= 19.683 (\Delta T)^3 \text{ W/m}^2 \\ &= 0.00001968 (\Delta T)^3 \text{ MW/m}^2 \end{aligned}$$

For Acetone:

$$c_2 = 2.3$$

$$qS = \{2.3(T_w - T_{sat})\}^{1/0.33}$$

$$qS = \{2.3(\Delta T)\}^{1/0.33}$$

$$qS = 12.167 (\Delta T)^3 \text{ W/m}^2$$

$$= 0.00001216 (\Delta T)^3 \text{ MW/m}^2$$

Critical Heat Flux (CHF)

Critical Heat Flux (CHF) is calculated by Kutateladze correlation.

$$q_{crit} = C_k \rho_v^{1/2} h_{fg} [g(\rho_l - \rho_v)\sigma]^{1/4}$$

- where q_{crit} = maximum heat flux for W/m^2
 ρ_v = density of saturated vapor, kg/m^3
 h_{fg} = enthalpy of vaporization, J/kg
 σ = Surface tension of liquid-vapor interface, N/m
 g = gravitational acceleration, m/s^2
 ρ_l = density of saturated liquid, kg/m^3
 C_k = 0.16, constant, for pool boiling

For Methanol:

- ρ_v = 1.222 kg/m^3
 h_{fg} = 1101 kJ/kg
 σ = 18.75 $\times 10^{-3}$ N/m
 g = 9.81 m/s^2
 ρ_l = 751 kg/m^3
 C_k = 0.16, constant, for pool boiling

$$q_{crit} = 0.16 \times (1.222)^{1/2} \times 1101 \left[9.81(751 - 1.222) \frac{18.75}{10^3} \right]^{0.25}$$

$$= 667.334 \text{ kW/m}^2$$

$$= 0.667 \text{ MW/m}^2$$

For Ethanol:

- ρ_v = 1.435 kg/m^3
 h_{fg} = 963 kJ/kg
 σ = 17.7 $\times 10^{-3}$ N/m
 g = 9.81 m/s^2
 ρ_l = 757 kg/m^3
 C_k = 0.16, constant, for pool boiling

$$q_{crit} = 0.16 \times (1.435)^{1/2} \times 963 \left[9.81(757 - 1.435) \frac{17.7}{10^3} \right]^{0.25}$$

$$= 624.67 \text{ kW/m}^2$$

$$= 0.62467 \text{ MW/m}^2$$

For Acetone:

$$\rho_v = 2.23 \text{ kg/m}^3$$

$$h_{fg} = 506 \text{ kJ/kg}$$

$$\sigma = 18.4 \times 10^{-3} \text{ N/m}$$

$$g = 9.81 \text{ m/s}^2$$

$$\rho_l = 750 \text{ kg/m}^3$$

$$C_k = 0.16, \text{ constant, for pool boiling}$$

$$q_{crit} = 0.16 \times (2.23)^{1/2} \times 506 \left[9.81(750 - 2.23) \frac{18.4}{10^3} \right]^{0.25}$$

$$= 412.084 \text{ kW/m}^2$$

$$= 0.412 \text{ MW/m}^2$$

